RLO/2439-77/2

UC 60

WIND ENERGY STATISTICS FOR LARGE ARRAYS OF WIND TURBINES (GREAT LAKES AND PACIFIC COAST REGIONS)

Annual Progress Report

C. G. Justus and W. R. Hargraves

School of Aerospace Engineering
Georgia Institute of Technology
Atlanta, GA 30332

Date Published - May 1977

Reporting Period - 1 May 1976 - 30 April 1977

PREPARED FOR THE UNITED STATES
ENERGY RESEARCH AND DEVELOPMENT
ADMINISTRATION

DIVISION OF SOLAR ENERGY

UNDER CONTRACT EY-76-S-06-2439

Georgia Tech Project E-16-681

Abstract

In an earlier study the wind and wind power statistics of large arrays of wind turbines in the New England and Central U.S. Regions were examined. This report examines arrays of simulated 0.5 MW, 1.5 MW and 2.0 MW wind turbines in the Great Lakes and Pacific Coast Regions. As with the earlier study, the parameters analyzed are: basic wind statistics, time and spatial correlations, mean wind power output, wind power frequency (availability without storage), and run duration of wind speed and array power (probabilities of wind and power lulls of various duration, without storage). New aspects of the present study include evaluation of diurnal as well as seasonal variations of wind and wind power, inclusion of density, wind shear, wind gusts and other factors in the model power output curve simulation, study of the possible relation between wind speed and degree days (known to affect a portion of utility demand), and development and verification of a simplified array simulation model. The basic results are similar to the earlier study, except that the Pacific Coast array had much lower spatial correlation because of terrain influence. No relationship between winds and degree days was observed although wind and temperature are related by virtue of a common diurnal variation pattern.

TABLE OF CONTENTS

LIST OF FIGURES

LIST OF TABLES

1. INTRODUCTION

This report presents results of analysis of simulated arrays of large wind energy conversion systems (WECS) in the Great Lakes and Pacific Coast area. This is a continuation of earlier array studies for the New England and Central U.S. Regions, reported by Justus (1976). The newly studied regions were made up of sites illustrated in Figures 1 and 2 and listed in Tables 1 and 2. Similar analysis techniques were used to those employed in the earlier array simulations. National Climatic Center wind data (for years 1971-1975) were used, and converted to wind turbine hub height by methods described by Justus and Mikhail (1976).

Three wind turbine designs were evaluated in this study, with rated powers of 0.5, 1.5, and 2.0 MW. Characteristics of these machine designs are given in Table 3. Power output is assumed to be zero below cut-in speed, to vary parabolicly between zero and full rated power up to rated speed, to remain at rated power between rated speed and a high value of cut-out speed.

As in the earlier studies, the array of WECS units is assumed to be made up of farms of wind turbines at the National Weather Service site locations, with an arbitrary number of WECS units per farm. Actual array computations done here assume the same number of WECS units per farm, but the array simulation model is adaptable to arbitrary numbers of units per farm [see equations (B-3) through (B-5)]. Power output statistics would not be extremely sensitive to variable numbers of WECS units per farm. Power output of the array is expressed per generator for comparison of statistics with individual machines.

New aspects of this study include:

- inclusion of density, wind shear, wind gusts and other factors in the power output curve simulation

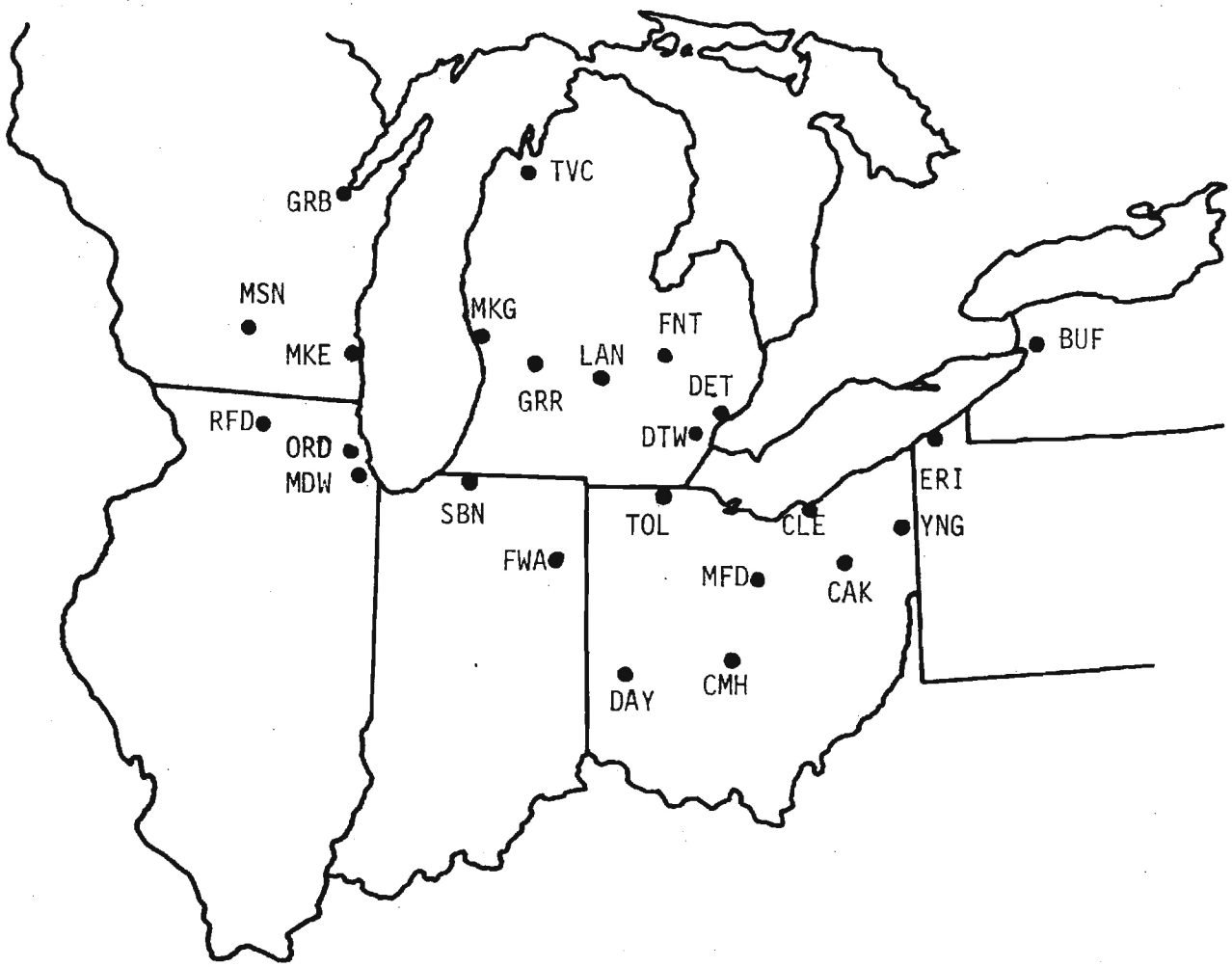

Figure 1. Map of the Great Lakes Sites.

Table 1

Great Lakes Sites

BUF	Buffalo, NY	LAN	Lansing, MI
CAK	Akron, OH	MDW	Chicago (Midway, IL
CLE	Cleveland, OH	MFD	Mansflied, OH
CMH	Columbus, OH	MKE	Milwaukee, WI
DAY	Dayton, OH	MKG	Muskegon, MI
DET	Detroit (City), MI	MSN	Madison, WI
DTW	Detroit (Metro), MI	ORD	Chicago (O'Hare), IL
ERI	Erie, PA	RFD	Rockford, IL
FNT	Flint, MI	SBN	South Bend, IN
FWA	Ft. Wayne, IN	TOL	Toledo, OH
GRB	Green Bay, WI	TVC	Traverse City, MI
GRR	Grand Rapids, MI	YNG	Youngstown, OH

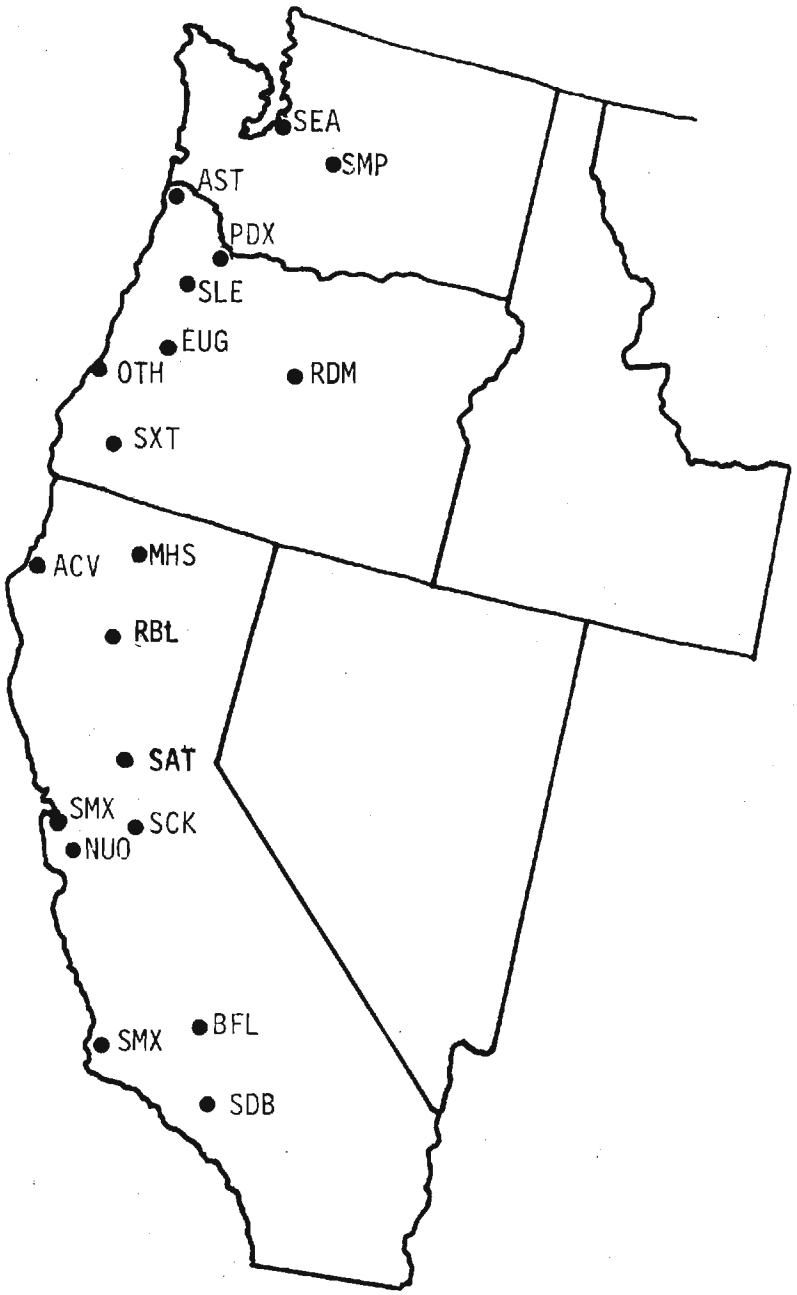

Figure 2. Map of the Pacific Coast Sites.

Table 2 - West Coast Sites

ACV	Arcata, CA	SAC	Sacramento, CA
AST	Astoria, OR	SCK	Stockton, CA
BFL	Bakersfield, CA	SDB	Sandberg, CA
EUG	Eugene, OR	SEA	Seattle/Tacoma, WA
MHS	Mt. Shasta, CA	SFO	San Francisco, CA
NUO	Sunnyvale, CA	SLE	Salem, OR
OTH	North Bend, OR	SMP	Stampede Pass, WA
PDX	Portland, OR	SMX	Santa Maria, CA
RBL	Red Bluff, CA	SXT	Sexton Summit, OR
RDM	Redmon, OR		

Table 3

Wind Turbine Characteristics

Rated Power, MW	0.5	1.5	2.0
Cut-In Speed at Hub Height			
m/s	4.6	6.6	5.3
mph	10.3	14.8	11.9
Rated Speed at Hub Height			
m/s	9.4	13.1	10.6
mph	21.0	29.3	23.7
Rotor Swept Diameter			
m	55.8	57.9	91.4
ft	183	190	300
Tower Height			
m	60.0	60.0	60.0
ft	197	197	197

- evaluation of diurnal as well as seasonal variation in wind power statistics
- study of the possible relationship between heating and cooling degree days (known to influence utility demand) and available wind energy
- development and verification of a model whereby wind data (either summarized as averages and standard deviations, or in time series form) can be used for a single "representative" site to simulate the statistical aspects of behavior of a WECS array of arbitrary size, configuration, and spatial correlation.

2. WIND STATISTICS

Table 4 and Table 5 show seasonal mean wind speeds for the Great Lakes sites and the Pacific Coast sites, respectively. The seasons correspond to the following days of the year: winter, days 1-44 and 315-366; spring, days 45-134; summer, days 135-224; fall, days 225-314; annual, all days. These mean speeds are the 5-year averages for 1971-1975. The Great Lakes sites used in this study generally have higher mean speeds than the Pacific Coast sites used. Buffalo, New York (BUF), and Muskegon, Wisconsin (MKG), are the best sites in the Great Lakes area while Sandberg, California (SDB), has the highest mean speed in the Pacific Coast area. All data used in this study come from airport locations, and hence are not likely to be indicative of winds at the best nearby wind power sites. This difference is more significant for the Pacific Coast sites, where substantial terrain effects are found within the study region.

Mean wind speeds by month are shown in Figure 3 and Figure 4. These values were evaluated by averaging over all sites and all years for the corresponding month for each area of study. As seen, the Great Lakes mean speed reaches a maximum in January and a minimum in August. This contrasts with the Pacific Coast area which has two minimums, one in December and one in September, and 2 maximums, one in May and a secondary maximum in November. The Great Lakes array has significantly higher mean speeds in the winter months and slightly lower mean speeds in the summer than the Pacific Coast area.

Diurnal variation by season is shown in Figure 5 and Table 6 for the Great Lakes area and in Figure 6 and Table 7 for the Pacific Coast area. Both areas have a maximum at 1600 hours and a minimum at 400 hours, independent of season. As expected, the summer variation is greater than the winter. In the Great Lakes area the winter means are always greater than the summer values, but in the Pacific Coast area the summer afternoon winds are well above the corresponding winter winds. Overall the mean winds in the Great Lakes are higher than those in the Pacific Coast but the summer winds in the Pacific Coast are better than those in the Great Lakes.

Table 4

Mean Wind Speed (m/s) at 60 m (197 ft) Hub Height for Great Lakes Sites

	Winter	Spring	Summer	Fall	Annual
BUF	9.1	8.3	7.1	7.6	8.1
CAK	8.0	7.7	5.9	6.6	7.0
CLE	8.4	7.8	6.3	6.9	7.3
CMH	7.8	7.6	5.7	6.2	6.8
DAY	8.1	7.9	6.1	6.5	7.2
DET	7.5	6.9	6.0	6.4	6.7
DTW	8.7	8.4	6.8	7.5	7.8
ERI	9.0	8.1	6.8	7.8	7.9
FNT	8.0	7.5	6.2	6.8	7.1
FWA	8.3	8.1	6.5	6.9	7.5
GRB	7.8	7.6	6.5	7.1	7.2
GRR	7.9	7.5	6.2	6.6	7.0
LAN	7.9	7.5	5.8	6.5	6.9
MDW	7.7	8.0	6.6	7.1	7.4
MFD	8.9	8.4	6.7	7.5	7.9
MKE	8.8	8.4	7.5	7.9	8.1
MKG	8.7	8.0	6.7	7.5	7.7
MSN	7.2	7.3	6.1	6.7	6.8
ORD	8.2	8.0	6.4	7.4	7.5
RFD	7.8	7.9	6.2	6.9	7.2
SBN	8.2	8.0	6.2	6.8	7.3
TOL	7.2	7.1	5.3	5.9	6.4
TVC	6.8	6.1	5.8	6.2	6.2
YNG	8.1	7.7	6.0	6.7	7.1
	—	—	—	—	—
AVG	8.1	7.7	6.3	6.9	7.3

Table 5

Mean Wind Speed (m/s) at 60 m (197 ft) Hub Height for Pacific Sites

	Winter	Spring	Summer	Fall	Annual
AST	7.2	5.6	6.1	6.0	5.8
BFL	4.8	6.0	6.0	5.1	5.5
EUG	6.4	5.5	6.0	5.8	5.5
OTH	7.1	6.3	7.9	6.7	6.3
RBL	6.6	6.2	6.3	6.3	5.8
RDM	6.2	5.2	6.0	5.8	5.2
SAC	5.1	5.7	6.5	4.9	5.7
SCK	5.8	6.6	7.0	5.7	6.3
SDB	9.0	9.5	7.6	8.0	8.5
SEA	6.8	6.1	5.8	6.1	6.2
SFO	5.8	8.1	8.5	6.7	7.3
SMP	7.9	7.4	7.2	7.2	7.5
SMX	5.7	4.8	-	5.7	4.9
SXT	7.9	7.3	6.2	6.8	7.8
	---	---	---	---	---
AVG	6.5	6.5	6.7	6.1	6.2

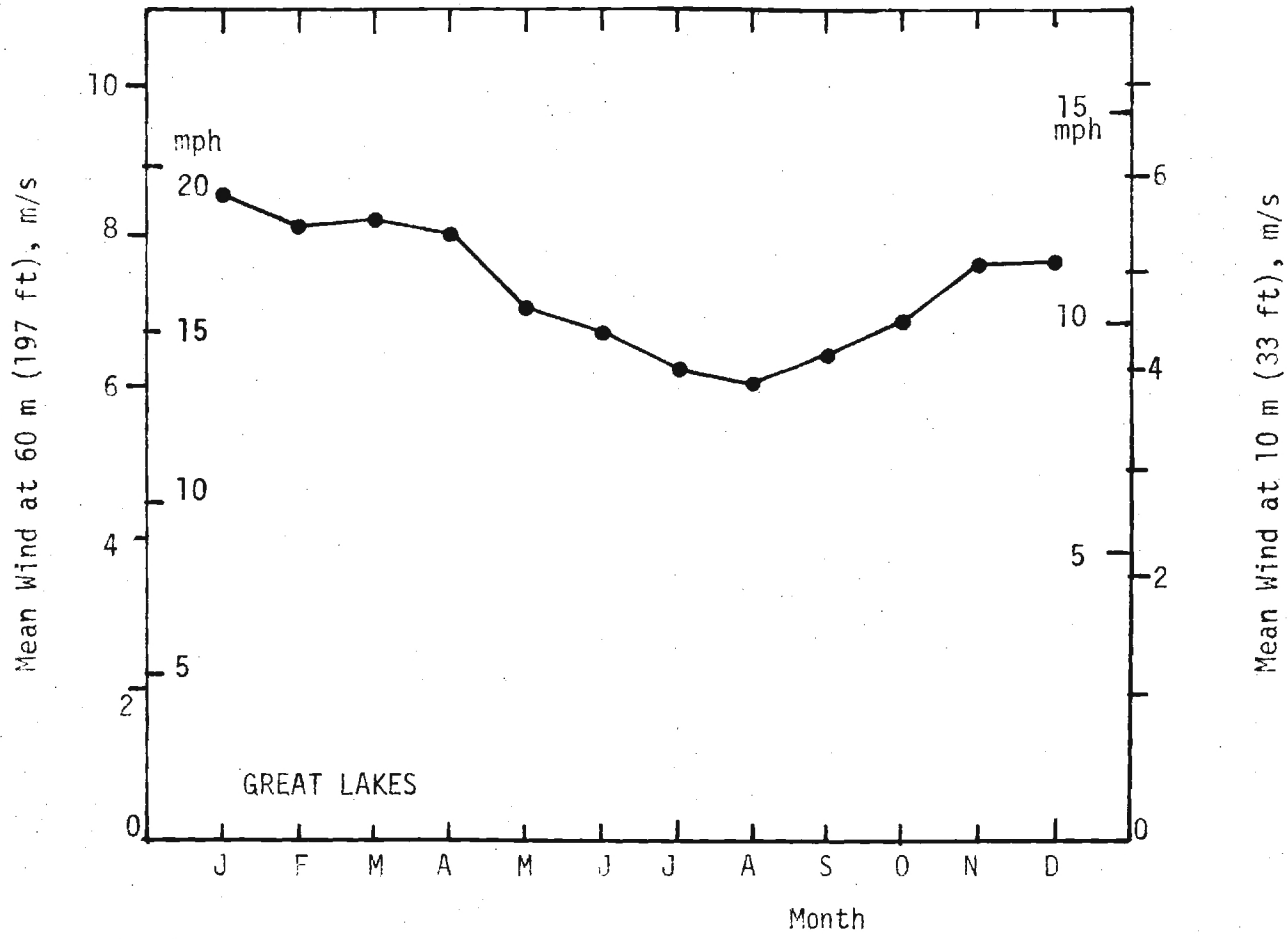

Figure 3. Mean Winds Annual Variation for the Great Lakes Region.

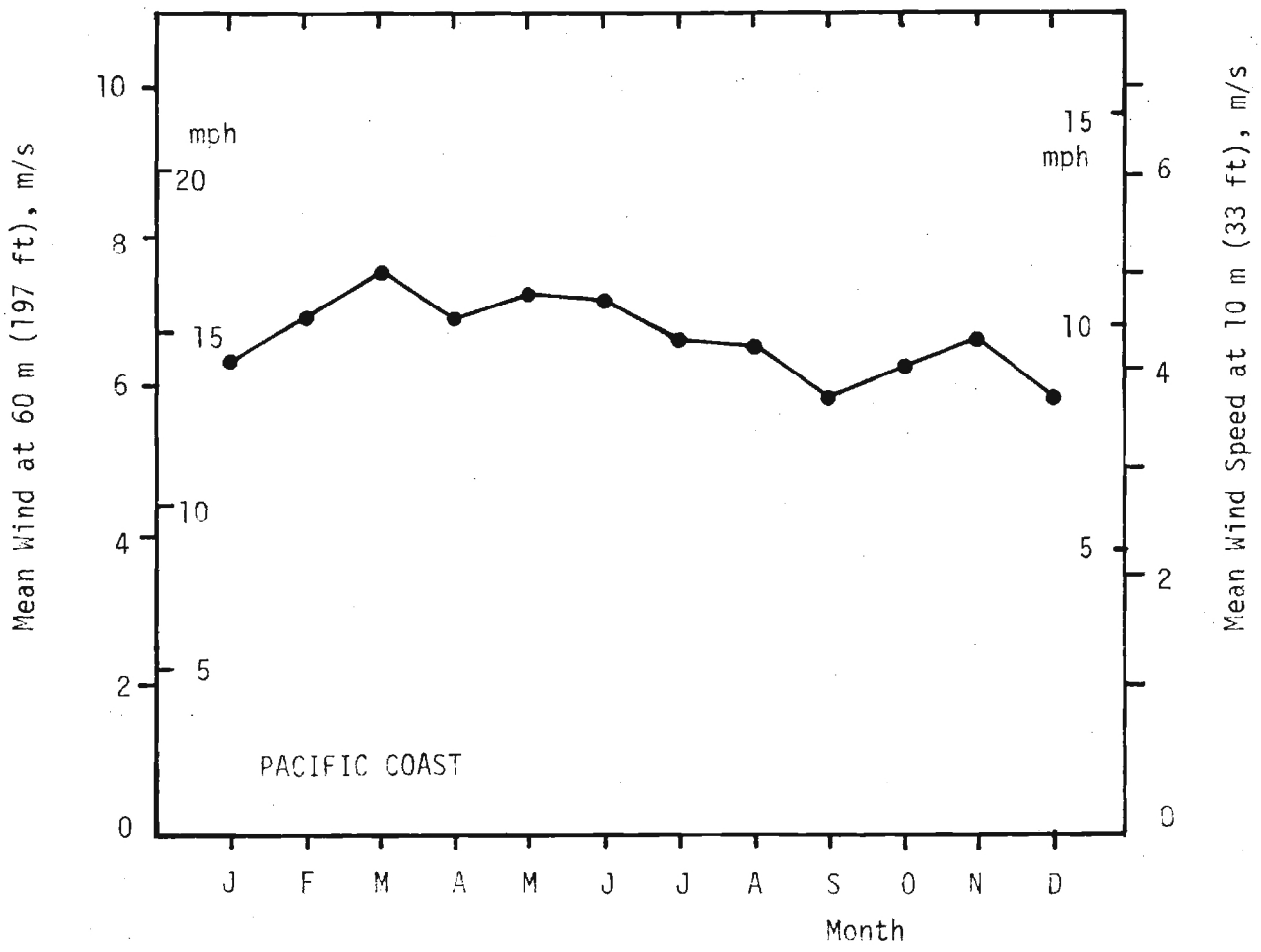

Figure 4. Mean Winds Annual Variation for the Pacific Coast Region.

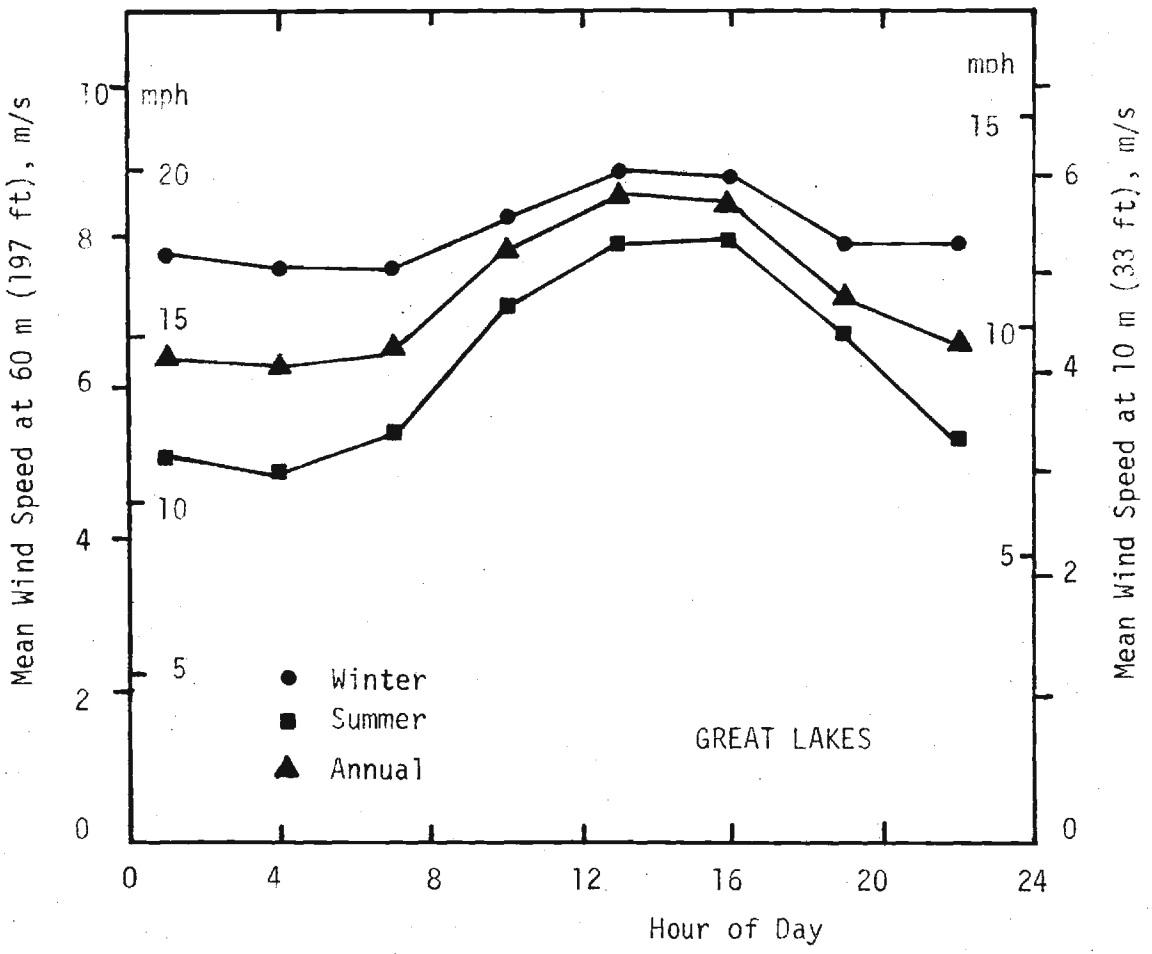

Figure 5. Diurnal Variation of Mean Wind by Season for the Great Lakes Region.

Table 6

Seasonal and Diurnal Variations of 60 m (197 ft) Hub Height Mean Wind Speed (m/s) for the Great Lakes Array.

Season \ Hour	1	4	7	10	13	16	19	22	Avg
Winter	7.8	7.6	7.6	8.3	8.9	8.8	7.9	7.9	8.1
Spring	6.7	6.6	6.9	8.6	9.2	9.2	7.9	6.9	7.7
Summer	5.1	4.9	5.4	7.1	7.9	8.0	6.7	5.3	6.3
Fall	6.2	6.0	6.1	7.7	8.4	8.2	6.5	6.4	6.9
Annual	6.4	6.3	6.5	7.9	8.6	8.5	7.2	6.6	7.3

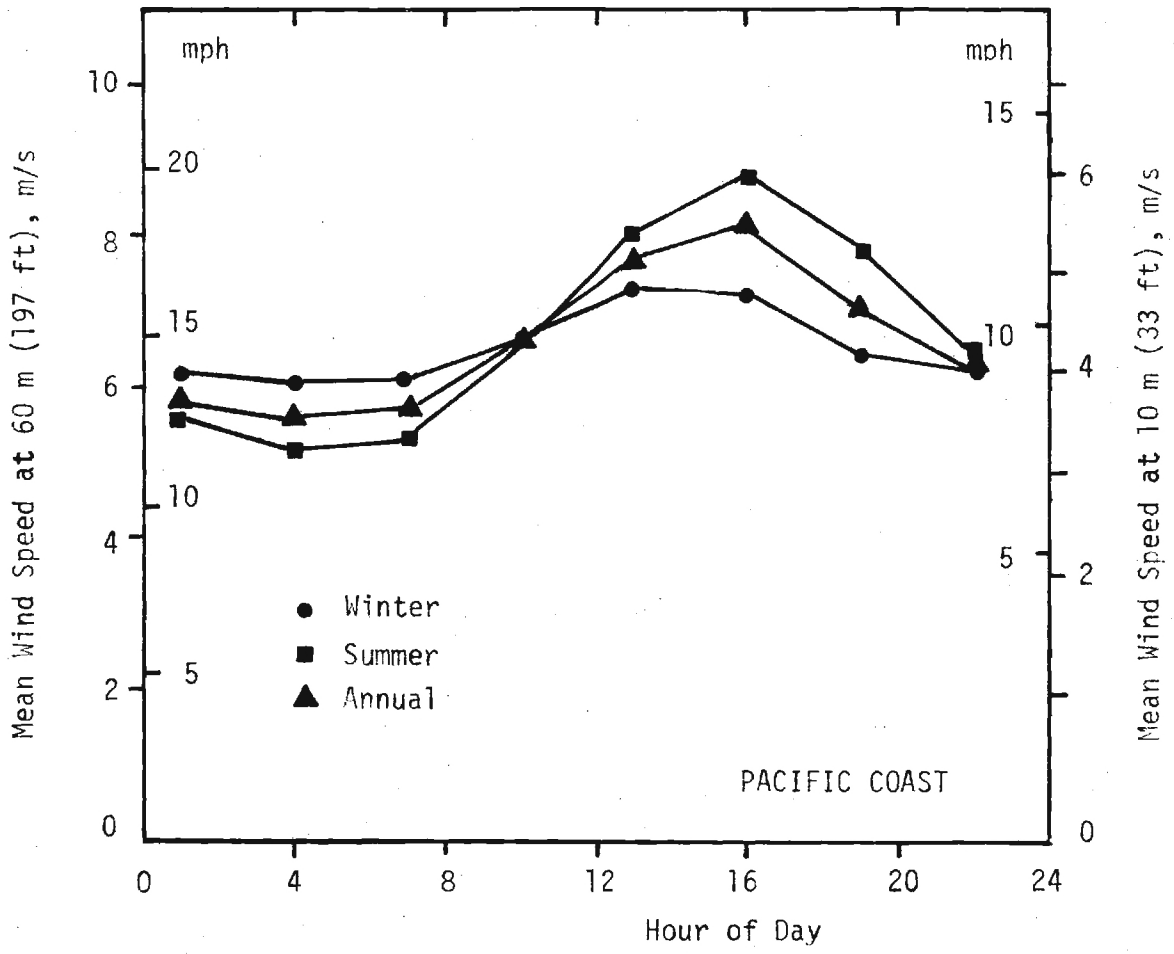

Figure 6. Diurnal Variation of Mean Wind by Season for the Pacific Coast Region.

Table 7

Seasonal and Diurnal Variations of 60 m (197 ft) Hub Height Mean Wind Speed (m/s) for Pacific Array

Season \ Hour	1	4	7	10	13	16	19	22	Avg
Winter	6.2	6.1	6.1	6.6	7.3	7.2	6.4	6.2	6.5
Spring	6.0	5.9	6.0	7.2	8.2	8.7	7.5	6.5	7.0
Summer	5.6	5.2	5.3	6.5	8.0	8.8	7.8	6.3	6.7
Fall	5.4	5.3	5.3	6.2	7.3	7.5	6.2	5.7	6.1
Annual	5.8	5.6	5.7	6.6	7.7	8.1	7.0	6.2	6.6

3. WIND SPEED CORRELATIONS

Time Autocorrelation

Time autocorrelation functions for the Great Lakes array (Figure 7) and the Pacific Coast array (Figure 8) show strong diurnal effects in the summer season. During the winter season the Pacific Coast array has slight diurnal influence and the Great Lakes influence is about nil. This is in agreement with the diurnal variation seen in Figure 5 and Figure 6, and with the time autocorrelation results obtained earlier for the New England and Central U.S. Regions. As in the earlier studies, the time autocorrelation is of departures of one minute average wind speeds from the monthly mean speed for the site. Results of Figures 7 and 8 are averaged over all sites in the respective arrays. Large values ($\rho \geq 0.5$) of the time autocorrelation for the 3 hour lag are an indication that, for most purposes, the 8 observations per day give adequate time resolution.

Spatial Cross Correlation

Spatial cross correlation of the one minute mean wind speed departures from the monthly mean was computed as a function of inter-site separation by the same method as in the earlier array study. Figure 9 (Great Lakes area) and Figure 10 (Pacific Coast area) show these results for the winter and summer seasons. All correlation values were averaged together by intervals of 50 km in separation (i.e. all 0 - 50 km separations averaged, all 50 - 100 km separations averaged, etc.). For the Great Lakes the number of site-pairs in the 0 - 50 km separation interval is 30, with 225 in the 50 - 100 km interval and 390 in the 100 - 150 km interval. The number then varies between 84 and 15 out to the 900 - 950 km interval. The 950 - 1000 km interval has 15 site-pairs included.

Figure 9 shows correlation values for the Great Lakes starting well below one and decreasing gradually. There are not any zero or negative correlations out to 850 km separation distance. Winter cross correlation values are higher

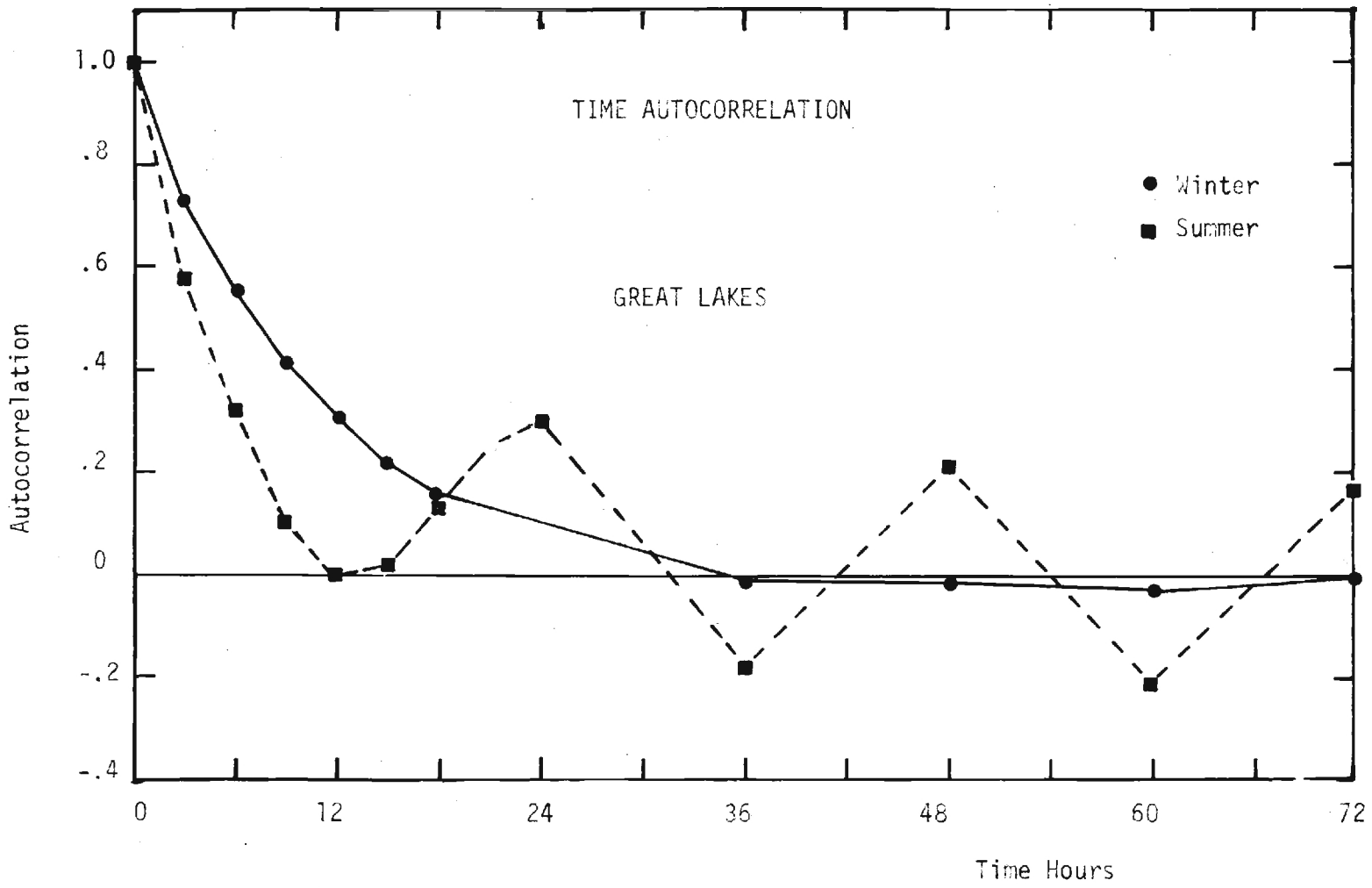

Figure 7. Time Autocorrelation of Wind Speed for the Great Lakes Region.

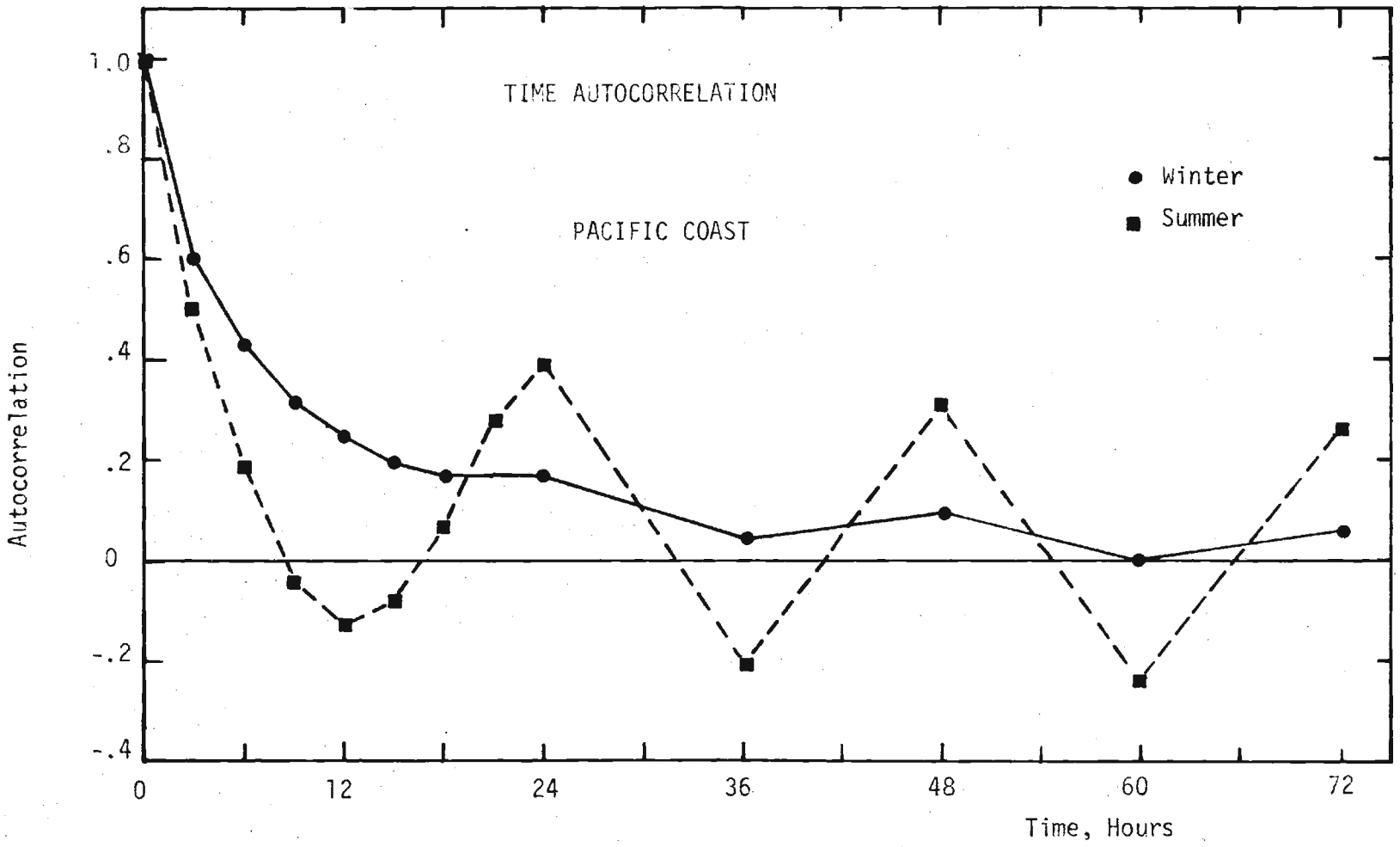

Figure 8. Time Autocorrelation of Wind Speed for the Pacific Coast Region.

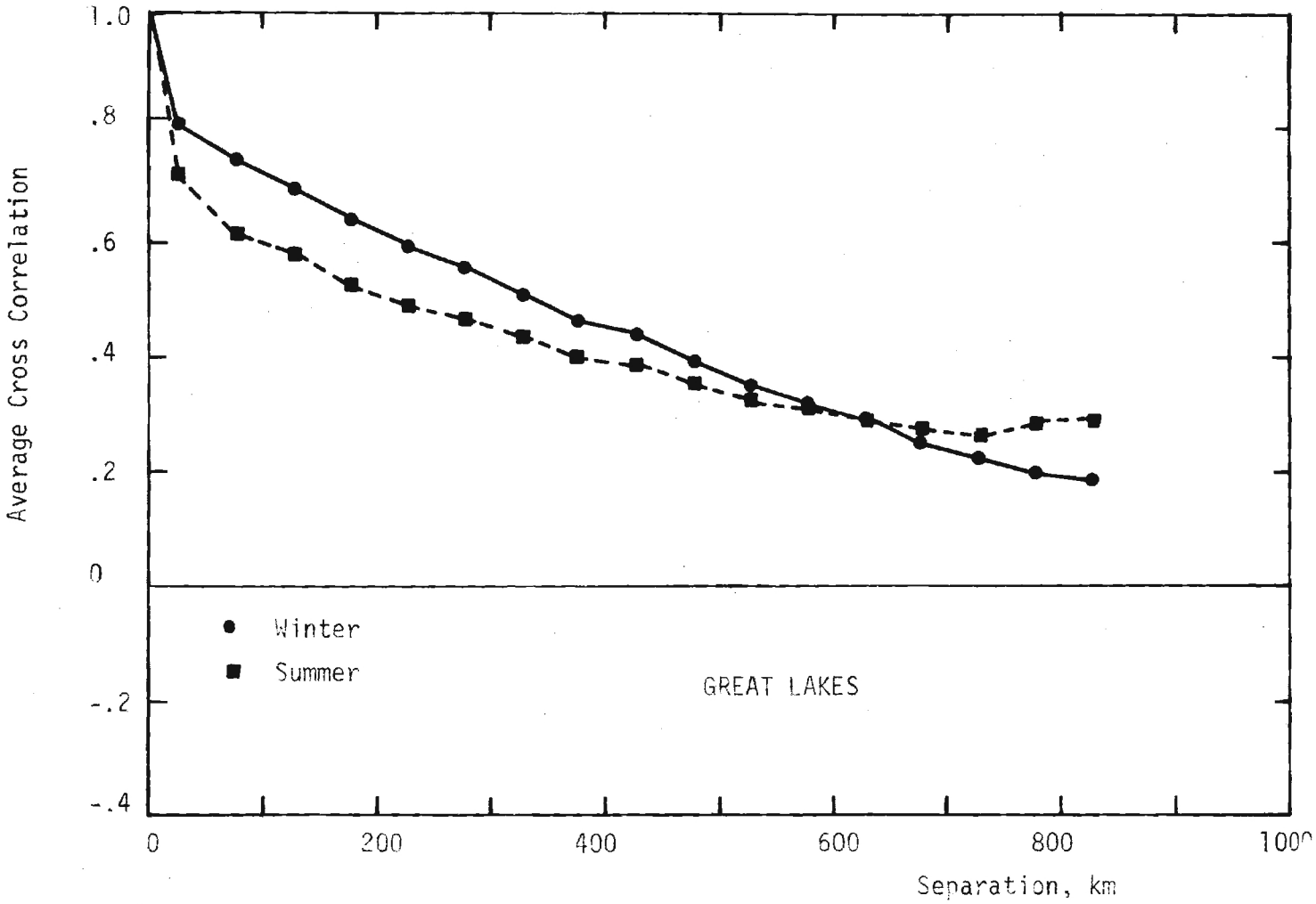

Figure 9. Average Spatial Cross Correlation Versus Separation for the Great Lakes Region.

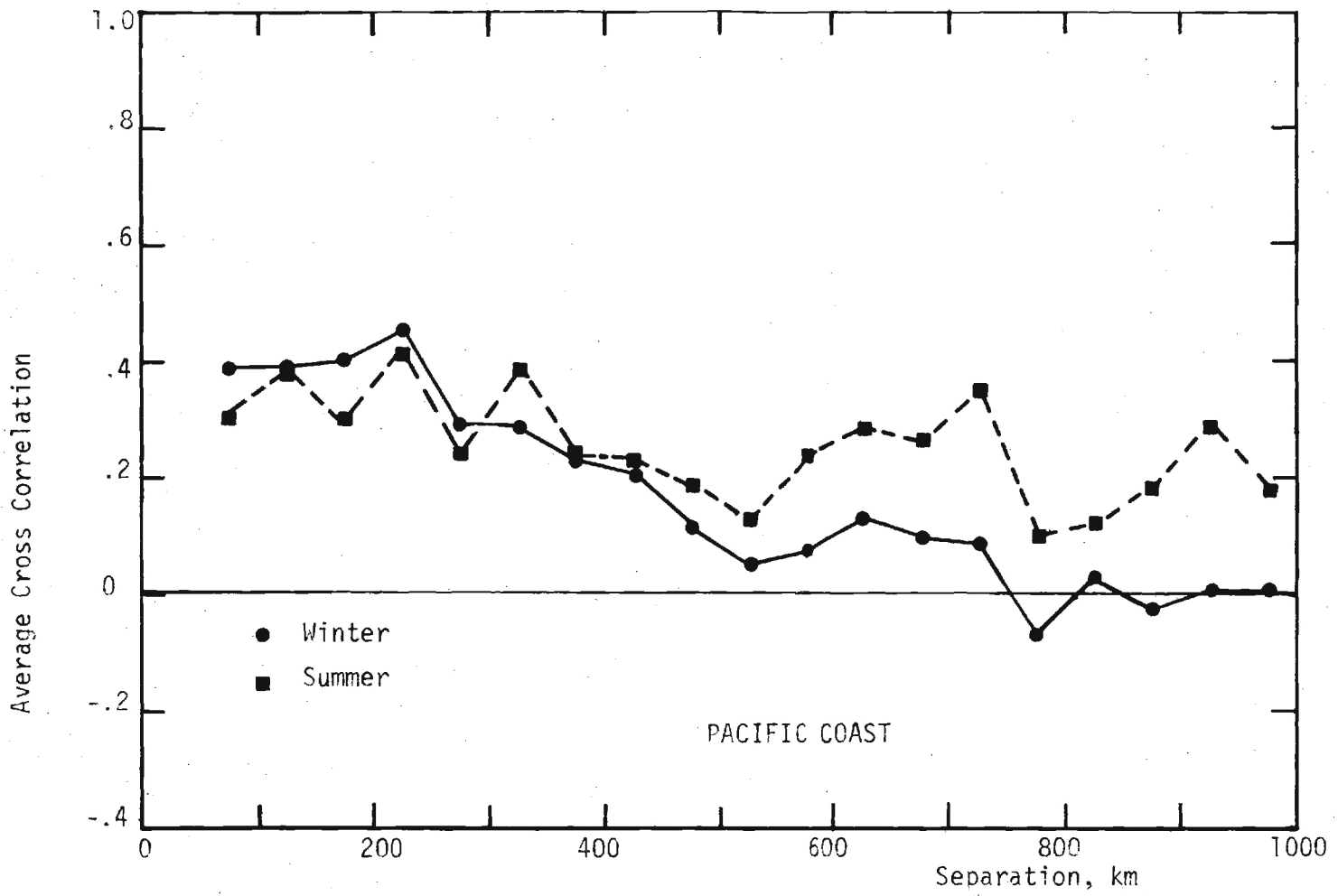

Figure 10. Average Spatial Cross Correlation Versus Separation for the Pacific Coast Region.

than summer values out to a separation distance of approximately 650 km. From 650 - 850 km the summer correlation values are greater than winter.

The Pacific Coast correlation values (Figure 10) are unusual. The values are less than .45 at all separation distances and show very sporadic behavior. The winter values are near-zero or less than zero for separations greater than 750 km. The summer values remain positive and can even have relatively large correlations at large distances (.35 at 750 km separation compared with .40 at 250 km separation). Summer behavior is very sporadic.

At this time the unusual behavior of the Pacific Coast correlations can only be explained as terrain influence. Many Pacific Coast sites are located in valleys or on mountains where the wind flow could be easily affected by the terrain.

The average effective cross correlation for an array is found by averaging over all the individual site-pair cross correlations, regardless of separation. Figure 11 shows these values for both areas of study. The Pacific Coast correlations are very low. Both areas exhibit considerable seasonal variation. The Pacific Coast has a maximum correlation in July and a minimum in December, while the Great Lakes has a maximum in January and a minimum in August. The phase of the Great Lakes seasonal variation of average correlation corresponds to the phase of seasonal variation of mean wind speed. Low wind speeds have low correlation and high wind speeds have high correlation. The Pacific Coast area is generally the reverse of this, i.e. high mean wind speeds have low correlation values and low wind speeds have higher correlation values.

The array average correlation $\bar{\rho}$ and the number of sites in the array are the two main parameters affecting the array power distribution differences from single site distributions. See Appendix B for the application of $\bar{\rho}$ in the modeling of arrays. For taking advantage of the array diversity, low correlation values are desirable.

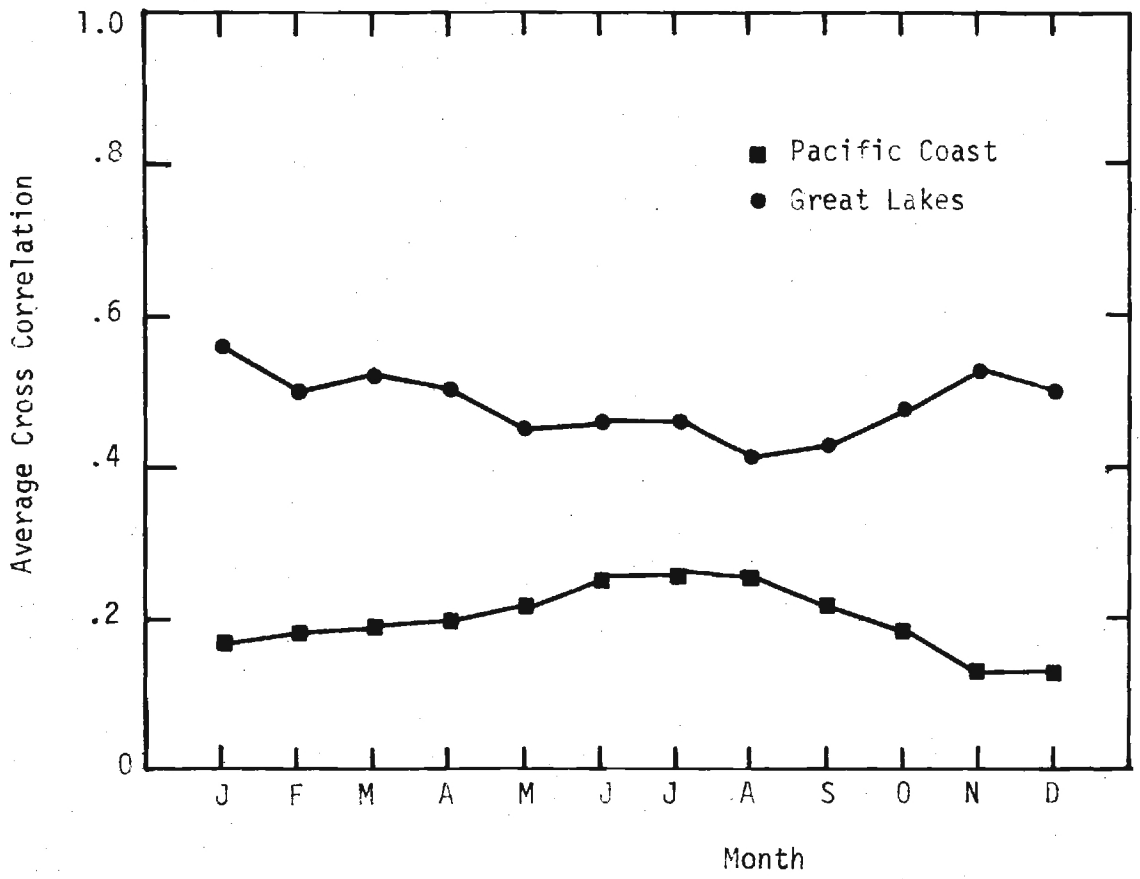

Figure 11. Array Average Spatial Cross Correlation for Both Regions, by Month.

Degree Days/Wind Speed Correlation

Figures 12 and 13 show mean daily hub height wind speeds versus degree days (mean daily temperature relative to 18° C(65° F)) for summer and winter. There seems to be no consistent trend over the seasons or between sites, based on these diurnal average data. It is well known that in many utility service areas a portion of the total demand is correlated with heating or cooling degree days. The results of Figures 12 and 13 would imply no relationship between wind speed and wind power availability and demand, at least as related to temperature statistics. Hourly data for which wind speed and utility demand data were correlated separately for each hour of the day (and separately for each season) also confirmed no significant wind speed/demand correlations (this was done as part of a separate study by JBF-NEGEA-Georgia Tech on evaluation of cost effectiveness of WECS for electric utilities, and not reported in detail here, but will be presented in the final report of that project).

Neither of the above results negates the fact that wind speed and utility demand are related on a diurnal cycle (because each of these has its own diurnal variation). This fact is illustrated by Figures 14 and 15 which are linear regressions of mean wind versus temperature for the Great Lakes Region (from Decennial Summary Data). The apparent relationship between wind and temperature in Figures 14 and 15 is due in fact to the diurnal cycle of both wind and temperature, which remain to influence the data when all hours are combined, i.e. both low winds and low temperatures occur at night and high winds and high temperatures occur during the daytime. In contrast the results of Figures 12 and 13 show no dependence of daily average winds on daily average temperature, and the separate hourly study for the JBF-NEGEA-Georgia Tech project indicates no dependence of hourly wind speed on hourly temperature when data are referenced to expected values for the hour (rather than to daily mean).

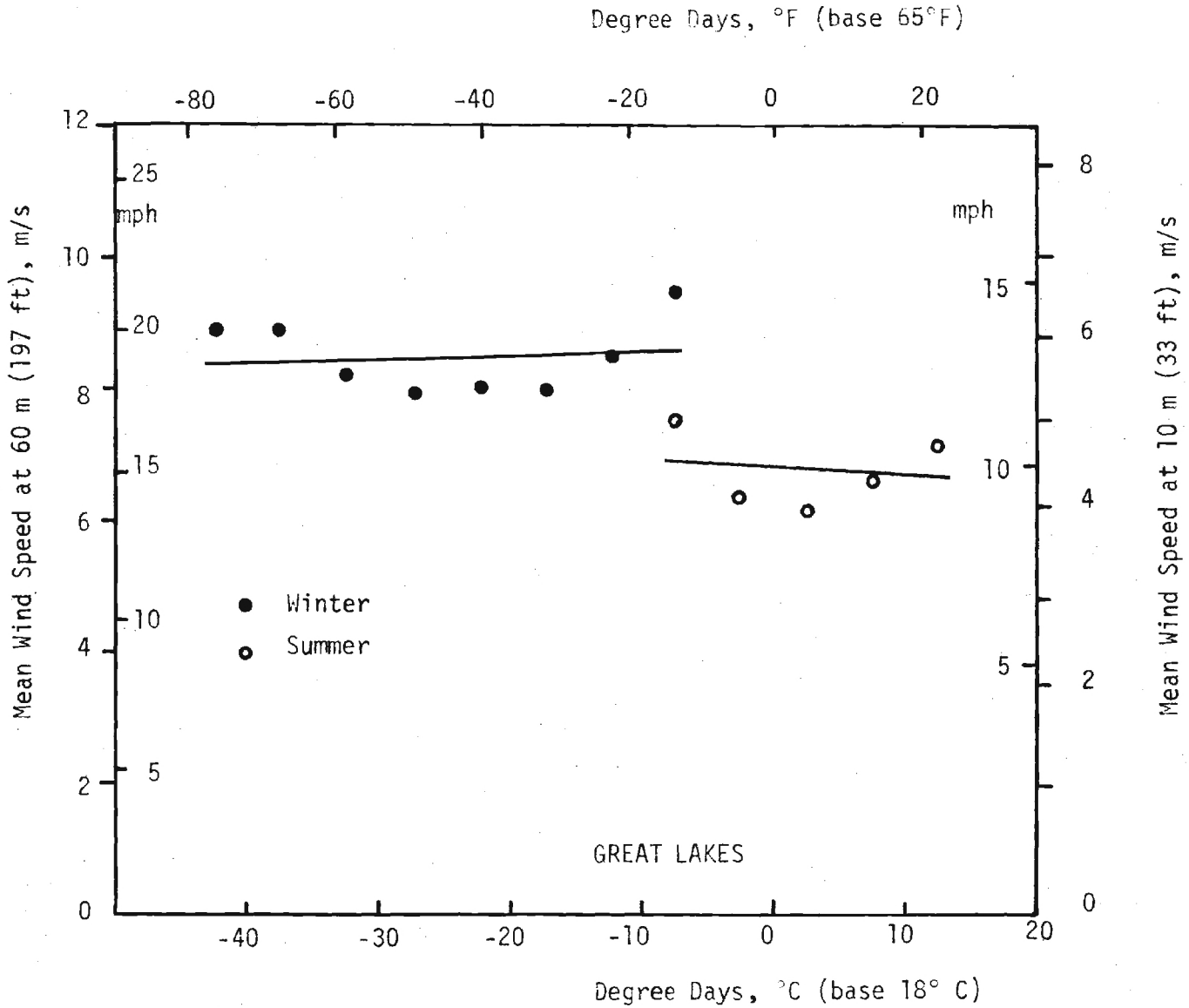

Figure 12. Regression of Mean Wind Speed Versus Degree Days for the Great Lakes Region.

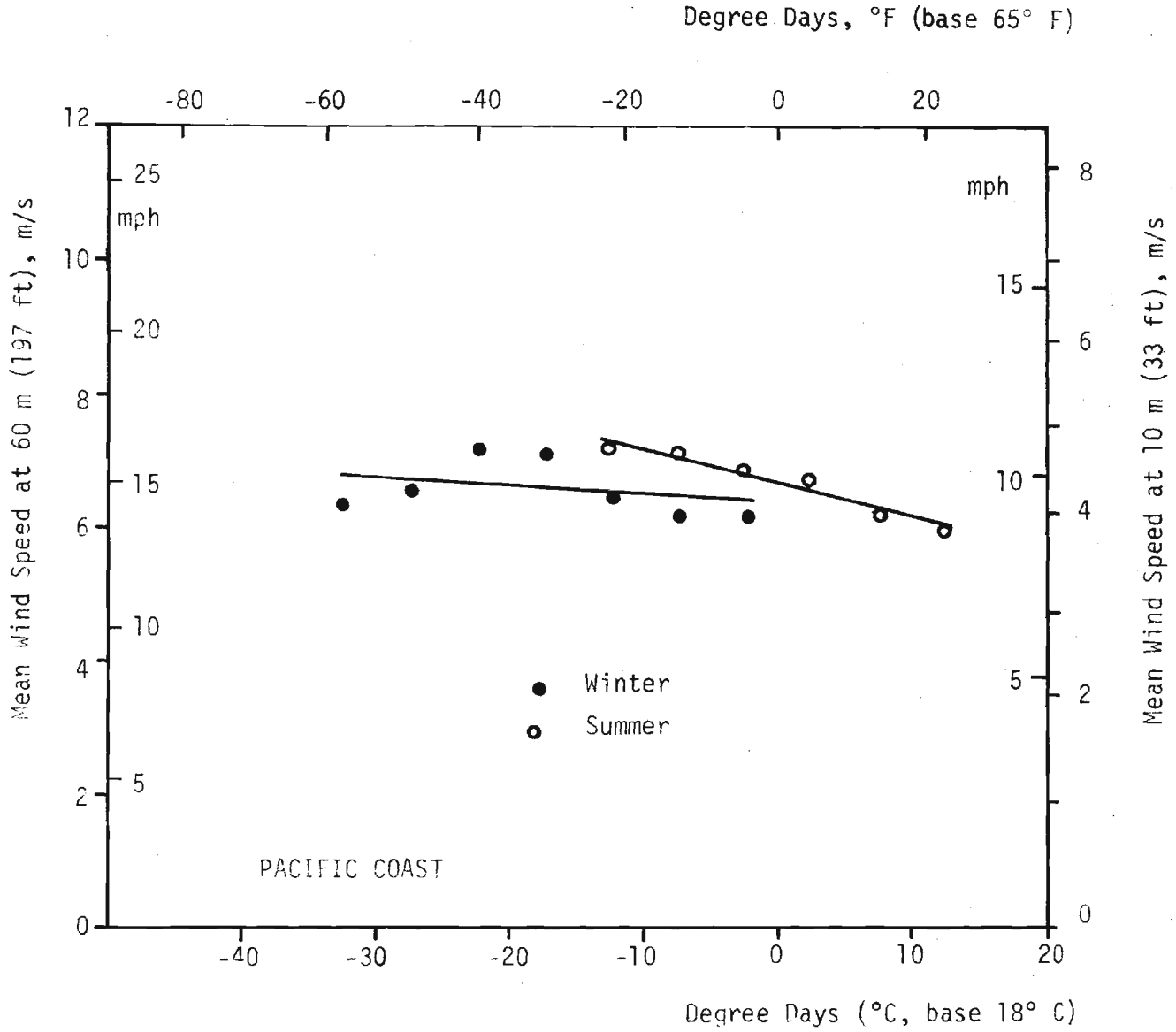

Figure 13. As in Figure 12 for the Pacific Coast.

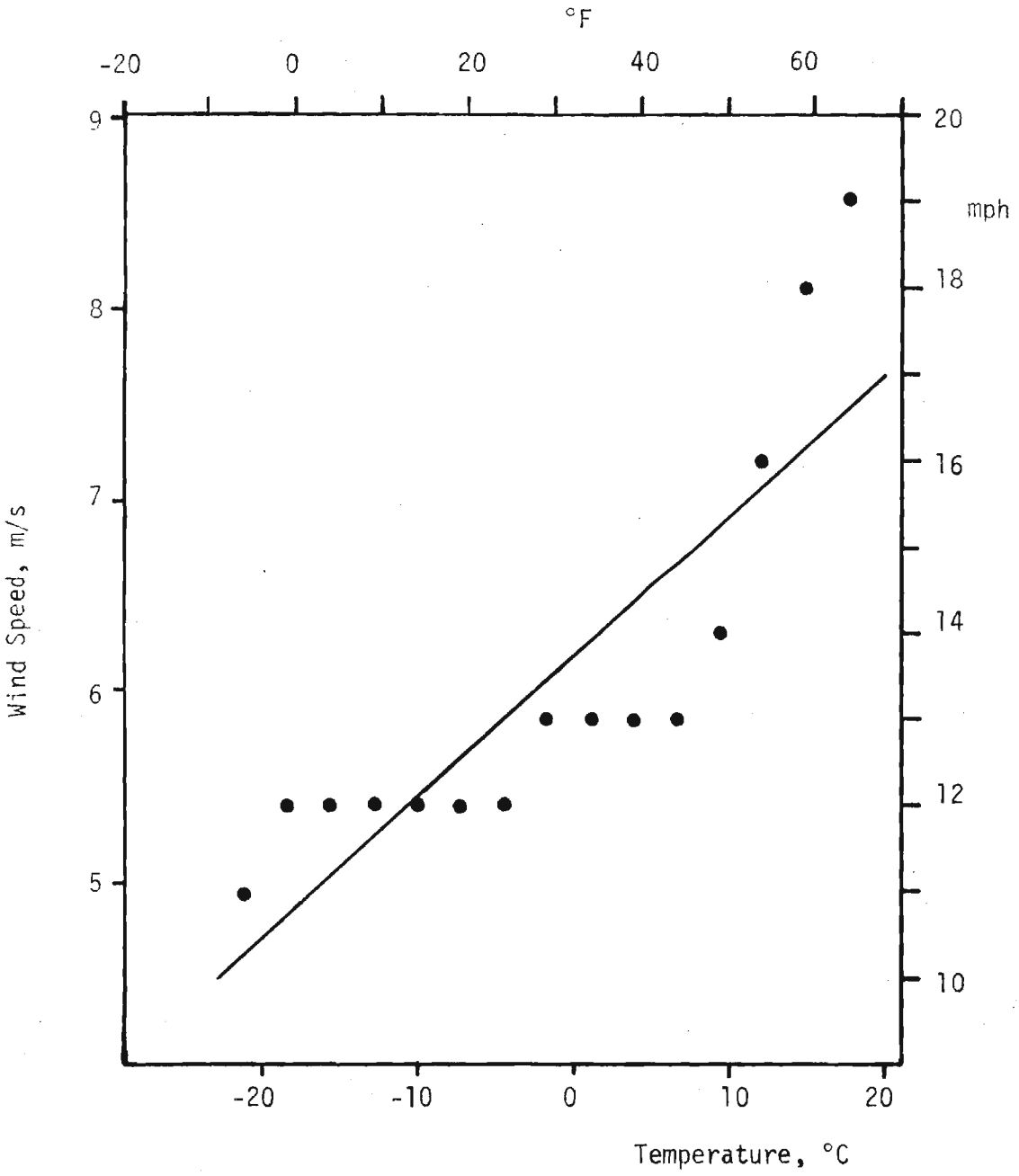

Figure 14. Linear Regression of Hourly Wind Speed and Hourly Temperature for the Great Lakes Region (from Decennial Summary Data) for Winter.

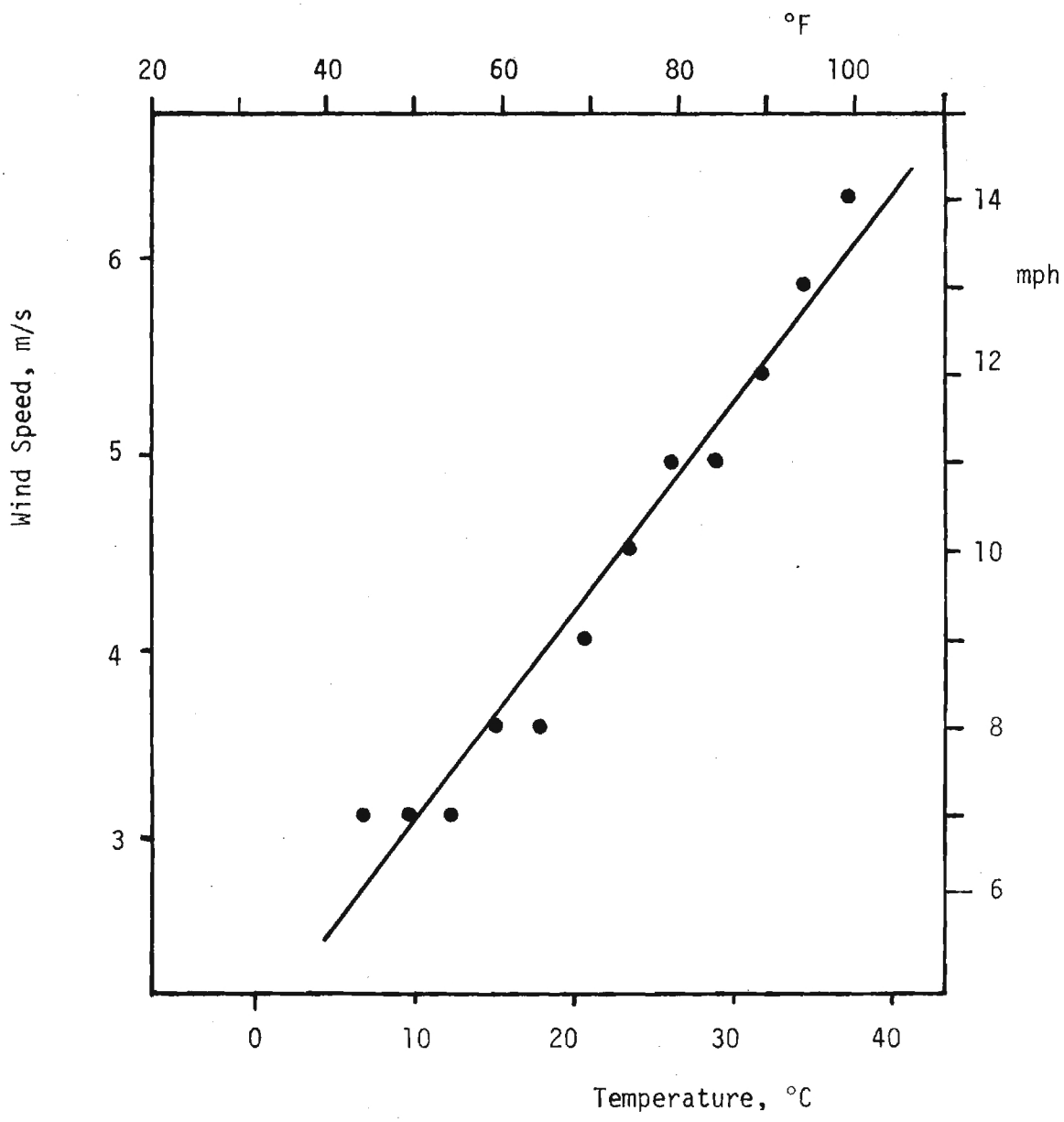

Figure 15. As in Figure 14 for Summer.

4. MEAN OUTPUT WIND POWER

One minute average winds, adjusted to 60 m (197 ft) hub height, were used in power output curves (see Appendix A) to compute instantaneous output power from three different designs of wind turbines: with rated powers of 500, 1500, and 2000 kW. Output power from these wind turbines was averaged over one month intervals and corresponding months over 5 years (1971 - 1975) were averaged to yield monthly mean power output. (See Figures 16 and 17). Output power was also averaged over seasons by time of day for each wind turbine and for both areas of study. Figures and tables of these results are presented in Appendix C.

Figures 16 and Figure 17 show that the monthly variations in mean output power follow in phase with the monthly variations in the mean wind. The 2000 MW (2 MW) turbine has the greatest power variation over the year. But if power variation is expressed as a percent of rated power, the 2 MW and the 500 kW turbines compare favorably. In the Great Lakes area, the 2 MW turbine varies from a maximum output power level of 1051.5 kW, 53% of rated, to a minimum of 429.5 kW, 21% of rated. The 500 kW unit varies from a maximum of 317.7 kW, 64% of rated, to a minimum of 157.8 kW, 32% of rated. The 1.5 MW turbine produces a maximum of 489 kW, 24% of rated, and a minimum of 131.5 kW, 9% of rated. The cut-in and rated speeds of the 1.5 MW unit are the largest of the three turbines, which is the reason it doesn't compare favorably with the other two units in terms of power output or in variation magnitude.

The same effect is noticed in the diurnal variation of output power shown in Appendix C. For example, in the Great Lakes array, for the summer season (Figure C-1), which has the largest variation, the minimum output power for the 500 kW turbine is 98 kW, 20% of rated, and the maximum is 288 kW, 58%

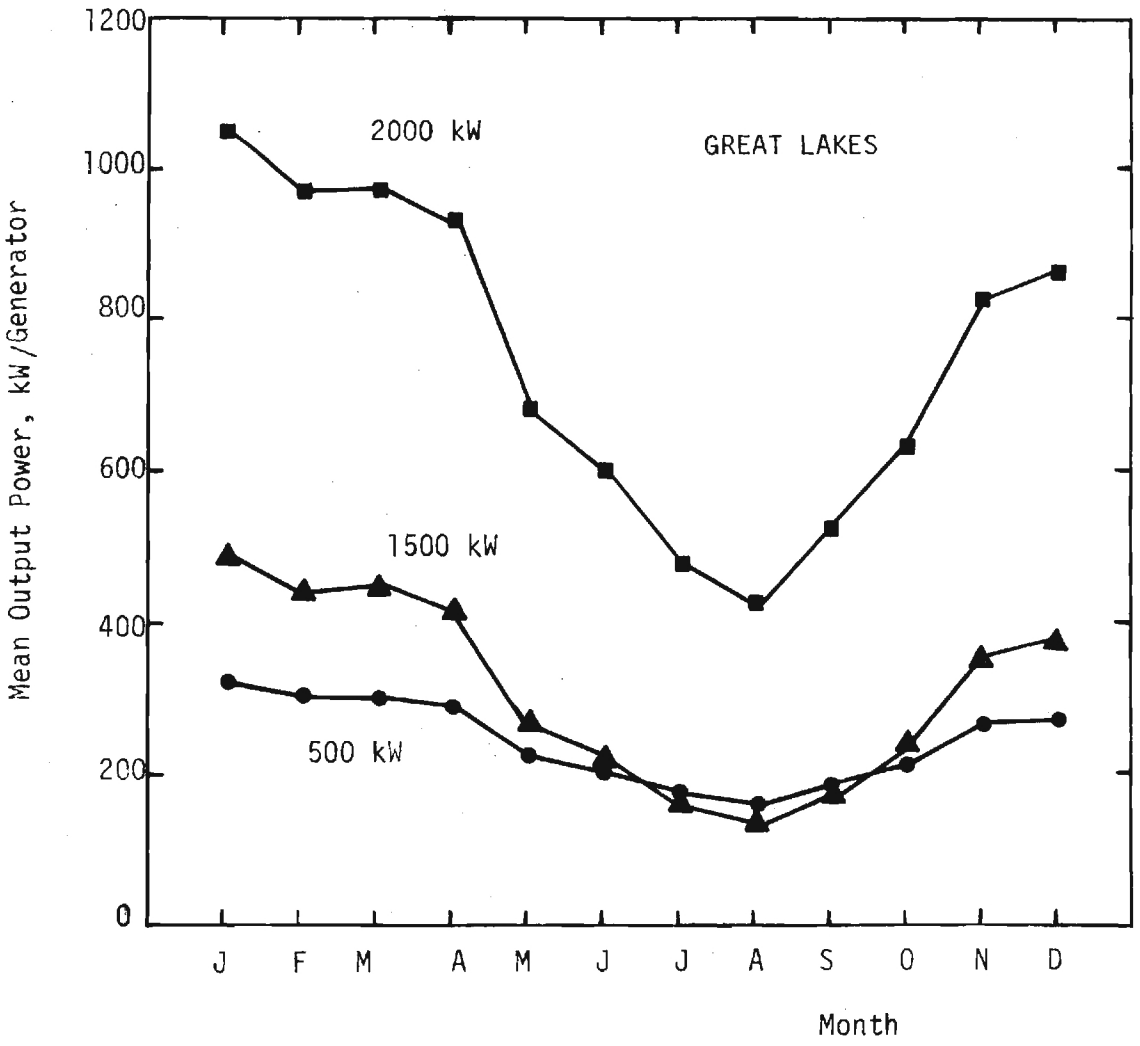

Figure 16. Monthly Mean Output Power of the Three WECS Studied - Great Lakes Region.

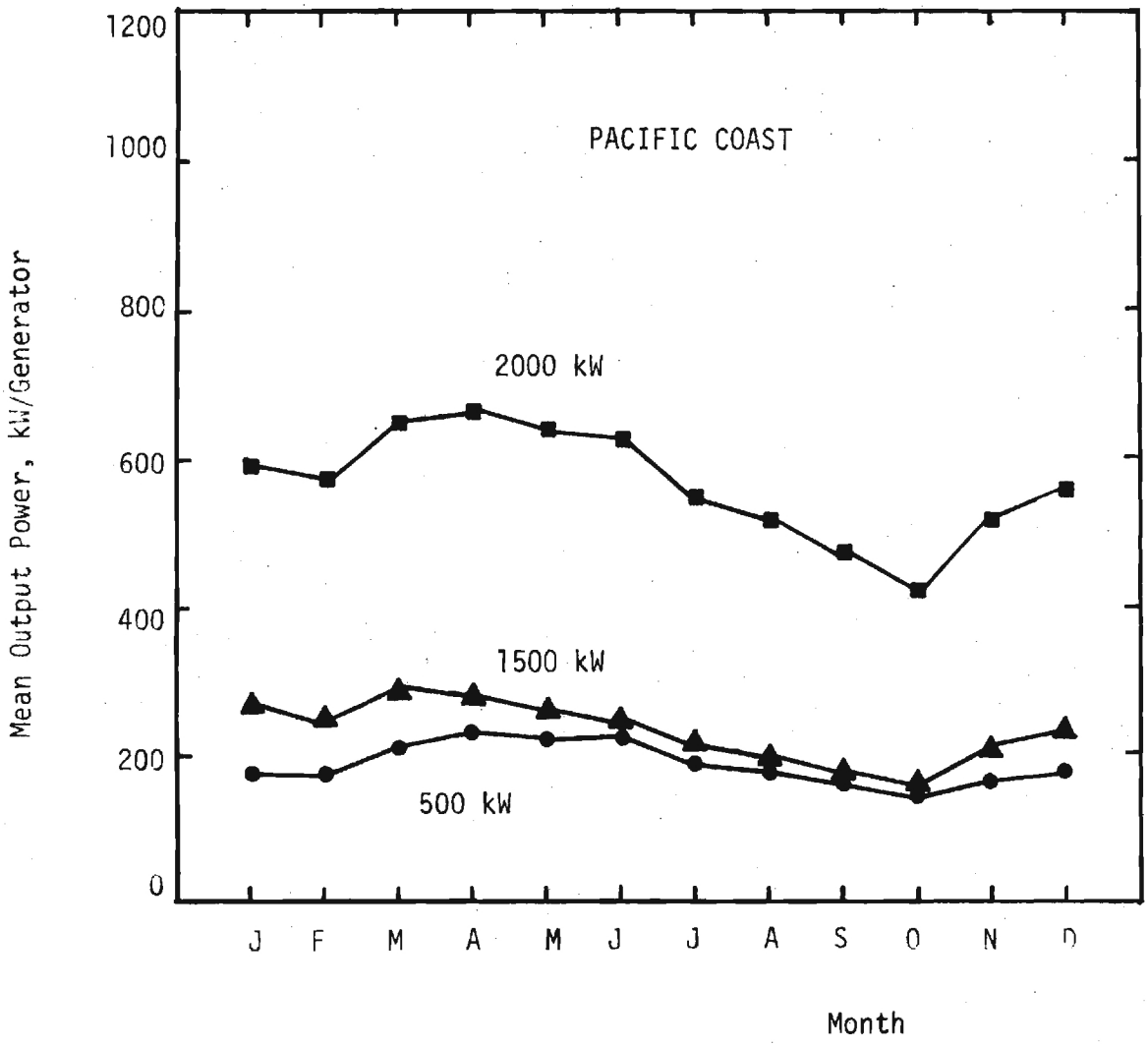

Figure 17. Monthly Mean Output Power for the Three WECS Studied - Pacific Coast Region.

of rated. The 2 MW unit produces a minimum power of 249 kW, 12% of rated and a maximum of 875 kW, 44% of rated. The minimum value of the Mod 1 is 73 kW, 5% of rated and the maximum values is 331 kW, 22% of rated. Again this difference is due to the higher cut-in and rated speed of the 1500 kW unit.

Notice that in the Pacific Coast array (Figures C-4 through C-6), the summer maximum occurs at 1600 hours and is greater than the winter maximum. This could be of significance in reducing the summer air conditioning load.

The major parameter influencing mean output power from an array is the ratio of mean array wind speed $\bar{V}$ to WECS rated speed V_r. Provided $\bar{V}/V_r$ is in the range $0.4 \leq \bar{V}/V_r \leq 1$, a simple linear relationship $\bar{P}/P_r = a + b\,(\bar{V}/V_r)$ may be used to estimate mean power per generator relative to rated power P_r for the WECS units in the array [compare equation (B-10)]. The coefficients a and b depend slightly on the wind speed distribution, on machine design parameters (power coefficient versus wind speed), and on the hub height. Outside the range $0.4 \leq \bar{V}/V_r \leq 1$, the linear relationship must be expanded to include parabolic or cubic terms in $\bar{V}/V_r$. Details of mean power output coefficents and their dependence on wind and machine parameters are currently under investigation and will be presented in later reports.

5. WIND POWER FREQUENCY (AVAILABILITY WITHOUT STORAGE)

Frequency distributions of individual site output power were evaluated by direct "counting up" within power intervals of observed single site powers $P(V_i)$ for each time i, where $P(V_i)$ is the wind turbine output power as a function of the observed wind speed V_i (adjusted to hub height). Frequency distributions of array power were similarly evaluated for array power in the various power intervals, where at each time i, the array power $\bar{P}_i$ was evaluated by summing over the n individual sites in the array.

$$\bar{P}_i = \sum_{j=1}^{n} P_j(V_i) \qquad (1)$$

Figures 18 - 21 show single site observed array and array model (Appendix B) power output frequency distributions for the summer and winter seasons for the 2000 kW turbine. Figures 22 - 25 present the same data in non-cumulative form.

The cumulative probabilities (Figures 18 - 21) best show the effects of array influence on power availability, while the non-cumulative presentations (Figures 22-25) best show the physical differences between single site and array power distributions. As shown in Figures 22 - 25, the array power distributions have significantly lower probabilities of zero power (i.e. all array units below cut-in) or full rated power (i.e. all array units at or above rated speed). Conversely the array has significantly higher probabilities of power levels at or near the average output power (i.e. the diversity of wind across the array acts as a smoothing "filter" on the power output, de-emphasizing the extremes and enhancing the near-average power values).

The frequency distribution curves can be used to determine the improvement in power output availability which can be achieved by dispersing the wind turbines into arrays. For example, Figure 18 shows that for the 2000 kW turbine during winter, a power of 500 kW in the array is 73% available, while for

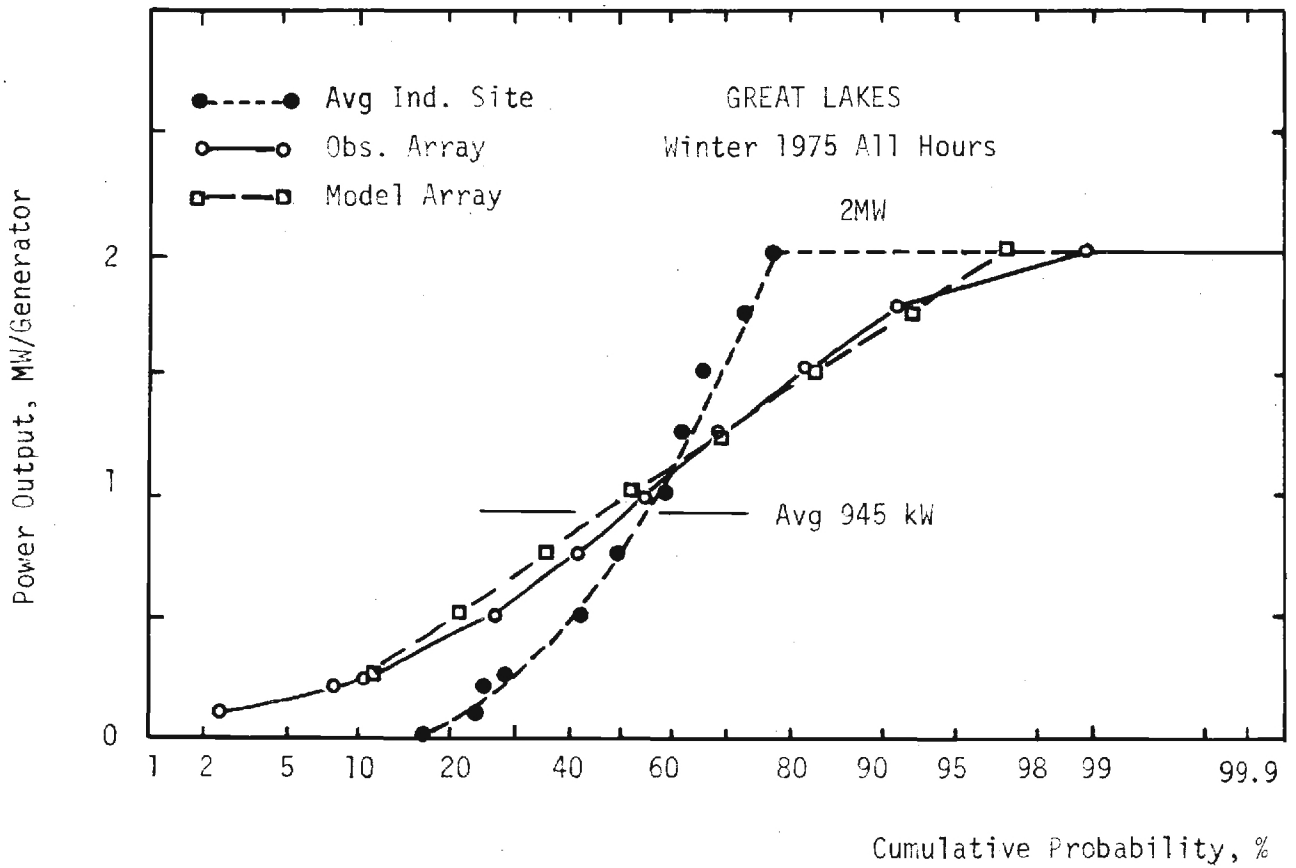

Figure 18. Cumulative Frequency of Various Power Output Levels for 2 MW WECS Individual Site, and Array Configuration for Great Lakes Winter 1975.

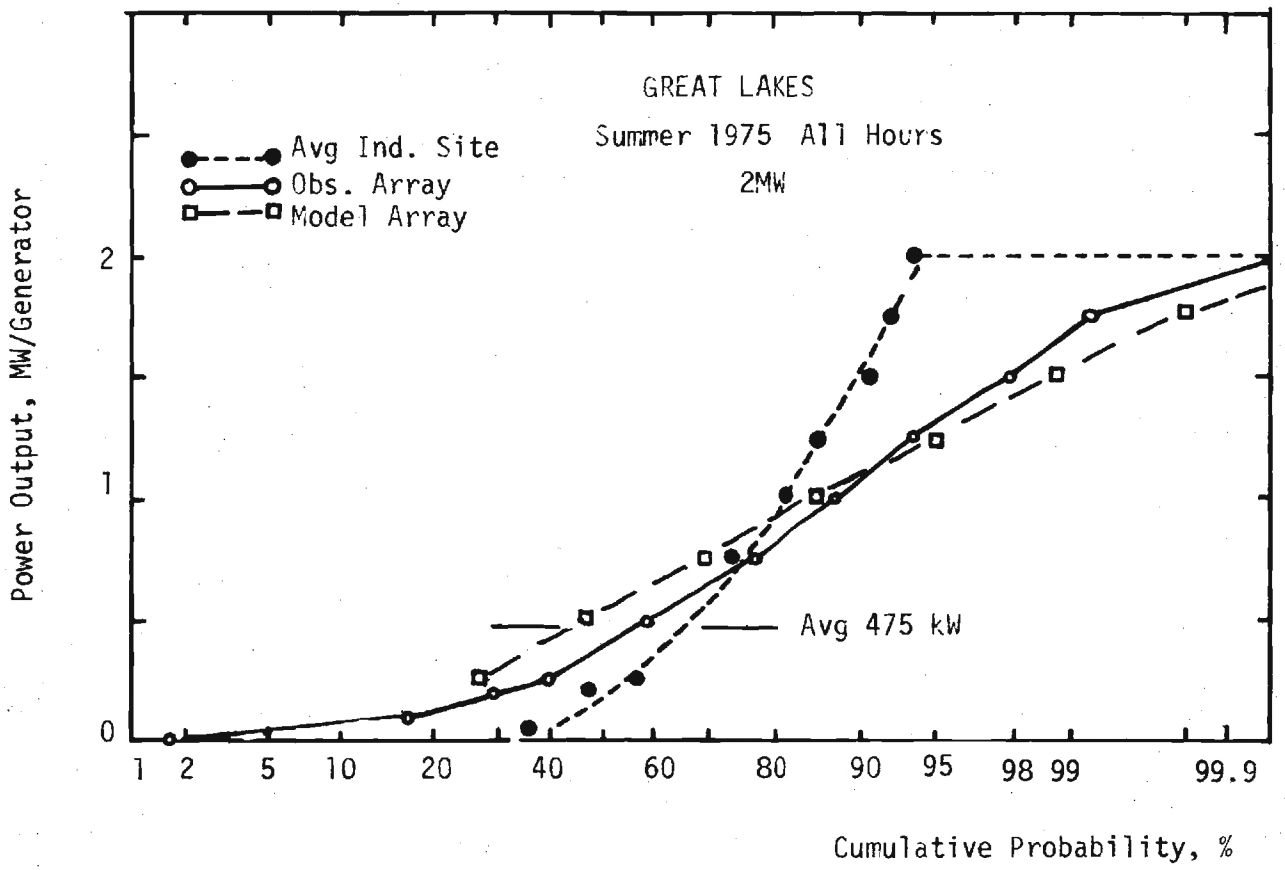

Figure 19. As in Figure 18 for Summer.

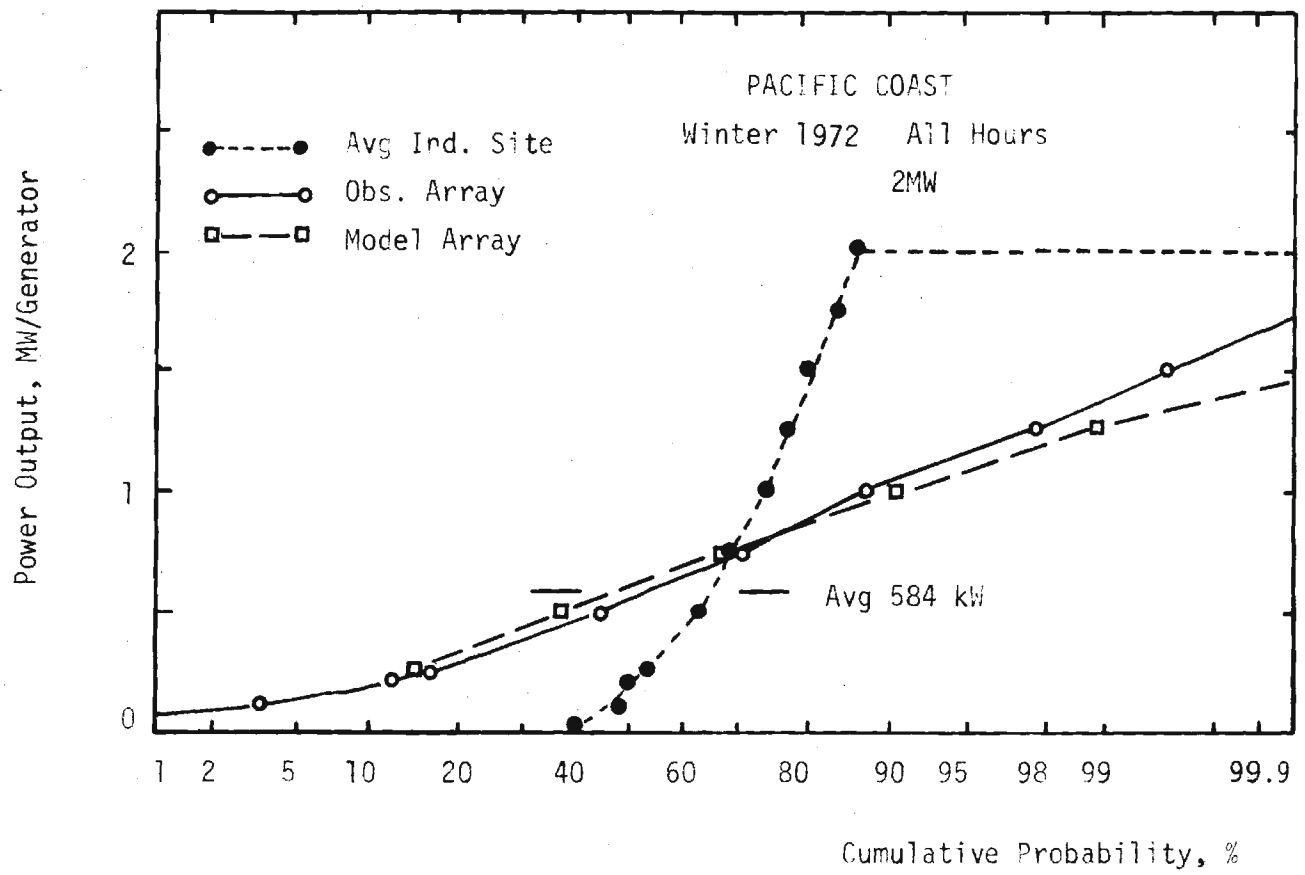

Figure 20. As in Figure 18 for Pacific Coast Winter.

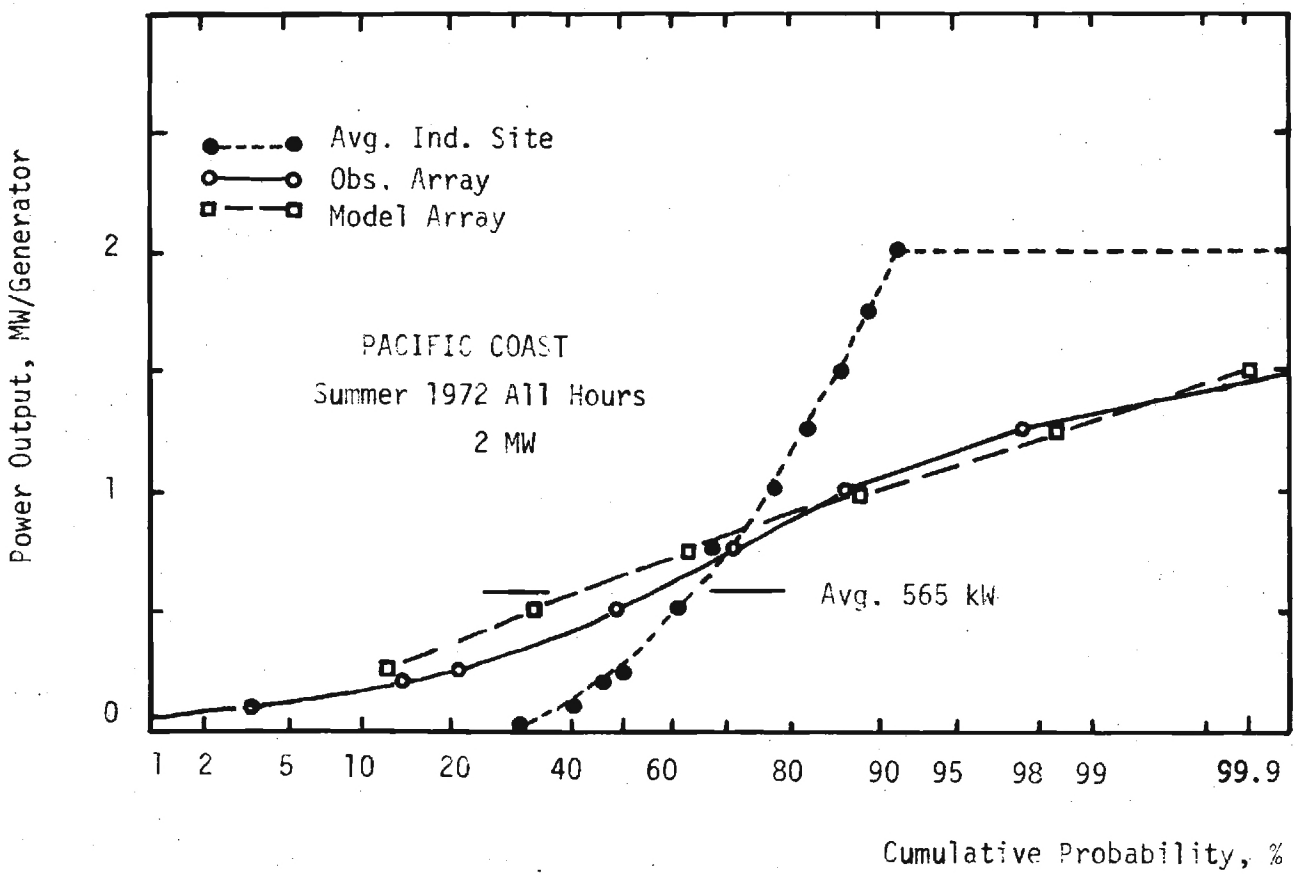

Figure 21. As in Figure 18 for Pacific Coast Summer.

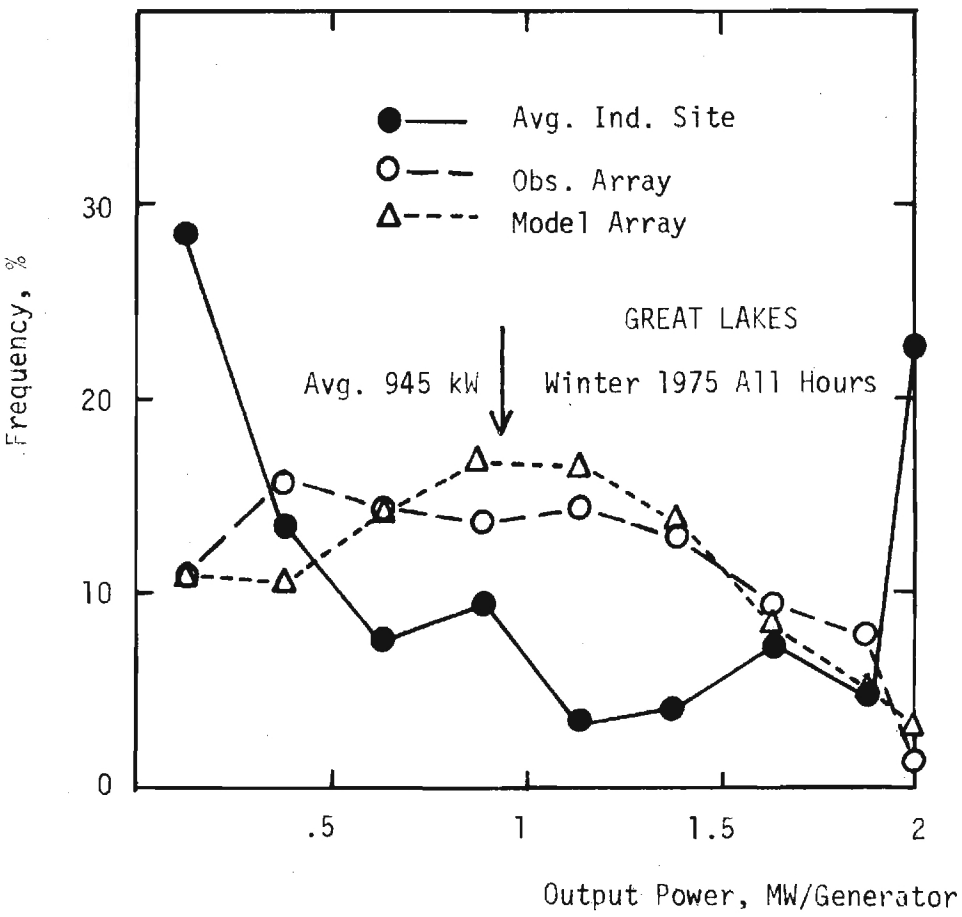

Figure 22. Frequency of Power Output for 2 MW WECS, Great Lakes, Winter 1975.

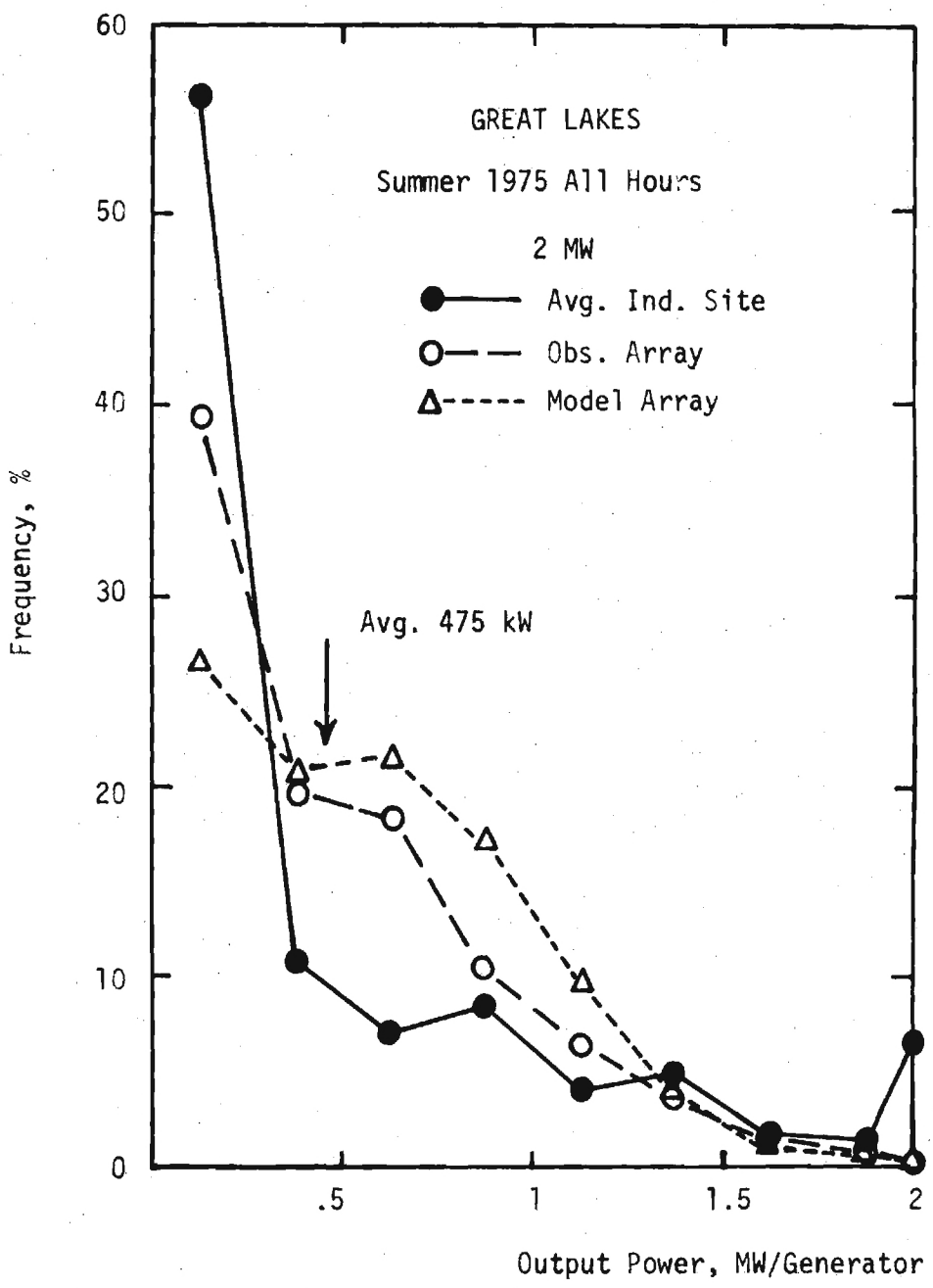

Figure 23. As in Figure 22 for Summer.

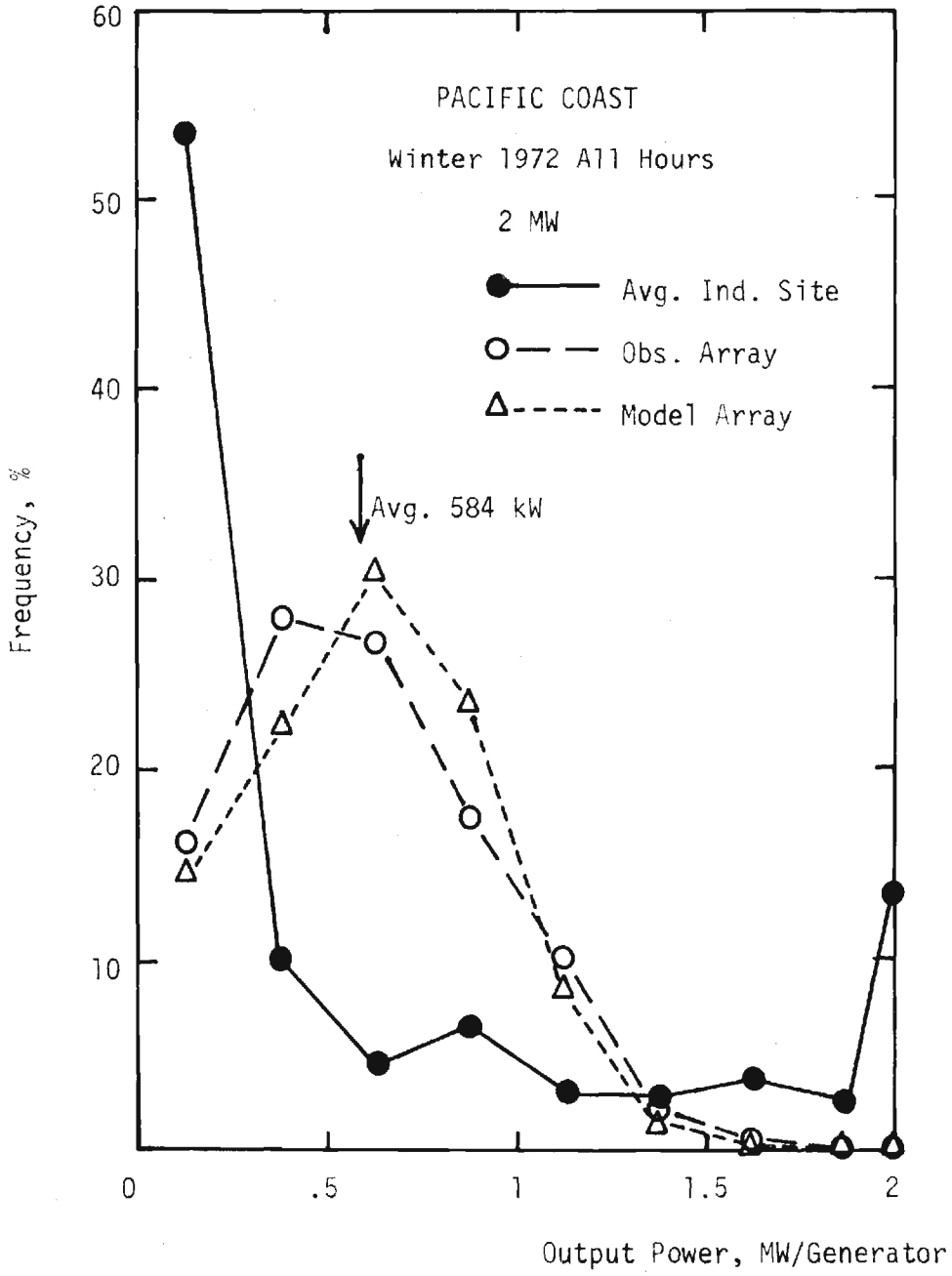

Figure 24. As in Figure 22 for Pacific Coast, Winter.

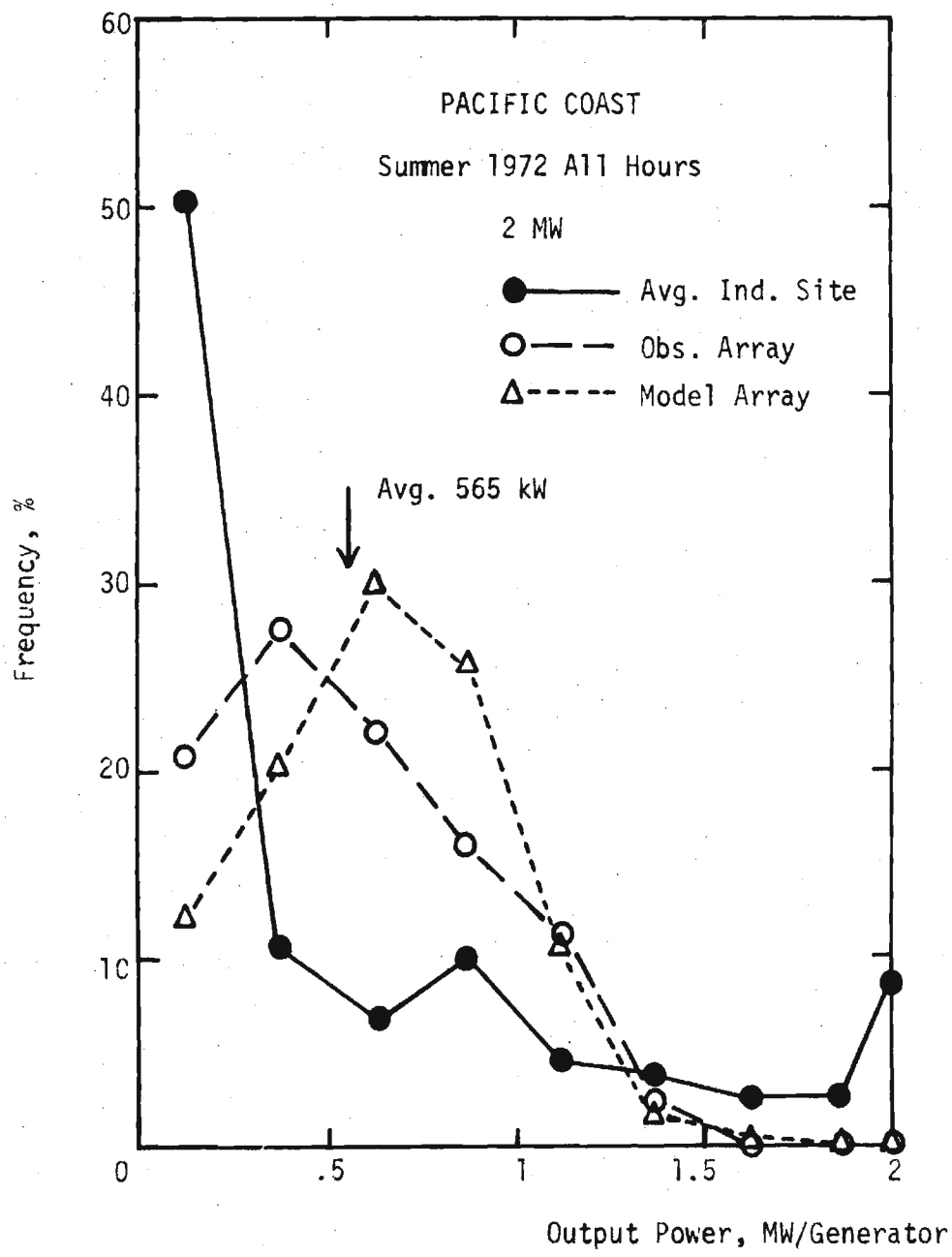

Figure 25. As in Figure 22 for Pacific Coast, Summer.

the single site it is 58% available. For an output power of 750 kW the array has 59% availability and the single site 51% availability. Similar results are seen in each of the figures.

Appendix D also show the availability of certain power levels for the two areas of study. A level of 100 kW is given for the 500 kW and the 1500 kW turbine in Tables D-1 and D-2 (Great Lakes) and Tables D-5 and D-6 (Pacific Coast). For the 2000 kW unit, levels of 200 kW and 500 kW are presented in Tables D-3 and D-4 (Great Lakes) and Tables D-7 and D-8 (Pacific Coast). These tables show that very significant increases in power availability (especially in the near peak load afternoon hours) are achievable with the array configurations studied.

The simulated array model based on individual site (or average site) statistics is seen to work reasonably well in describing actual array performance (Figures 18 - 21 and 22 - 25). Details of this array simulation model are given in Appendix B.

The wind power availability data presented in this chapter relate directly to the credited capacity achievable with WECS arrays without storage. A significant amount of capacity credit for WECS would allow capital cost displacement as well as fuel cost savings, hence would be an important factor in establishing cost effectiveness for the WECS. Since no power generating units, even conventional fossil fuel system, have 100% availability, the most logical method of assigning credited capacity is on the basis of system wide loss-of-load probability. Thus, WECS of a certain total rated power, added to a conventional mix of power generation, would receive capacity credit for that rated power amount of conventional units it could displace without lowering the total system loss-of-load probability. These would be complicated calculations, dependent on the details of reliabilities, etc. of the conventional units being displaced, but would hinge on the availabilities of various power levels of WECS

output, especially during peak load periods. These availability factors can be significant for the arrays studied here [for example, 99.3% availability for 500 kW/generator from the 2 MW WECS Pacific Coast array in summer at 1600 hours (Table D-8)].

Similarly the economic benefit of fuel saved by WECS power depends not only on the average power (by season and time of day) but on the dependability of that power. The percentage availability data relate also to this area of utility analysis of WECS cost effectiveness. The enhanced power availabilities of the arrays studied (as shown in Tables in Appendix D) mean that significantly more peak load period fuel (the most expensive used) can be reliably displaced by wind power, hence improving the potential cost effectiveness of wind power used only as a fuel saver.

6. RUN DURATION STATISTICS FOR SPEED AND POWER

Run Statistics for Speed

Average and maximum length of runs for hub height (60 m) return speeds of 5, 7.5, and 10 m/s are shown in Tables 8 and 9 for the Great Lakes area and the Pacific Coast area respectively. As expected, as the return speed increases the amount of time that the wind stays above the return values (run durations above) decreases and the time the wind stays below the return speed (run durations below) increases.

In the Great Lakes area the wind stays above a given return speed longer and once the wind has gone below the return value, it remains below for a shorter length of time than in the Pacific Coast area. This is due to the fact that the Great Lakes area sites used in this study generally had stronger winds than the Pacific Coast area sites used.

Figures 26 - 33 give the probability of run duration below or above a given speed level evaluated for each of the return speeds for the summer and winter seasons. For example, in Figure 26 when the wind speed drops below 10 m/s there is approximately a 35% probability that the wind speed will remain below 10 m/s for a day or longer [hence a 65% probability that, once the wind speed drops below 10 m/s it will remain below 10 m/s less than one day]. Notice that for the Great Lakes area, run durations of greater than 6-12 hours can be represented by a straight line but this line cannot be continued back through the run duration data points for durations less than 6-12 hours. For the Pacific Coast a straight line for run durations longer than 6-12 hours cannot be continued for runs of duration longer than about 2 days. Thus the results are not consistent with the theoretically justifiable exponential run duration probability with a single time scale. If the exponential form for run duration probability is to apply at all, these results must be interpreted in terms of an exponential form

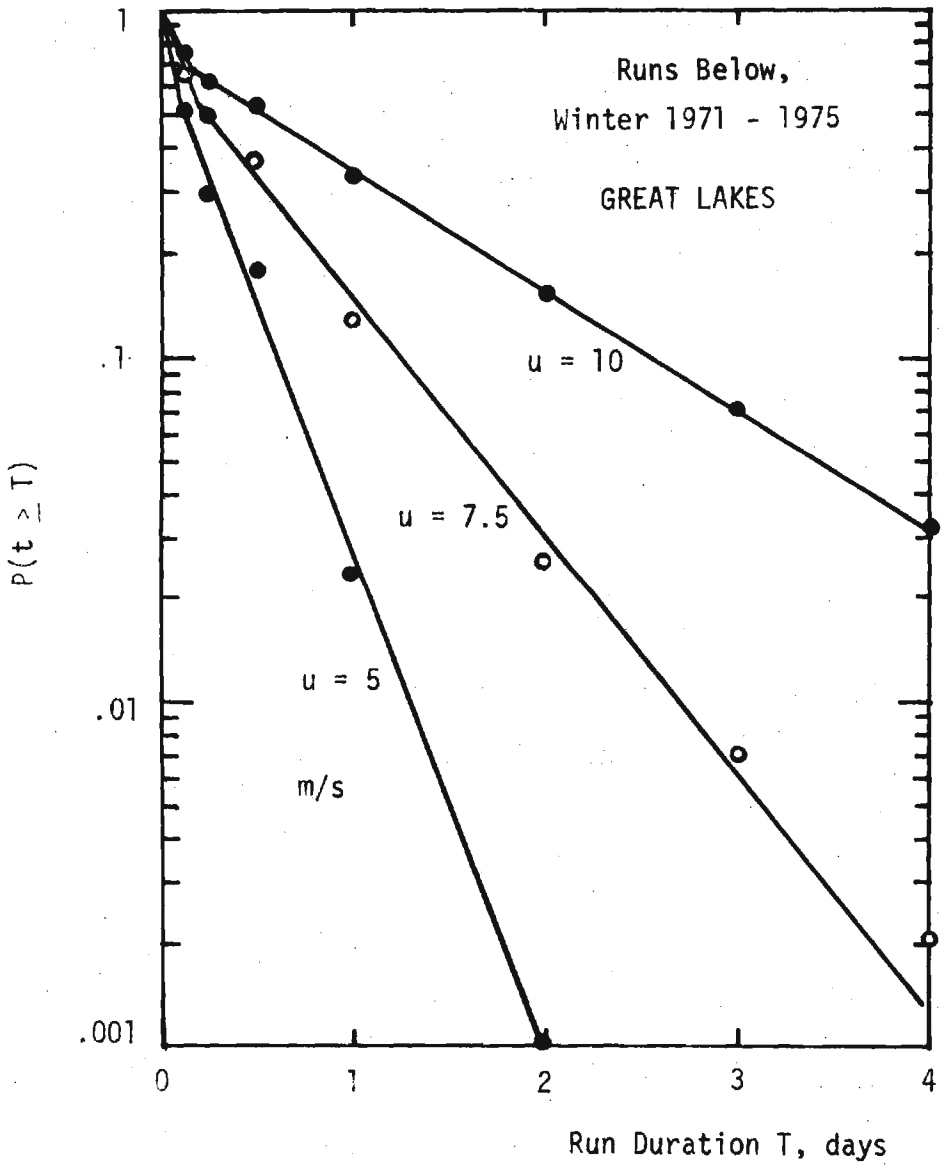

Figure 26. Probabilities of Run Duration (Runs Below) for Various Return Speeds, Great Lakes, Winter.

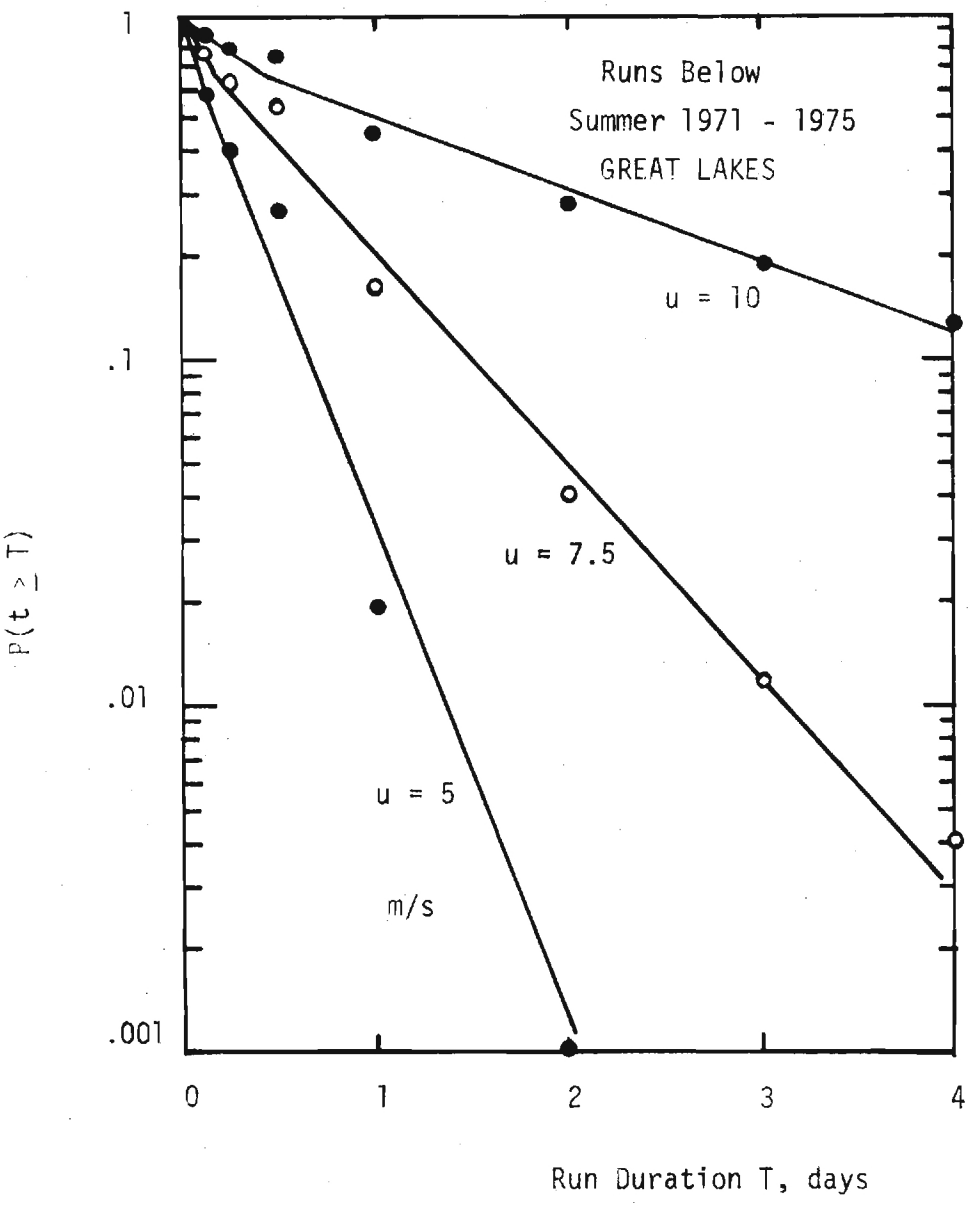

Figure 27. As in Figure 26 for Summer.

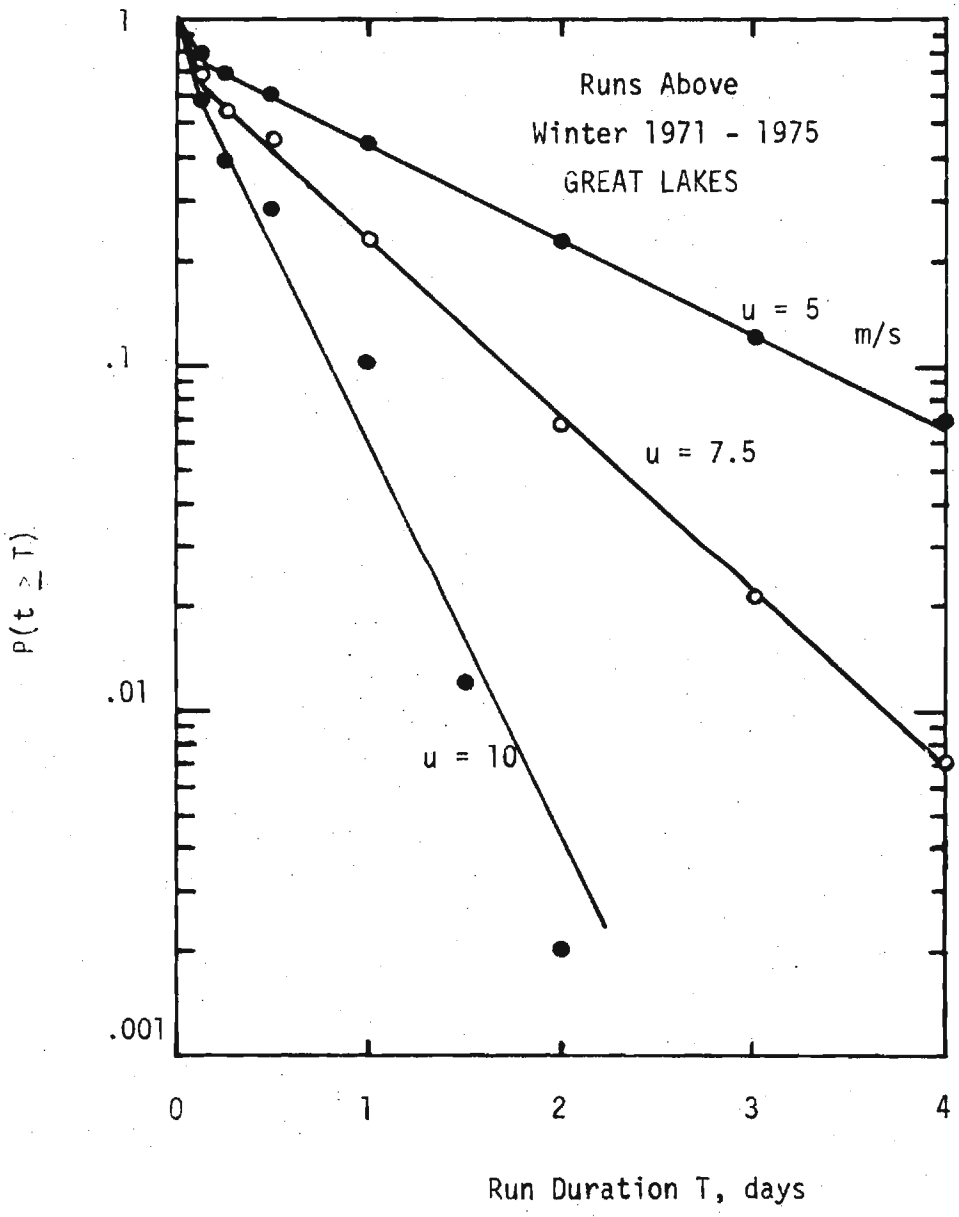

Figure 28. As in Figure 26 for Runs Above.

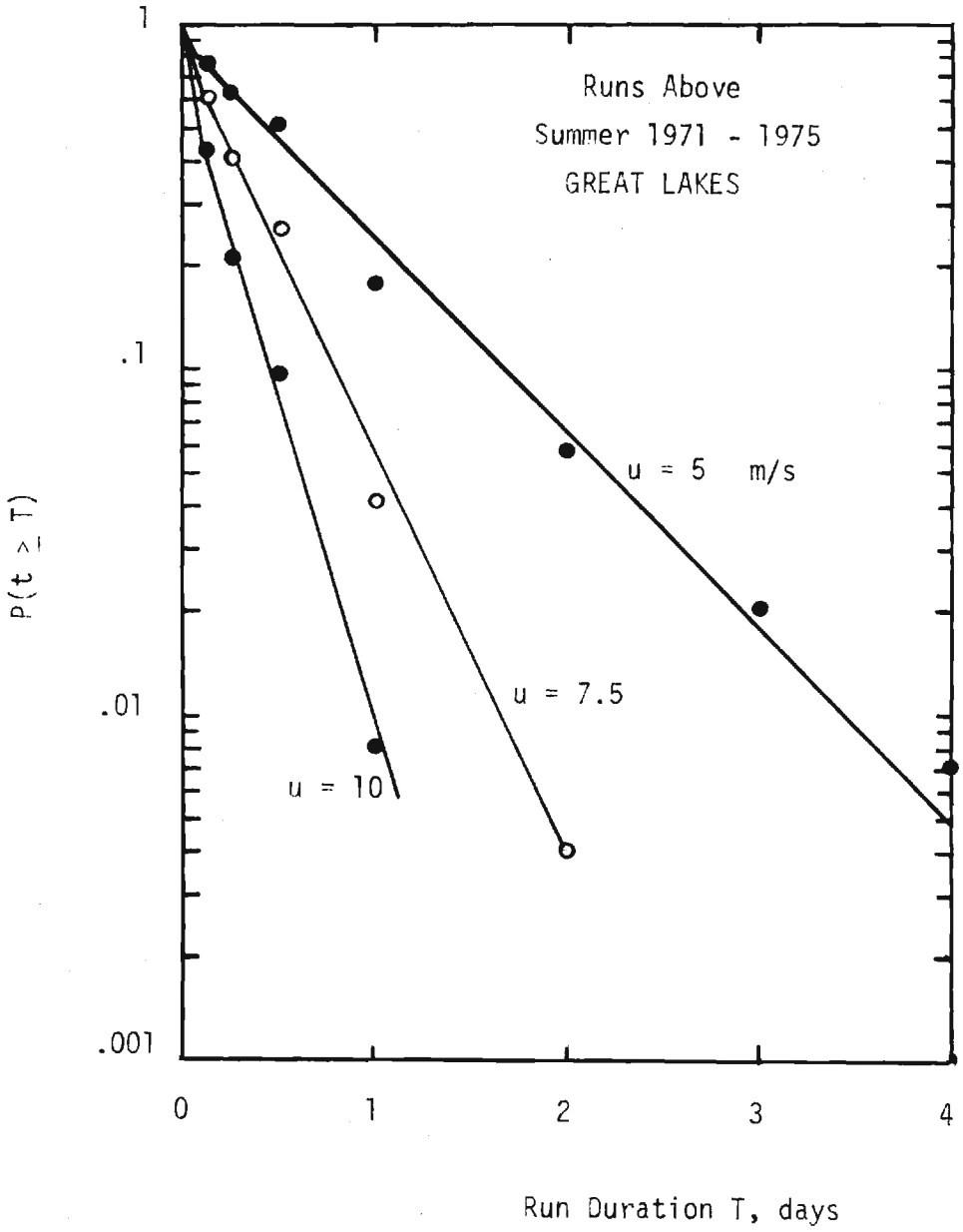

Figure 29. As in Figure 26 for Runs Above in Summer.

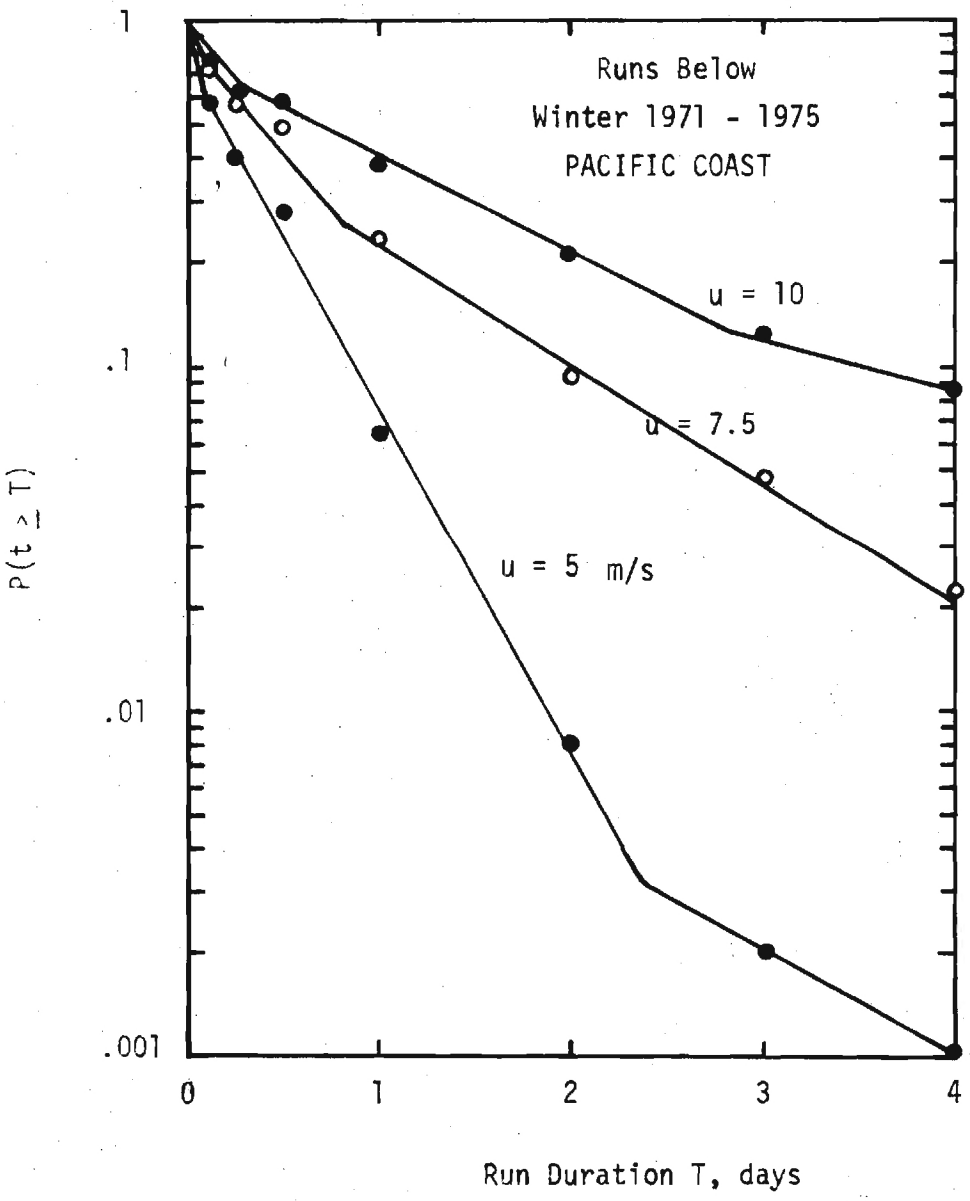

Figure 30. As in Figure 26 for Pacific Coast.

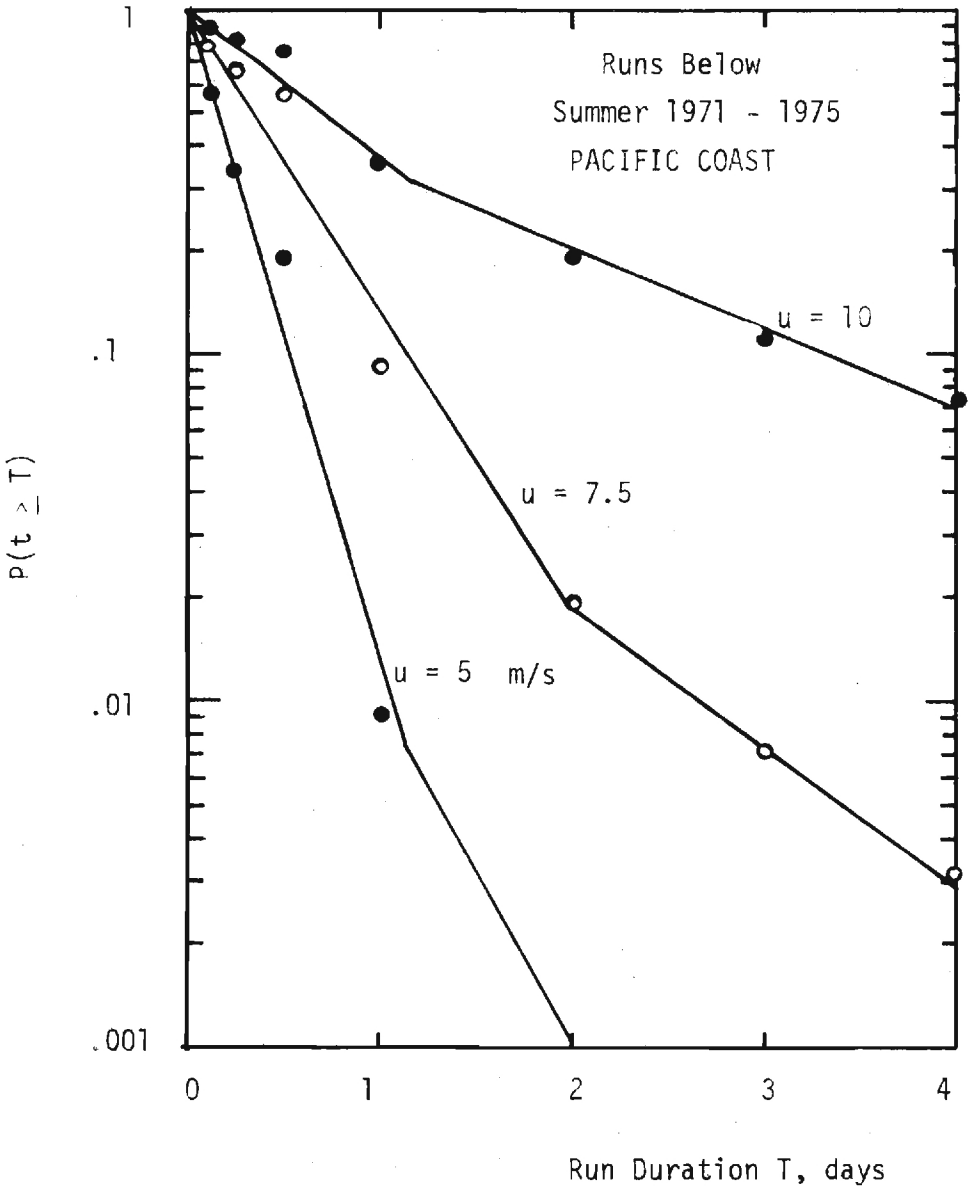

Figure 31. As in Figure 26 for Pacific Coast, Summer.

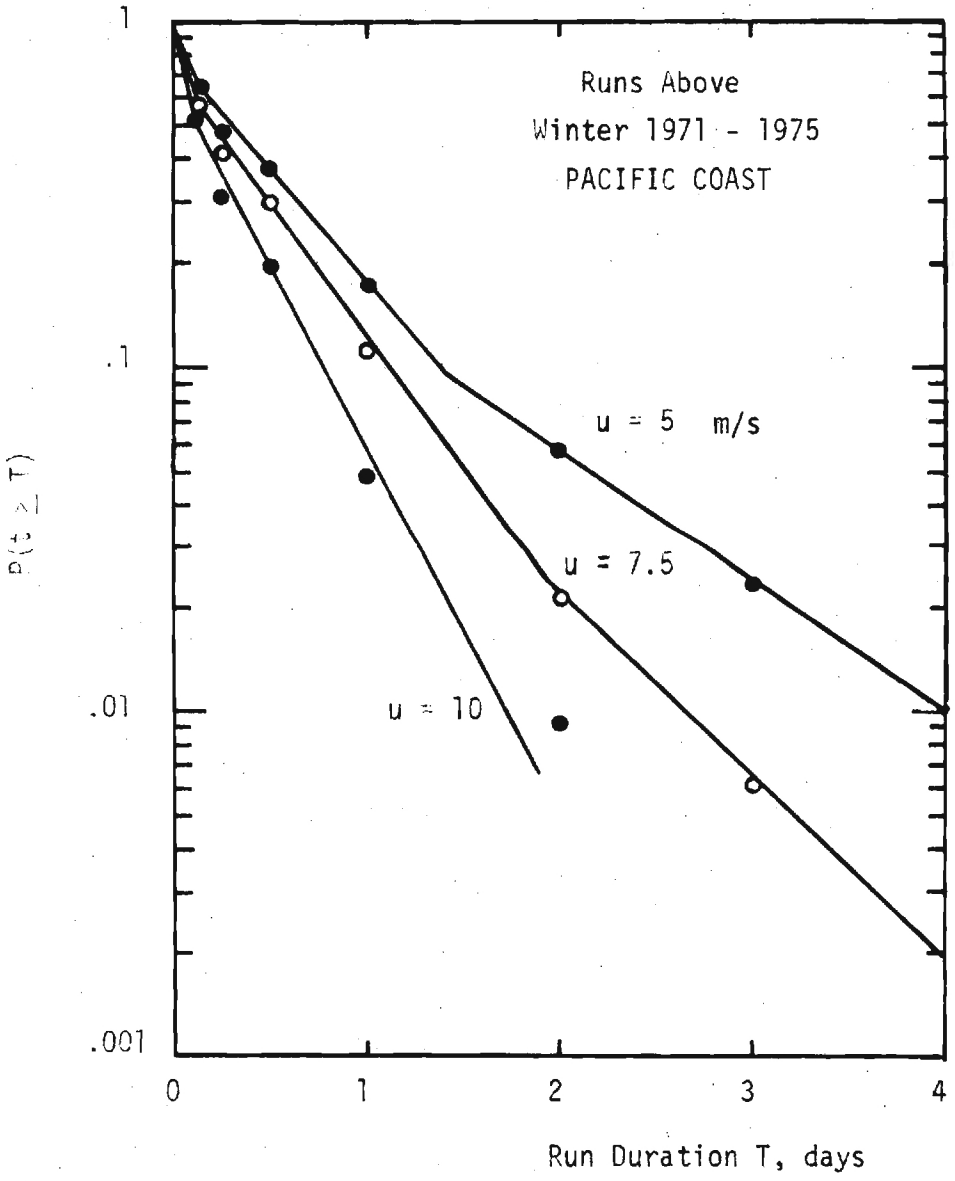

Figure 32. As in Figure 26 for Pacific Coast Run Above.

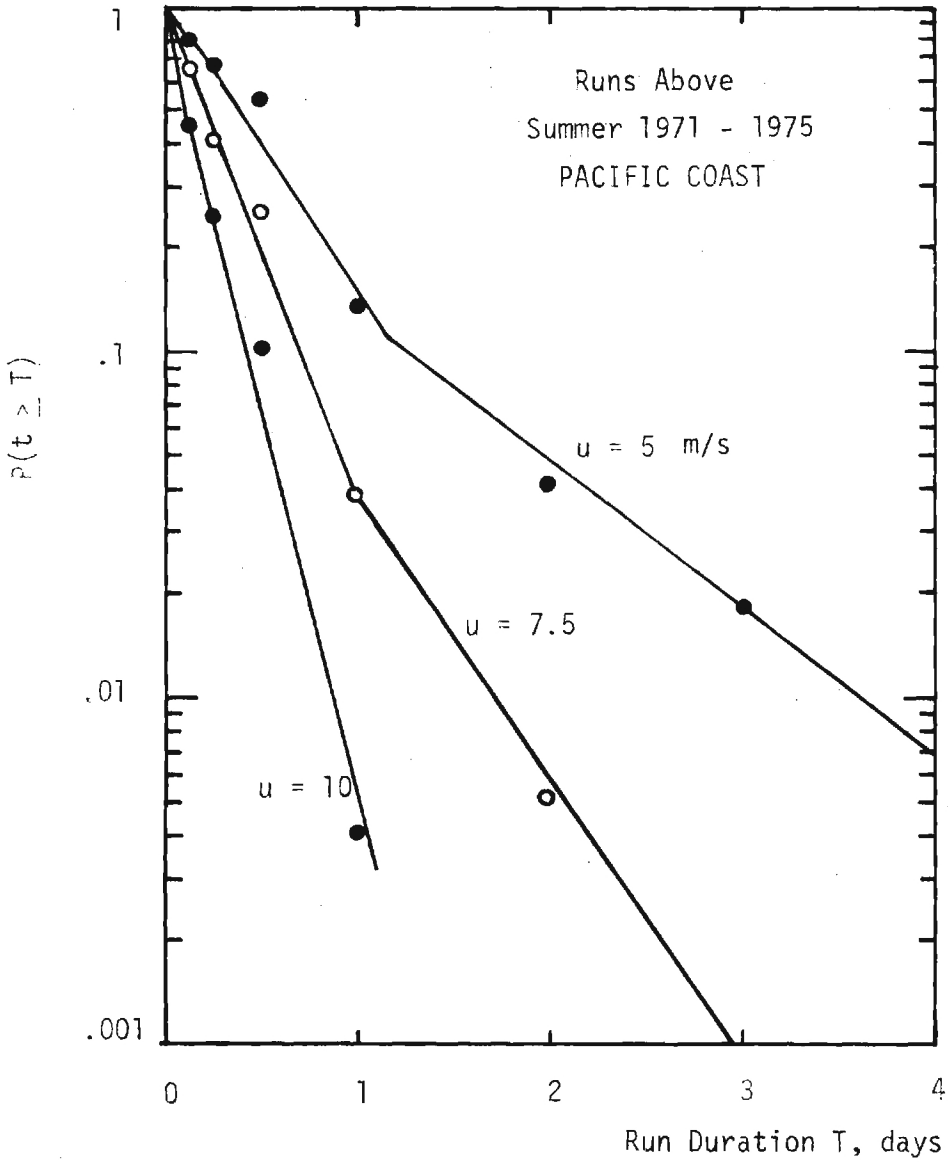

Figure 33. As in Figure 26 for Pacific Coast, Runs Above, Summer.

Table 8

Average and Maximum Run Duration (Length of Run in Hours) for Hub Height (60 m) Return Speeds of 5, 7.5, and 10 m/s (Great Lakes Array)

	Return Speed	Winter		Spring		Summer		Fall		Annual	
	m/s	AVG	MAX	AVG	MAX	AVG	MAX	AVG	MAX	AVG	MAX
Above	5.0	32.5	417	25.8	297	15.9	282	20.5	336	23.7	417
	7.5	15.8	180	13.5	183	8.2	96	10.6	114	12.0	183
	10.0	9.6	108	8.4	87	5.4	54	6.7	60	7.5	108
Below	5.0	6.8	57	6.5	66	7.7	87	7.6	69	7.1	87
	7.5	11.7	144	11.5	147	15.3	183	14.3	231	13.2	231
	10.0	24.0	300	25.4	489	44.2	528	35.0	381	31.9	528

Table 9

Average and Maximum Run Duration (Length of Run in Hours) for Hub Height (60 m) Return Speeds of 5, 7.5, 10.0 m/s (Pacific Coast Array)

	Return Speed m/s	Winter AVG	Winter MAX	Spring AVG	Spring MAX	Summer AVG	Summer MAX	Fall AVG	Fall MAX	Annual AVG	Annual MAX
Above	5.0	14.0	261	15.7	246	15.1	285	12.3	309	14.3	309
	7.5	10.3	138	9.6	108	8.4	87	8.0	117	9.1	138
	10.0	7.5	96	6.7	75	5.7	42	6.1	42	6.5	96
Below	5.0	8.9	120	6.8	66	6.8	90	8.1	111	7.6	120
	7.5	18.8	285	13.7	186	13.5	288	17.8	312	15.9	312
	10.0	32.9	522	29.2	540	33.4	378	40.2	456	33.6	540

with more than one time scale, e.g.

$$p(t) = A\, e^{-t/T_1} + B\, e^{-t/T_2} + C\, e^{-t/T_3} \qquad (2)$$

where for most of the Great Lakes data only the two time scales T_1 and T_2 are required (i.e. two linear segments in the $p(t < T)$ graphs) and for the Pacific Coast data (which generally had 3 linear segments in the $p(t < T)$ graphs) all three scales T_1, T_2, and T_3 would be required. The cumulative probability of run duration $p(t \geq T)$ found from integration of (2) would be given by

$$p(t \geq T) = (A/T_1)\, e^{-T/T_1} + (B/T_2)\, 2^{-T/T_2} + (C/T_3)\, e^{-t/T_3} \qquad (3)$$

from which the normalization $p(t \geq 0) = 1$ yields the constraint condition

$$(A/T_1) + (B/T_2) + (C/T_3) = 1 \qquad (4)$$

Corotis (1976), using higher resolution hourly wind data rather than 3 hourly values used here, found that for short run duration ($T \lesssim 24$ hours) the probability of run duration was accurately represented by

$$p(t) = a\, t^{-b} \qquad (5)$$

or by cumulative probability

$$p(t \geq T) = [A/(1 - b)]\, T^{1-b}. \qquad (6)$$

This model does not provide a good fit with our results of Figures 26 - 33 which are equally nonlinear on log-log plots [whereas equations (5) or (6) would be linear on a log-log representation]. However, Corotis in both private communication and in his reports (Corotis, 1977) has indicated that the exponential form for long duration runs is not inconsistent with his results, since his relation (5) is meant to apply only to short run duration. Corotis (1976) found interesting relations between his a and b parameters (equation 5), and the mean wind

speed, which may hold in analogous form for the parameters A, B, and C of the multiple time scale exponential model (equation 3). However, this level of detailed analysis has not been pursued at this stage.

Run Statistics for Array Power

For an analysis of the probability of array power lulls of various durations, without storage, the statistics of array power run durations were evaluated at three power levels - 100 kW, 200 kW, and 500 kW per generator. An array power run duration for a given power level is defined as the time required after array power goes below the given power level until the array power returns above that level. Tables 10 and 11 show the average, average maximum, and 5 year maximum run durations in hours for the three power return levels and for each area of study. The average maximum run duration is the average of the 5 yearly maximums for each season. The 5 year maximum is the absolute maximum observed for a particular season over the 5 year period.

Figures 34 - 37 give probability of run duration below a given power level (i.e. power lulls) evaluated for each of the three power levels of the 1.5 MW generator for the summer and winter seasons. For example, from Figure 35 once the power drops below 500 kW per generator there is approximately a 41% probability of the power staying below the 500 kW level for a day or longer before returning above that level [hence a 59% chance of power returning above 500 kW per generator in less than a day].

It should be noticed that for each power run duration - probability curve there seems to be no single straight line relationship for run durations over the range evaluated. Hence, a simple exponential model cannot explain the array power run duration statistics. The data are also not linear on log-log plots - hence the Corotis power law model is not applicable. Unambiguous application of a multiple time scale exponential model cannot be made either.

Table 10

Average, Average Maximum and 5 Year Maximum Run Durations (Length of Runs Below, in Hours) for Various Power Levels and Wind Turbines in the Great Lakes Array

Wind Turbine	Return Power kW	WINTER			SPRING			SUMMER			FALL			ANNUAL		
		AVG	AVG MAX	5YR MAX	AVG	AVG MAX	5YR MAX	AVG	AVG MAX	5YR MAX	AVG	AVG MAX	5YR MAX	AVG	AVG MAX	5YR MAX
500 kW	100	8.6	22.6	48	8.7	13.8	18	10.6	19.2	42	10.3	21.8	33	9.6	19.4	48
	200	15.1	47.8	90	12.3	37.8	90	18.6	67.0	111	17.1	61.8	99	15.8	53.6	111
	500	160.6	244.7	513	169.2	276.4	366	-	-	-	198.8	260.4	477	172.4	259.8	513
1500 kW	100	11.2	33.4	69	9.9	20.6	45	13.5	36.0	87	13.0	42.6	90	11.9	33.2	90
	200	16.9	54.4	138	14.8	46.4	90	22.3	89.0	159	19.6	73.8	117	18.4	65.9	159
	500	30.6	96.8	168	40.5	151.4	285	79.1	212.6	360	60.0	156.2	282	52.5	154.3	360
2000 kW	100	5.5	8.3	15	6.3	10.9	15	7.9	13.0	15	7.0	12.4	18	6.8	11.5	18
	200	7.8	19.4	42	8.1	13.4	18	9.7	17.0	21	9.2	18.2	24	8.7	17.0	42
	500	13.8	43.6	87	11.6	33.0	90	17.5	54.4	87	15.9	58.8	99	14.7	47.5	99

Table 11

Average, Average Maximum and 5 Year Maximum Run Durations (Length of Runs Below, in Hours)

for Various Power Levels and Wind Turbines in the Pacific Coast Array

Wind Turbine	Return Power kW	WINTER			SPRING			SUMMER			FALL			ANNUAL		
		AVG	AVG MAX	5YR MAX	AVG	AVG MAX	5YR MAX	AVG	AVG MAX	5YR MAX	AVG	AVG MAX	5YR MAX	AVG	AVG MAX	5YR MAX
500 kW	100	8.5	26.0	60	6.2	13.8	18	6.3	12.4	15	8.3	19.2	42	7.3	17.9	60
	200	18.5	107.2	210	11.5	29.2	45	13.1	22.8	39	19.2	70.4	183	15.6	57.4	210
	500	-	-	-	-	-	-	-	-	-	-	-	-	-	-	-
1500 kW	100	10.1	34.2	66	7.2	18.4	45	8.1	15.0	18	10.2	30.8	66	8.9	24.6	66
	200	15.4	75.4	138	11.4	30.8	69	12.7	20.8	39	16.6	64.6	141	14.0	47.9	141
	500	66.3	237.2	429	42.0	147.2	237	61.4	158.2	258	100.2	236.6	597	67.5	194.8	597
2000 kW	100	4.9	8.6	21	3.9	6.3	12	4.0	6.4	9	4.9	10.1	15	4.4	7.9	21
	200	7.6	20.0	60	5.6	11.2	15	5.6	11.0	15	7.4	16.0	21	6.5	14.6	60
	500	14.9	79.0	138	10.5	26.2	45	11.7	18.2	21	15.7	56.4	141	13.2	45.0	141

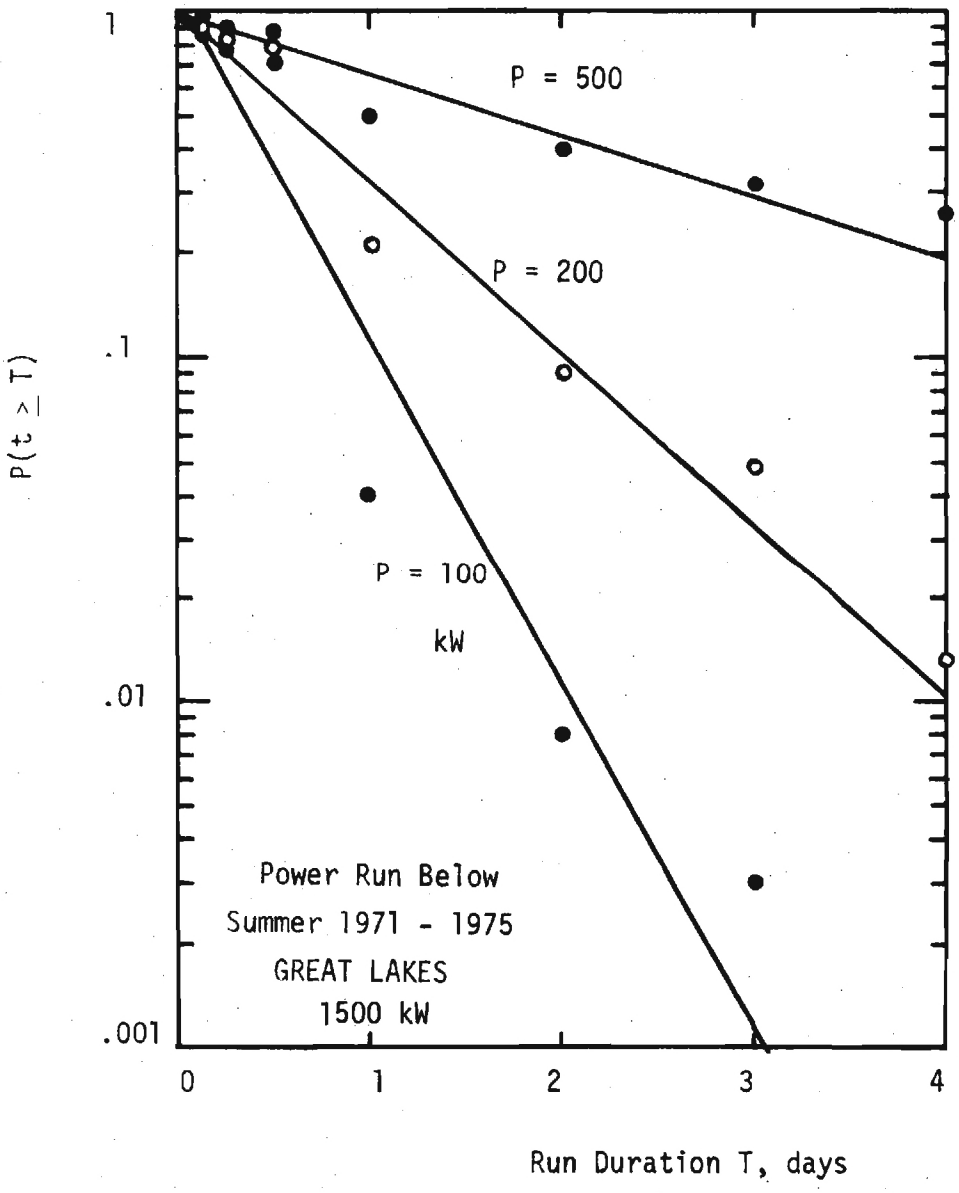

Figure 34. Probabilities of Run Duration (Runs Below) for Various Array Return Powers, Great Lakes, Summer, 1.5 MW WECS.

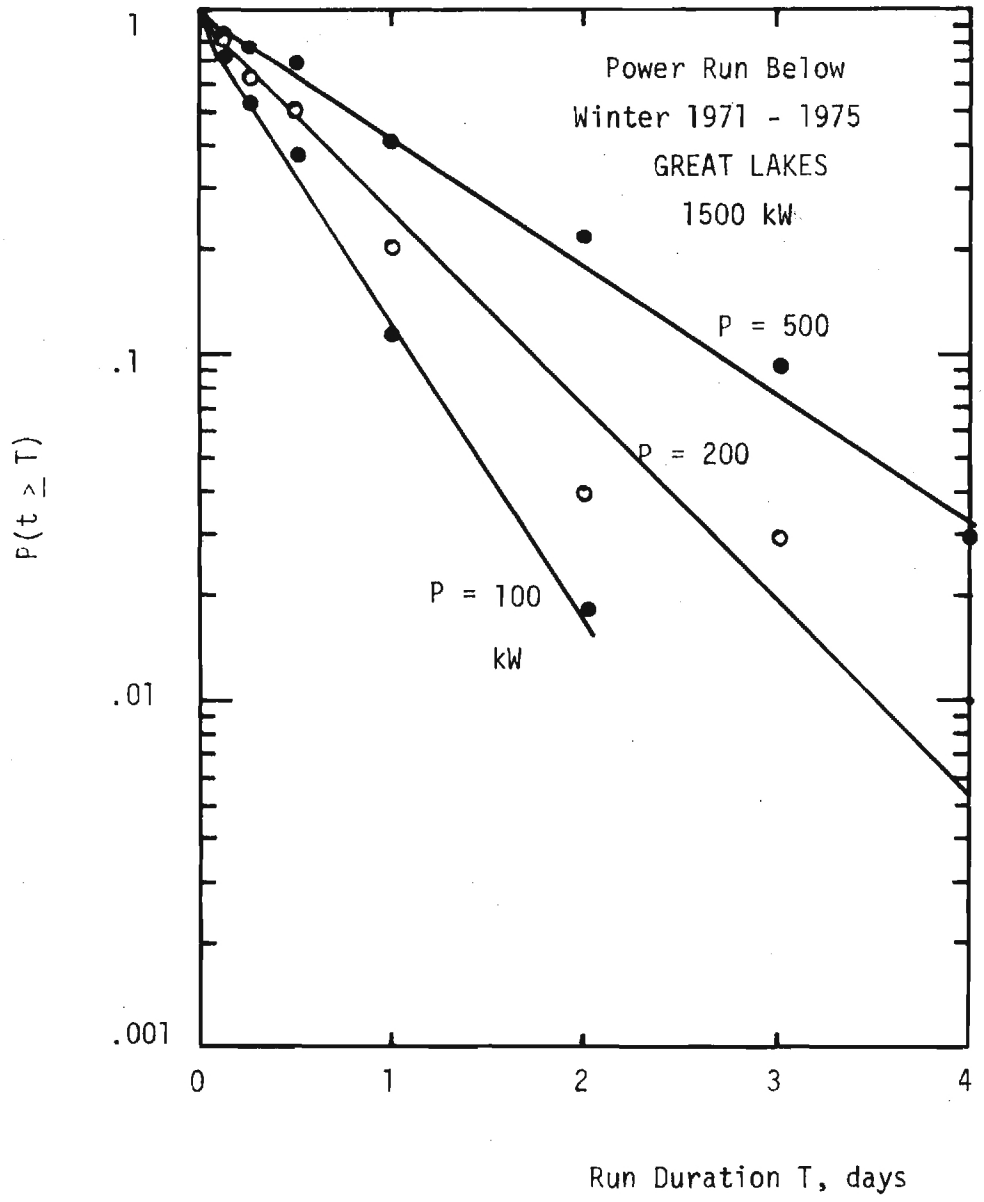

Figure 35. As in Figure 34 for Winter.

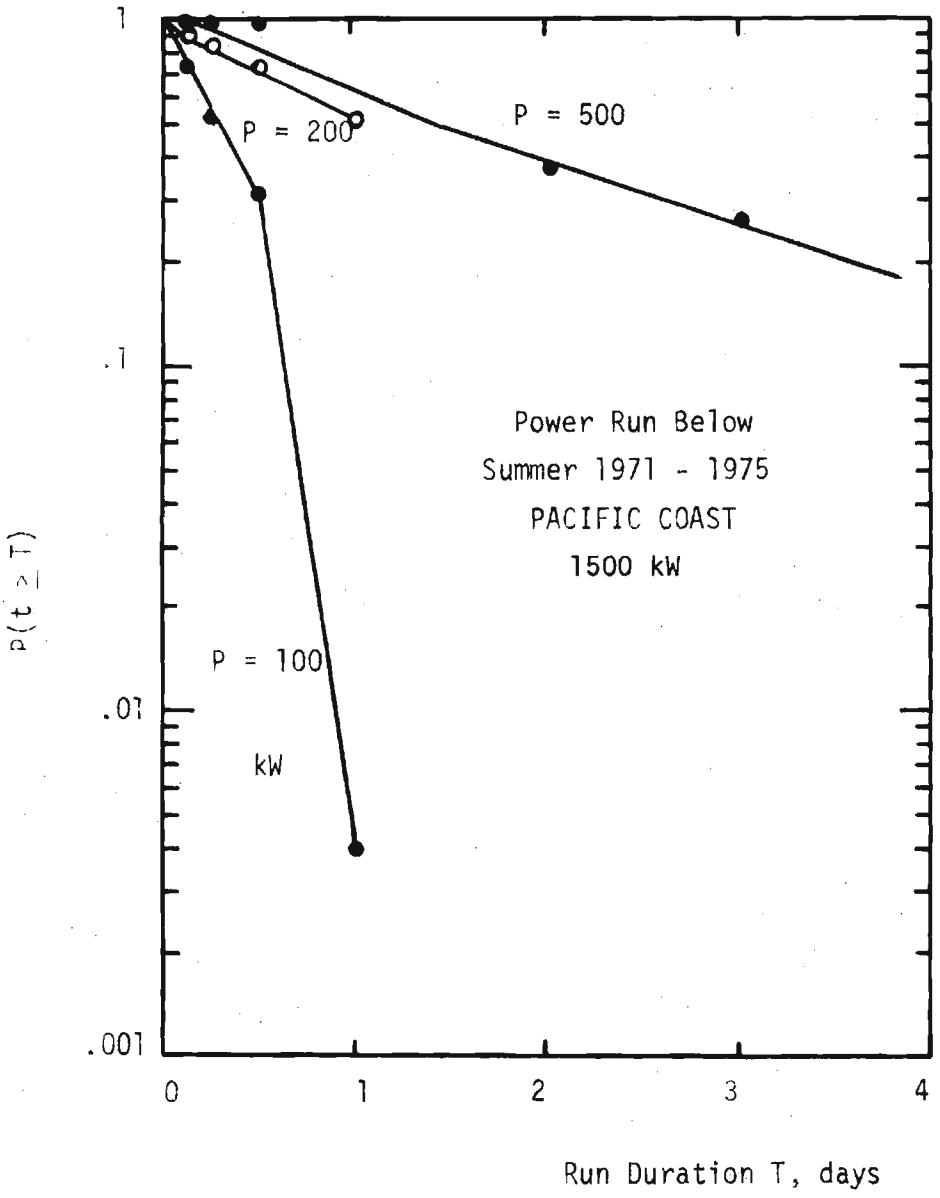

Figure 36. As in Figure 34 for Pacific Coast.

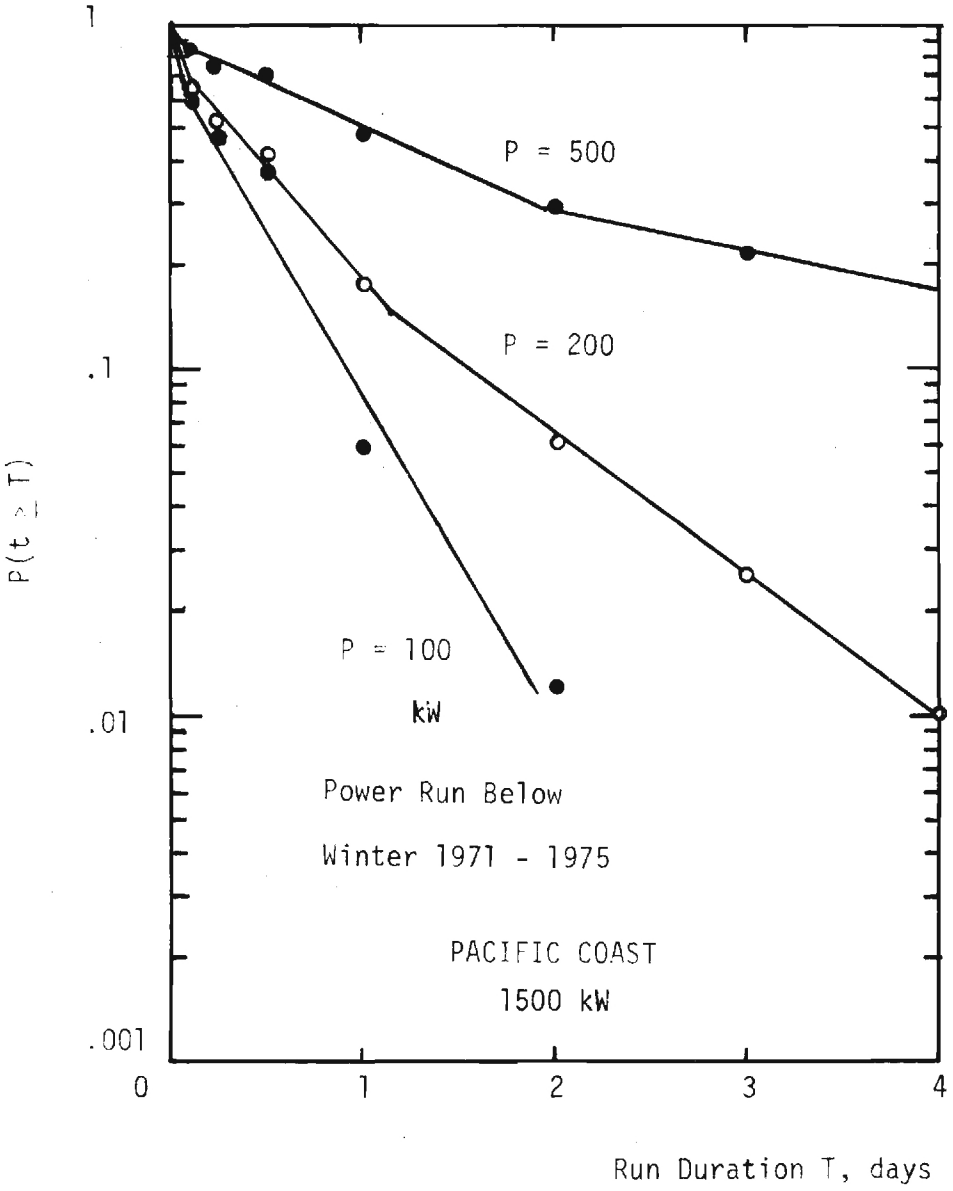

Figure 37. As in Figure 34, for Pacific Coast, Winter.

Table 12

Approximate Run Duration (in Days) Associated with 90% to 99% Probability for Various Array Output Power Levels.

Area			Great Lakes			Pacific Coast		
kW/Generator			100	200	500	100	200	500
Season	Wind Turbine	Availability %						
Winter	1.5 MW	90	1.1	1.7	2.7	1.0	1.6	5.4
		95	1.5	2.3	3.5	1.3	2.3	7.5
		99	2.3	3.5	5.4	2.0	4.0	12.0
	2.0 MW	90	0.5	0.7	1.5	0.3	0.6	1.5
		95	0.7	1.0	2.0	0.5	0.8	2.3
		99	1.2	1.6	3.1	1.0	1.5	4.2
Summer	1.5 MW	90	1.1	2.0	5.5	1.0	3.4	5.3
		95	1.3	2.7	7.3	1.3	4.5	7.0
		99	2.1	4.0	11.2	1.9	6.8	10.8
	2.0 MW	90	0.8	0.9	1.3	0.2	0.4	2.5
		95	0.9	1.1	1.7	0.3	0.6	3.2
		99	1.2	1.5	2.6	0.4	0.8	4.9

Hence development of a suitable model for array power run duration statistics must await further study.

Table 12 summarizes the run duration results for array output power from the 1.5 MW and 2.0 MW wind turbines in both regions studied. In this table the run durations (in days) associated with 90%, 95% and 99% availability of 100, 200 and 500 kW per generator are tabulated. These run duration values were interpolated or extrapolated from Figures 34 - 37 for the 1.5 MW and analogous data for the 2 MW machines. The run duration statistics can be interpreted as probabilities of power lulls in the absence of storage: e.g. (from Table 12) the 1% probable duration for a period in which the array power remains continuously below 500 kW per generator for the 2 MW wind turbine is 3.1 days for the Great Lakes array in winter (i.e. once power output goes below 500 kW per generator, there is a 99% probability power will stay below this level for 3.1 days or less and a 1% probability of such a lull lasting 3.1 days or longer).

In addition to information on the probability of various lengths of power lulls for arrays without storage, the power run duration statistics of this section also provide an approximate analysis of power availability for arrays with storage. Thus, for the Great Lakes 2 MW array in winter, if the storage started completely charged at the beginning of a power lull below 500 kW per generator, 95% of the time power would return above 500 kW/generator in less than 2.0 days so approximately 24 MW hours of storage capacity (500 kW x 48 hours) would meet such lulls with 95% dependability.

7. CONCLUSIONS

Of the two sets of regional sites studied for this report, the Great Lakes sites have the higher annual average wind speed and the Pacific Coast sites have the lower spatial cross correlation, due to terrain influence. Compared to the previously studied New England and Central U.S. region sites, the Pacific Coast region sites have the lowest wind speed and the Great Lakes Regions sites have the second highest wind speed (only the Central U.S. sites had higher). Of course, the airport sites used in these array studies are very likely not the best wind sites in the regions examined. Differences in these airport and the best wind locations are probably largest in the Pacific Coast region where the more significant terrain features would offer better opportunity for good hilltop locations for WECS units.

Although similar diurnal patterns were observed for winds in both of the presently studied regions (with peak winds near 1400 hours), the Pacific Coast region was interesting because its summer afternoon winds were higher than its winter afternoon winds.

The 2.0 MW wind turbine with its large rotor diameter and relatively low cut-in and rated speed showed better overall power output characteristics than the lower rated power 0.5 MW machine or the high rated speed 1.5 MW machine. Significant improvements in wind power availability were noted for the array configuration (e.g. 92% availability of 200 kW/generator from 2.0 MW WECS in winter for Great Lakes array, versus 75% for individual site, or 88% versus 50% for the similar Pacific Coast statistics).

The simplified model for evaluating array statistics (Appendix B) appears to produce satisfactory results, thus eliminating the need for extensive and costly simultaneous time series analysis of multiple sites for evaluation of

array characteristics, at least insofar as power distribution statistics are concerned. A time series model for arrays based on individual representative sites has additional verification required relative to the adequacy of its time variation simulation accuracy.

Run duration statistics for both wind speed and wind power output seem to indicate a multiple time scale exponential process although, with the scatter of the computed results, this process is not convincingly proved nor are other models necessarily ruled out. The run statistics of the Pacific Coast region are more complex than for the Great Lakes Region. Run duration results indicate that array power lulls below 200 kW per generator would have 99% probability of lasting less than 1 - 2 days for the 2 MW generator arrays. For 500 kW per 2 MW generator the 99 percentile runs below would be 3 - 5 days duration. The 95 percentile run durations below 200 kW per 2 MW generator would be 0.5 - 1 day or 3 - 5 days at 95 percentile for 500 kW per 2 MW generator. These statistics are most valuable to interpret as probabilities of power lulls of various durations, in the absence of storage, although they also have application as approximate analysis of storage requirements to meet various levels of power reliability.

APPENDIX A

WIND POWER PERFORMANCE CURVE MODEL (INCLUDING EFFECTS OF WIND GUSTS, SHEAR, DIRECTION SHIFTS, AND DENSITY EFFECTS)

In a uniform axial flow speed V_h at standard density ρ_o with power coefficient C_p and rotor swept area A, the shaft power output of a wind turbine would be:

$$P_o = 0.5\, C_p\, \rho_o\, V_h^3\, A. \tag{A-1}$$

When C_p variations with speed and blade pitch angle, mechanical and electrical losses etc. are taken into account, the electrical power output of the wind turbine can be reasonably approximated by the relations:

$$P(V_h)/P_r = \begin{cases} 0 & V_h \leq V_{in} \\ A + BV_h + CV_h^2 & V_{in} \leq V_h \leq V_{rated} \\ 1 & V_{rated} \leq V_h \leq V_{out} \\ 0 & V_h > V_{out} \end{cases} \tag{A-2}$$

where A, B, and C coefficients are determined by the three conditions

$$\begin{aligned} P(V_{in})/P_r &= A + BV_{in} + CV_{in}^2 = 0 \\ P(V_r)/P_r &= A + BV_r + CV_r^2 = 1 \\ P(V_m)/P_r &= A + BV_m + CV_m^2 = P_m/P_r \end{aligned} \tag{A-3}$$

where the "mid-point speed" V_m is $(V_{in} + V_{rated})/2$ and the "mid-point power" P_m is given by

$$P_m/P_r = P_f(V_m/V_r)^3 \tag{A-4}$$

where P_f is an adjustment factor which for most wind turbines is between 0.9

and 1.1 (for a wind turbine whose precise power curve is not known $P_f = 1$ can be assumed).

An approach, valid for the level of detail required in machine design, for the evaluation of the effects on power output by wind shear and wind gust level has been presented by Wilson and Lissaman (1974). However, for simple and straightforward computation in performance evaluation and systems analysis applications, a simpler, less rigorous approach is suggested. The corrections derived here for wind gust, shear, and density effects are found to be relatively small, but not completely insignificant. Thus, for power performance applications, the simplified correction methods derived here seem appropriate.

Corrections for Wind Shear

The effects of wind shear can be approximated by evaluating the shear affected energy flux (power) P through a disk of radius R (centered at hub height Z_h), relative to the uniform speed energy flux $P_o = \rho_o V_h^3 \pi R^2/2$, where ρ_o is air density and V_h is the speed at height Z_h. For a wind shear given by a power law wind profile $V(Z)/V_h = (Z/Z_h)^n$, the shear affected power flux, relative to P_0 is given by:

$$P/P_0 = (2/\pi) \int_0^{\pi} (1 + R \cos \theta/Z_h)^{3n} \sin^2 \theta \, d\theta. \qquad \text{(A-5)}$$

Therefore, P/P_0 is a function of the rotor radius relative to hub height R/Z_h and the wind profile exponent n. Figure A-1 shows equation (A-5) values of P/P_0 plotted versus exponent n for several values of relative radius R/Z_h. This figure shows that for exponent $n = 0$ (uniform flow) P/P_0 is constant at a value of 1, while for an exponent of $n = 1$, (linear shear across the blade area) the effect of shear could be important, provided the rotor blades are of sufficiently large diameter (high R/Z_h values).

Rather than a numerical integration of (A-5), actual evaluation of P/P_0 is done by the approximate relation:

$$P/P_0 = a(R/Z_h) + b(R/Z_h)\, n + c(R/Z_h)\, n^2 \qquad \text{(A-6)}$$

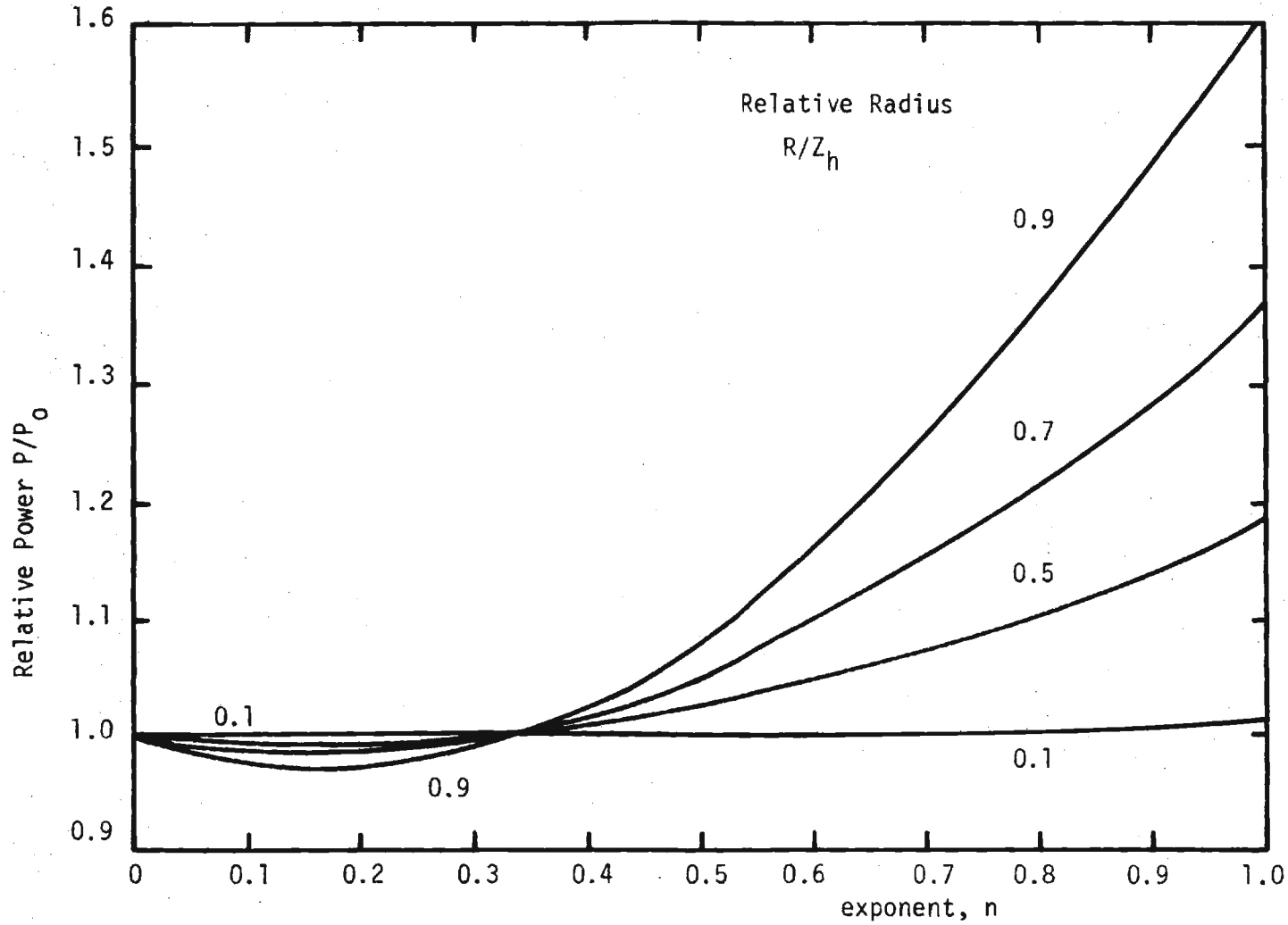

Figure A-1: Circular Integrated Relative Power P/P_o for Circular Area of Relative Radius R/Z_h for Various Wind Profile Exponents n.

where the coefficients are given by

$$a(R/Z_h) = 0.9949 - 0.0194\,(R/Z_h) - 0.020\,(R/Z_h)^2 \qquad \text{(A-7)}$$

$$b(R/Z_h) = 0.0350 - 0.1267\,(R/Z_h) - 0.255\,(R/Z_h)^2 \qquad \text{(A-8)}$$

$$c(R/Z_h) = 0.0441 - 0.1579\,(R/Z_h) - 0.980\,(R/Z_h)^2 \qquad \text{(A-9)}$$

and the exponent n for each hourly value of wind speed is calculated from equations in Justus and Mikhail (1976). The relations (A-7) through (A-9) were found by least square fit of parabolic variation through numerically integrated values for (A-5), followed by least squares parabolic fit of the variation of the parabolic coefficients (a, b, and c) thus determined. An approximate average correction, with n = 0.17 and $R/Z_h = 0.8$, is $P/P_o = 0.98$, which agrees approximately with Wilson and Lissaman's estimate for the effects of wind shear on the Grandpa's Knob machine with the same n value and R/Z_h value.

Although in practice the effective exponent n is evaluated for the hour-by-hour data, it is instructive to consider some statistics of the exponent values to be encountered. Data from the transition matrix for wind speed changes between vertical levels from Crawford and Hudson (1970) indicate 50% probable shears which are equivalent to n = 0.6 at low speeds, with $n \simeq 0.3$ being the 50% probable shear at wind turbine operating speeds. The 99 percentile shears would range from n = 0.9 at low speed to n = 0.35 at high speed.

Gust Factor Corrections

If the power output is assumed to respond via relation (A-2) to wind speeds V which have periods of the order of a few seconds, but the average power output $\bar{P}$ over some longer time period (e.g. 1 min.) is desired, then $\bar{P}$ is given by:

$$\bar{P}/P_r = A + B\bar{V} + C\langle V^2 \rangle \qquad \text{(A-10)}$$

where $\bar{V}$ is the average wind speed over the desired time interval, and $\langle V^2 \rangle$ is the mean square, which can be written as

$$\langle V^2 \rangle = \langle (\bar{V} + v)^2 \rangle = \bar{V}^2 + \sigma_u^2 \qquad \text{(A-11)}$$

where σ_u^2 is the mean square speed gust intensity about the mean wind speed for the time period. Thus

$$\bar{P}/P_r = A + B\bar{V} + C\bar{V}^2 + C\langle v^2 \rangle = A + B\bar{V} + (1 + \sigma_u^2/\bar{V}^2)C\bar{V}^2. \qquad \text{(A-12)}$$

From data contained in Crawford and Hudson (1970), Ramsdell (1975), Sissenwine et al (1973), Singer (1960), and Singer et al (1961). The mean ratio $\sigma_u/\bar{V}$ appropriate to the rotor swept area should be about 0.2 for turbulent gusts about the one minute mean. All of these reports are consistent with gust factors (mean plus peak gust divided by mean) of about 1.3. A peak gust factor of 1.36 was obtained by Georgia Tech analysis of Kennedy Tower data. The rms gust would be somewhat smaller than the peak gust.

The controls should maintain output power equal to rated power above rated conditions except for fluctuations due to gusts of scale too small to completely immerse the blades. From the model spectrum of Ramsdell (1975)[his figure 115 and equation 8.6] it is estimated that about 1/3 of the wind speed variance due to turbulence is produced by wavelengths smaller than 2 rotor diameters. Thus, when the wind turbine is above rated speed, a fluctuation of output power equal to (1/3) $(3P_r \sigma_u^2/\bar{V}^2)$ would be produced by the small scale turbulence (which contributes variance (1/3) σ_u^2). This comes from an assumption that, above rated, power changes proportional to the cube of wind speed, and that $\langle (\bar{V} + v)^3 \rangle \simeq \bar{V}^3 + 3\langle v^2 \rangle \bar{V}$ leads to a $3\sigma_u^2/\bar{V}^2$ variation relative to rated power P_r, only 1/3 of which is not capable of being followed by the pitch control mechanism and leads to an actual output power fluctuation. Thus, with $(\sigma_u/\bar{V})^2 \simeq 0.04$, a 500 kW machine may fluctuate on the order of 20 kW about rated conditions due to wind speed fluctuations which do not completely immerse the

blade, and which the controllers cannot completely follow. This fluctuation would be both above and below the rated power, but the mean output (equal to rated power) would not be affected.

Wind Direction Change Corrections

Consider a wind turbine whose power output is affected by off-axis wind directions in a cosine response fashion, e.g. $P(V, \theta) = P(V,0) \cos \theta$. (As with shear and gust corrections, this is an over simplification, but appropriate in terms of level of ease of evaluation compared to more rigorous approaches). If winds are varying in direction θ in such a way that the turbine tracking system cannot follow, then the average of $\cos \theta$, $\langle \cos \theta \rangle$, becomes a correction factor which must multiply the on-axis power output. The average $\langle \cos \theta \rangle$ can be approximated by:

$$\langle \cos \theta \rangle \simeq 1 - \langle \theta^2 \rangle / 2 = 1 - \sigma_\theta^2 / 2. \qquad \text{(A-13)}$$

Data from Crawford and Hudson (1970) on the transition matrix of wind direction changes, from Ramsdell (1975) on $\sigma_V/\bar{V}$, and from Singer et al (1957) indicate that in the useful range of wind speeds σ_θ averages about 0.2 radians. Georgia Tech analysis of Kennedy tower data indicates σ_θ = 0.3 radians. Thus, the average correction factor $\langle \cos \theta \rangle$ from equation (A-17) is about 1 - .04/2 = 0.98. Instantaneous shifts considerably larger could produce a more pronounced effect, but the average effect would be only 2% less than nominal power.

In addition to wind direction changes with time, the power output would be affected by mean wind direction changes with height (wind veering or backing). From Crawford and Hudson (1970), the median wind veering or backing angle is about 20° over the extent of the WKY tower, or about 3° over the height from top to bottom of the rotor disk. This amount of wind change would not significantly affect mean power. Under extreme (95 percentile) wind veers or backing

conditions, the angle change would be about 15° from top to bottom of the rotor, which would have a 1 - 2% effect on output power.

Corrections for Density Variations

The output power of a given WECS will not only be a function of wind speed, but also the density of the atmosphere at the rotor height. The 500 kW WECS output performance curve is based upon the ICAO Standard Atmosphere Sea Level density, 1.219 kg per m^3. However, for a given wind speed the actual WECS power output will decrease as density decreases below the ICAO standard. Atmospheric density is related to temperature and pressure as follows:

$$\rho = p/RT \tag{A-14}$$

where ρ = density, p = absolute pressure, T = absolute temperature and R = gas constant for air. Temperature and pressure vary as a function of altitude. Also, they have a diurnal and seasonal pattern.

The density correction term ρ/ρ_o can be approximated by:

$$\rho/\rho_o = (\rho_o + \Delta\rho)/\rho = 1 + \Delta\rho/\rho_o = 1 + \Delta p/p_o - \Delta T/T_o \tag{A-15}$$

where ΔT is temperature departure from standard atmosphere value (288° K), and Δp is pressure departure from sea level due to site elevation Z (above sea level) and hub height Z_h (above ground). With Z and Z_h in meters

$$\Delta p/p_o = -\rho_o\, g(Z + Z_h)/p_o \simeq -1.2 \times 10^{-4}\ (Z + Z_h). \tag{A-16}$$

If hourly observation of station pressure (not sea level pressure) and temperature are available, these can be used directly in equation (A-15). For situations in which time series pressure and temperature are not available, mean density corrections by month can be evaluated from mean temperature data,

since diurnal and seasonal pressure fluctuations lead to considerably smaller density changes on a diurnal scale than the changes influenced by seasonal temperature variations. For this study the density corrections from TDF-14 tape data were employed directly on the 3 hourly observations.

Combined Corrections

The effects of angle change, density corrections, and wind shear can be combined and used as an effective speed V_{eff} in (A-12), and together with speed gusts σ_u the total power corrections are incorporated as follows:

$$\bar{P}(V_{eff})/P_r = A + BV_{eff} + (1 + \sigma_u^2/\bar{V}^2)\, CV_{eff}^2 \qquad \text{(A-17)}$$

$$V_{eff} = V_{obs}\,[(1 - \sigma_\theta^2/2)(P/P_o)(\rho/\rho_o)]^{1/3} \qquad \text{(A-18)}$$

where V_{obs} is the observed wind speed (converted to hub height), $(1 - \sigma_\theta^2/2)$ is the wind direction correction from (A-13), P/P_o is the shear correction from (A-6), and ρ/ρ_o is the density correction from (A-15).

If use of V_{eff} in (A-17) is such that $\bar{P}/P_r$ is < 0 use $\bar{P}/P_r = 0$, or if $\bar{P}/P_r$ calculates > 1 use $\bar{P}/P_r = 1$. (These conditions become the new cut-in and rated V_{eff} values).

APPENDIX B

SIMPLIFIED WIND SPEED AND POWER DISTRIBUTION MODEL FOR ARRAYS

Single Site and Array Wind Speed Distributions

The array simulation method employed is one whereby summarized (e.g. mean and standard deviations) or time series (i.e. hour by hour) data from a single "representative" site can be used to estimate the statistical behavior or an arbitrary sized array. The concept is based on the Weibull distribution model.

If a single "representative" site has mean speed $\bar{V}_1$ and standard deviation σ_1 (annually, or by season or month, or even by month and hour of the day), then an array of n sites with average spatial cross correlation $\bar{\rho}$ would have a corresponding array mean speed $\bar{V}_n$ and standard deviation σ_n of

$$\bar{V}_n = \bar{V}_1 \tag{B-1}$$

$$\sigma_n = \{\sigma_1^2 [1 + (n - 1) \bar{\rho}]/n\}^{1/2}. \tag{B-2}$$

Equation (B-2) is a generalization, to the case with correlation, of the well known result that $\sigma_n = \sigma_1/n^{1/2}$ would represent σ_n if the n sites were independent (i.e. zero correlation).

From (B-2) it is seen that the ratio σ_n/σ_1 of the standard deviation of the array wind speed distributions and the wind speed distribution of the "typical" individual site in the array depends on the mean array spatial cross correlation $\bar{\rho}$ and the number of sites in the array n. Figure B-1 shows a plot of the ratio σ_n/σ_1 versus $\bar{\rho}$ and n. Above about n = 10, the dependence on n is very slight.

In the more general case of an array made up of n sites, each site i being a farm with n_i WECS units, and each site having mean speed $\bar{V}_i$ and standard deviation σ_i, the array mean speed would be the weighted average of the indivi-

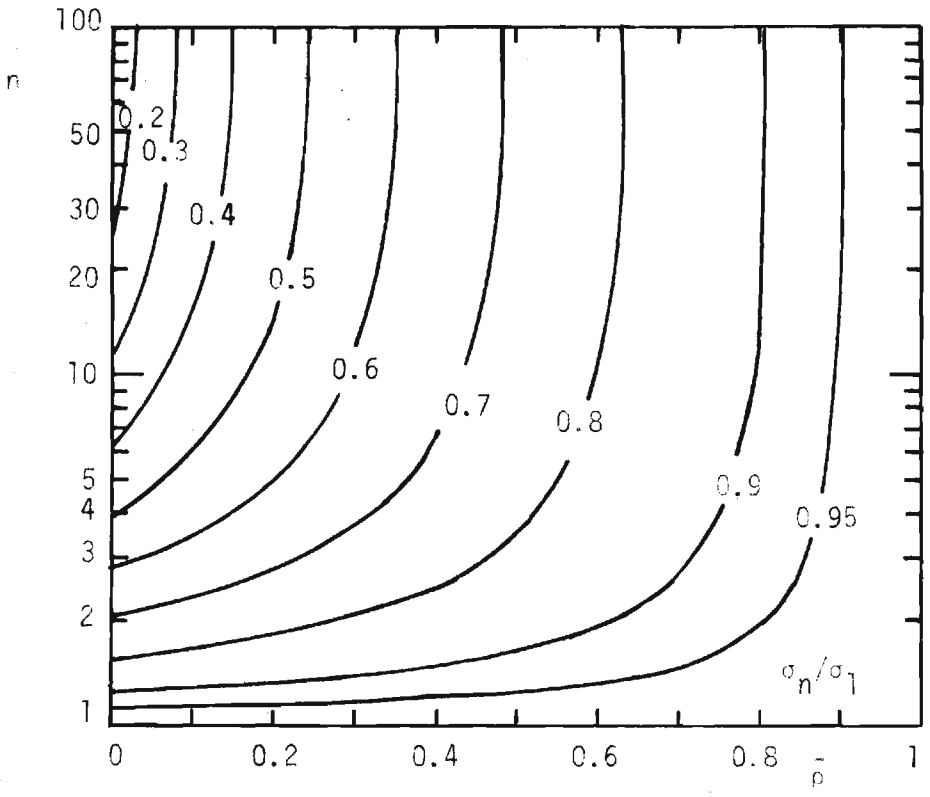

Figure B-1. Array to single site standard deviation ratio σ_n/σ_1 for array with n sites and cross correlation $\bar{\rho}$.

dual site mean speeds

$$\bar{V}_n = \sum_{i=1}^{n} n_i \bar{V}_i / N \qquad \text{(B-3)}$$

where the total number of WECS units N is

$$N = \sum_{i=1}^{n} n_i \qquad \text{(B-4)}$$

A weighted average standard deviation σ_o can be evaluated by

$$\sigma_o^2 = \sum_{i=1}^{n} n_i \sigma_i^2 / N \qquad \text{(B-5)}$$

and this σ_o used in place of the single site standard deviation σ_1 in (B-2) to compute array wind standard deviation σ_n.

Equations (B-3) and (B-5) [with σ_o used instead of σ_1 in (B-2)] are for the general case of an arbitrary number of generators at an arbitrary number of farm sites. For the single "representative site" case, equations (B-1) and (B-2) may be used directly. Such a representative site should be chosen so as to have a mean speed as close as possible to the array mean speed [because of (B-1)] and a standard deviation as close as possible to the rms average array standard deviation [because of equation (B-5)], with approximate equivalence of the mean speed being the more important of these two criteria.

From earlier studies (Justus, 1976, Justus et al, 1976), the wind speed distribution both for individual sites and for arrays is characterized by the Weibull function (with the array having a smaller standard deviation and larger Weibull shape factor k than the individual sites). Thus the distribution of array wind speed V_n for the n site array is given by

$$p(V_n) = (k_n/c_n)(V_n/c_n)^{k_n-1} \exp[-(V_n/c_n)^{k_n}] \qquad \text{(B-6)}$$

where the Weibull shape parameter k_n can be evaluated from

$$k_n = (\sigma_n/\bar{V}_n)^{-1.086} \qquad \text{(B-7)}$$

and the Weibull scale factor c_n can be evaluated by

$$c_n = \gamma \bar{V}_n / \Gamma (1 + 1/k_n) \tag{B-8}$$

where (B-7) is an empirical approximation to the theoretical relation between k and $\sigma/\bar{V}$

$$(\sigma/\bar{V})^2 = [\Gamma (1 + 2/k)/\Gamma^2 (1 + 1/k)] - 1 \tag{B-9}$$

and (B-8) is the theoretical relation between $c/\bar{V}$ and k multiplied by the empirical adjustment factor γ (found from observations to be about 1.02-1.03).

Single Site and Array Power Output Distributions

The array power output $P(V_n)$ per WECS unit in the array is assumed to be a linear function of the array wind speed V_n (at hub height)

$$P(V_n)/P_r = a + b(V_n/V_r) \tag{B-10}$$

where P_r is the rated power and V_r is the rated speed of the WECS units in the array. This model is based on array observations (Justus, 1976), which found the linear relation valid, with a =-0.32, b = 1.04 for the New England and Central U.S. regions. The present studies in the Great Lakes and Pacific Coast areas confirmed the validity of the linear relation, but found that a = -0.42, b = 1.14 would fit these observations better.

Based on the linear regression (B-10) and the Weibull distribution $p(V_n)$ from (B-6), the array average output power $\bar{P}_n$ would be:

$$\bar{P}_n/P_r = \int_0^\infty [a + b(V_n/V_r)]\, p(V_n)\, dV_n. \tag{B-11}$$

To evaluate the probability of various output power levels, the Weibull distribution for array speed is utilized. Thus if the probability of array power being between P_j and P_k is desired (e.g. P_j = 0.1 MW and P_k = 0.2 MW), then from the Weibull cumulative probability

$$p(P_j \leq P \leq P_k) = \exp[-(V_j/C_n)^{k_n}] - \exp[-V_k/C_n)^{k_n}] \qquad \text{(B-12)}$$

where V_j and V_k are the array speeds corresponding to the desired power intervals P_j and P_k, which from (B-10) are given by

$$\begin{aligned} V_j &= [(P_j/P_r) - a]\, V_r/b \\ V_k &= [(P_k/P_r) - a]\, V_r/b \end{aligned} \qquad \text{(B-13)}$$

Examples of these types of array power probability distributions are given in Figures 22 - 25.

Time Series Array Simulation with Single Site Data

In the above analysis mean speed $\bar{V}_1$ and standard deviation σ_1 by month and hour are used to infer probability distributions of array power appropriate to the given month and hour. For certain applications, however, it is necessary to have a simulation of hour-by-hour array power output. The simulation model which can be used for such applications is also based in the Weibull distribution and assumes that the array wind speed for a given time is the speed which would have probability in the array distribution which is equal to the probability of the observed single site wind at that time (based on the appropriate single site distribution). For example, if at a specific time the wind speed observed at the representative site (on which the array statistics are to be based) is V_1, and it is known that the Weibull distribution at the representative site is characterized by scale parameter C_1 and shape parameter k_1, then the cumulative probability $p(V \geq V_1)$ of that observation is

$$p(V \geq V_1) = \exp[-(V_1/C_1)^{k_1}]. \qquad \text{(B-14)}$$

The corresponding array speed V_n which would have equal probability would be

$$p(V \geq V_n) = \exp[-(V_n/C_n)^{k_n}]. \qquad \text{(B-15)}$$

Therefore, by equating (B-14) and (B-15), we obtain

$$V_n = C_n(V_1/C_1)^{k_1/k_n} \qquad \text{(B-16)}$$

as the array wind speed corresponding to the single site wind speed V_1. The array power for the given time when V_1 is observed would then be found by evaluating (B-10) with the value of V_n determined by (B-16).

An example application of this technique is illustrated in Figures B-2 and B-3, which were originally produced as part of the ongoing JBF-NEGEA-Georgia Tech study on electric utility cost effectiveness of wind energy. These data were computed in that study to evaluate the adequacy of "operating reserve" units to handle wind power fluctuations on a 1 hour to 1 day time scale. Figure B-2 shows, for a single site (Falmouth, MA in this case), the probability of finding a change in wind output power of various magnitudes over various time intervals. Power changes ΔP_x are shown relative to wind turbine rated power (500 kW in this example) and time intervals Δt are 1 hour to 12 hours. Probabilities of power changes are shown regardless of direction (i.e. increase or decrease). Thus a change ΔP_x of 0 can occur when $P(t)$ is zero and $P(t + \Delta t)$ remains zero or when $P(t)$ is rated power and $P(t + \Delta t)$ remains rated power. An example of how to read Figure B-2 is given as follows: the probability $p(|P(t + \Delta t) - P(t)| \leq 0.3P_r)$ is read as 70% for Δt = 4 hours. This means that there is a 30% chance that ΔP exceeds 150 kW (0.3 P_r) in Δt = 4 hours and a 70% chance that ΔP is less than (or at most) 150 kW over the same time interval. Comparison of this sample with Figure B-3, for a simulated array, shows that for Δt = 4 hours, the same power change level of 0.3 P_r has about 78% probability of not being exceeded (i.e. 22% probability of being exceeded).

Comparison of Figures B-2 and B-3 show that the simulated array (based on Falmouth as representative site, with n = 20, $\bar{\rho}$ = 0.7 as array simulation input parameters), has much lower probabilities of high power changes being exceeded, but higher probabilities of low power changes ($\Delta P_x \leq 0.2\ P_r$) being exceeded.

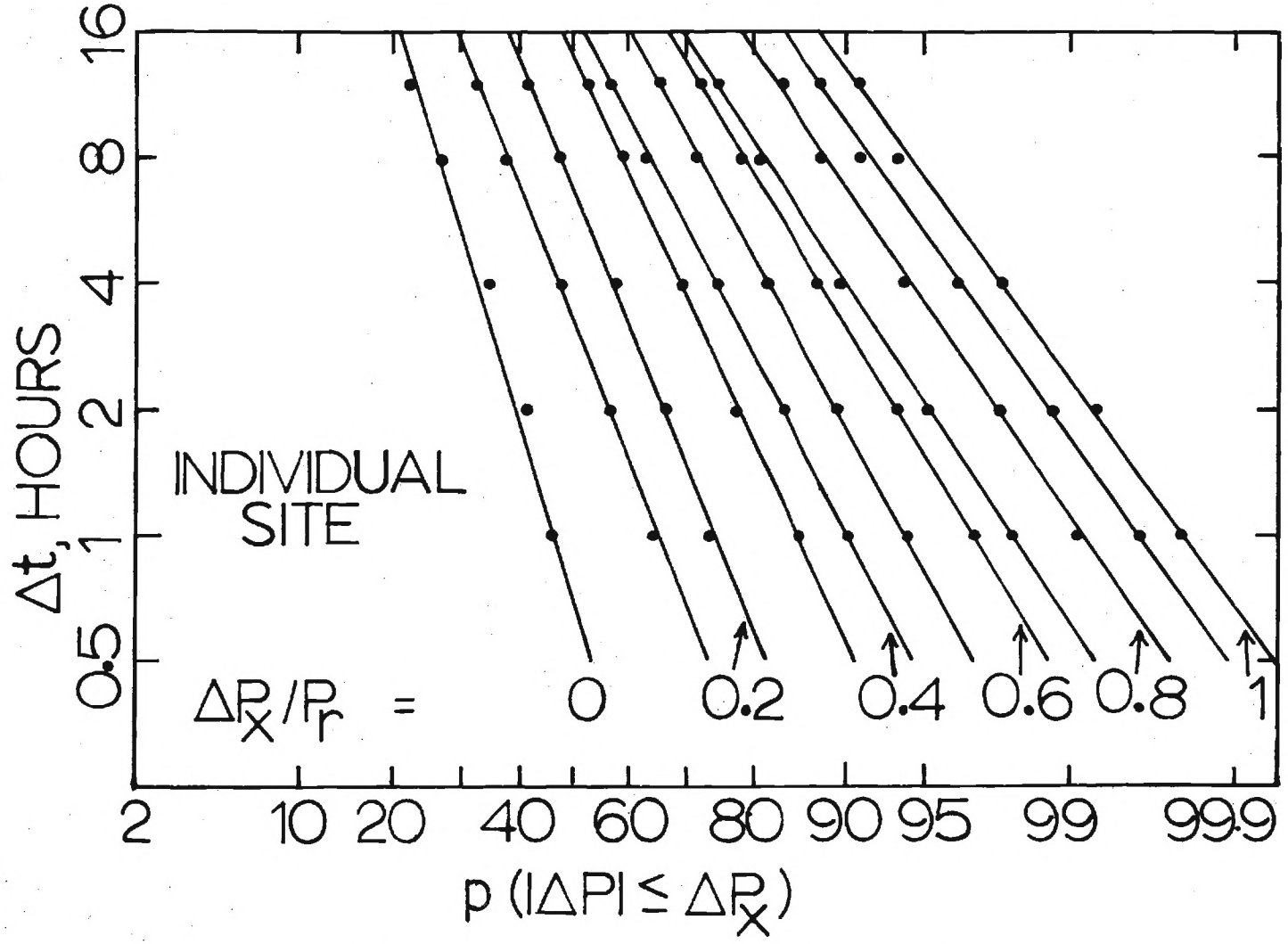

Figure B-2: Probability of wind power changes with time for individual site.

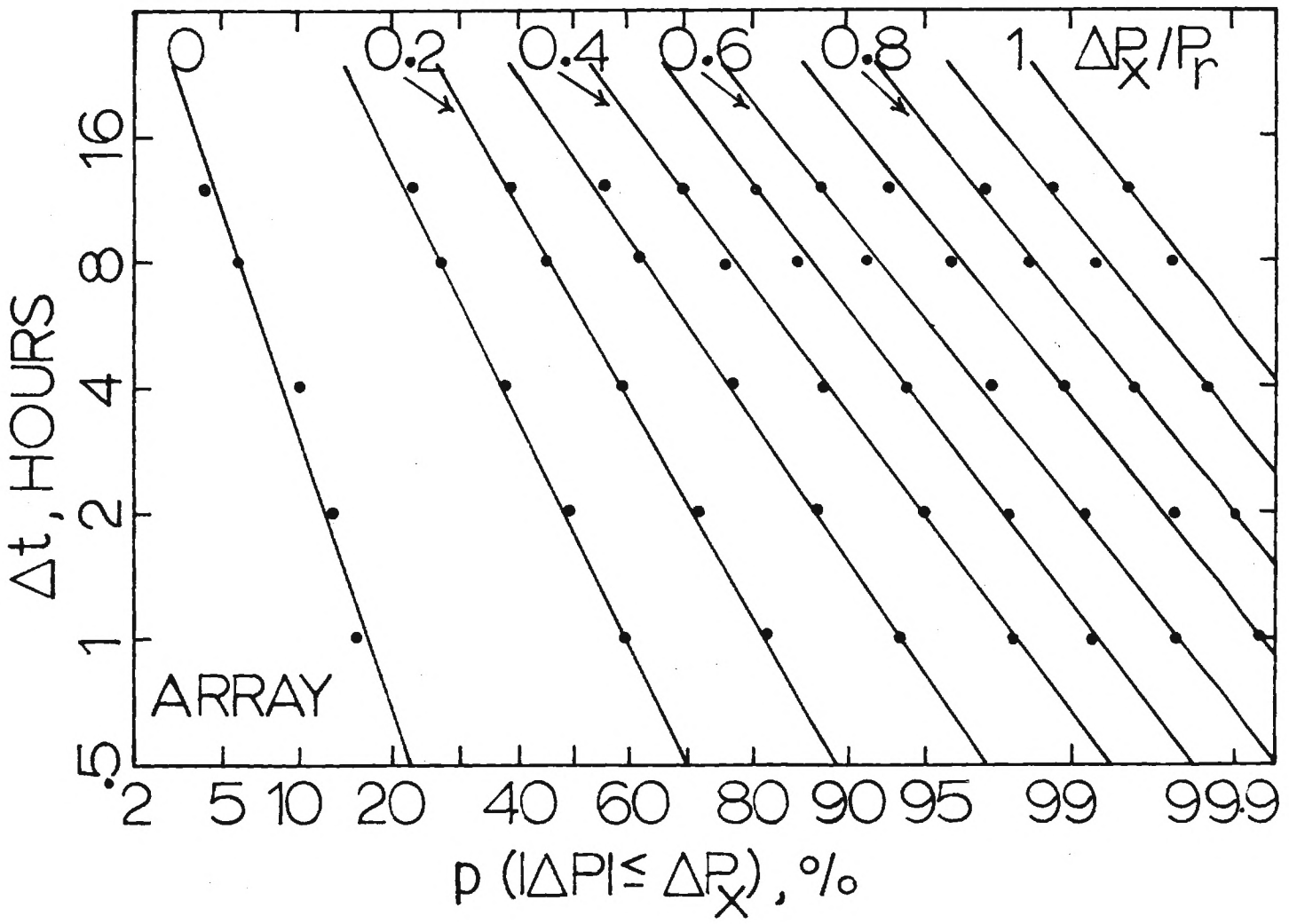

Figure B-3: Time series array model (equations B-14 through B-16) of array power (per generator) changes with time.

The higher array probabilities for low power changes are due to the significantly lesser frequency with which the array is in a state which permits near zero power change (e.g. zero or full power, c.f. Figures 22 - 25).

This proposed time series array model is amenable to verification by direct study of actual array power time changes over one hour and longer (e.g. the run duration analysis of this report, or direct array calculation of power change probabilities such as in Figure B-3). However, such direct comparisons have not yet been carried out, and will be left for further study.

APPENDIX C

SEASONAL AND DIURNAL VARIATIONS IN ARRAY MEAN OUTPUT POWER

This appendix give graphs and tables of the seasonal and diurnal variations of mean array power output for each of the three WECS designs studied. Figures C-1 through C-3 and Tables C-1 through C-3 are for the Great Lakes array 0.5 MW, 1.5 MW, and 2.0 MW WECS respectively, and Figures C-4 through C-6 and Tables C-4 through C-6 are corresponding results for the Pacific Coast array.

Output power level in these figures and tables is expressed in kW/generator. Thus for an array output of 100 kW/generator the total array output power would be 100 kW times the number of WECS units in the array.

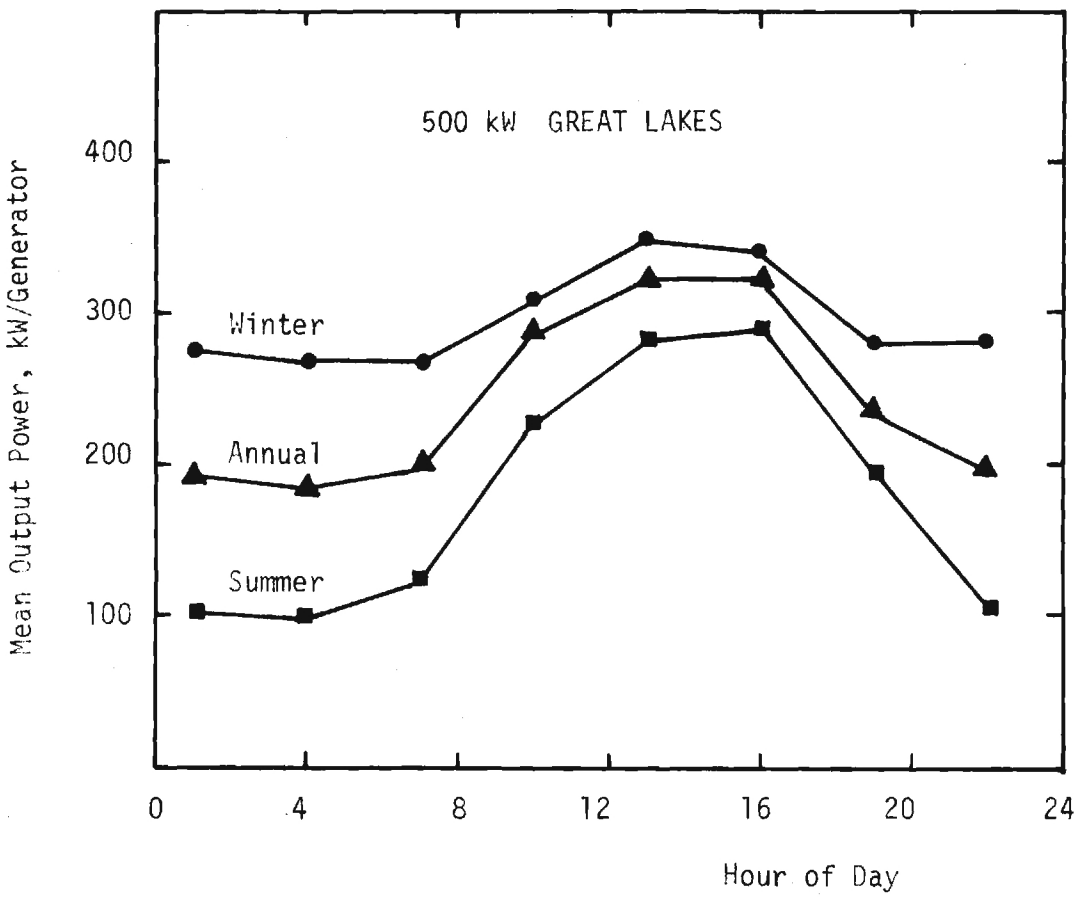

Figure C-1. Seasonal and Diurnal Variations of Mean Output Power for Great Lakes 500 kW WECS Array.

Table C-1

Seasonal and Diurnal Variations of Mean Output Power from Great Lakes Array of 500 kW Wind Turbines (kW per Generator).

Season \ Hour	1	4	7	10	13	16	19	22	Avg
Winter	275	269	268	309	347	340	280	281	296
Spring	206	204	227	324	354	356	278	212	270
Summer	105	98	123	229	282	288	193	108	178
Fall	174	167	171	270	312	300	183	184	220
Annual	190	184	197	283	324	321	233	196	241

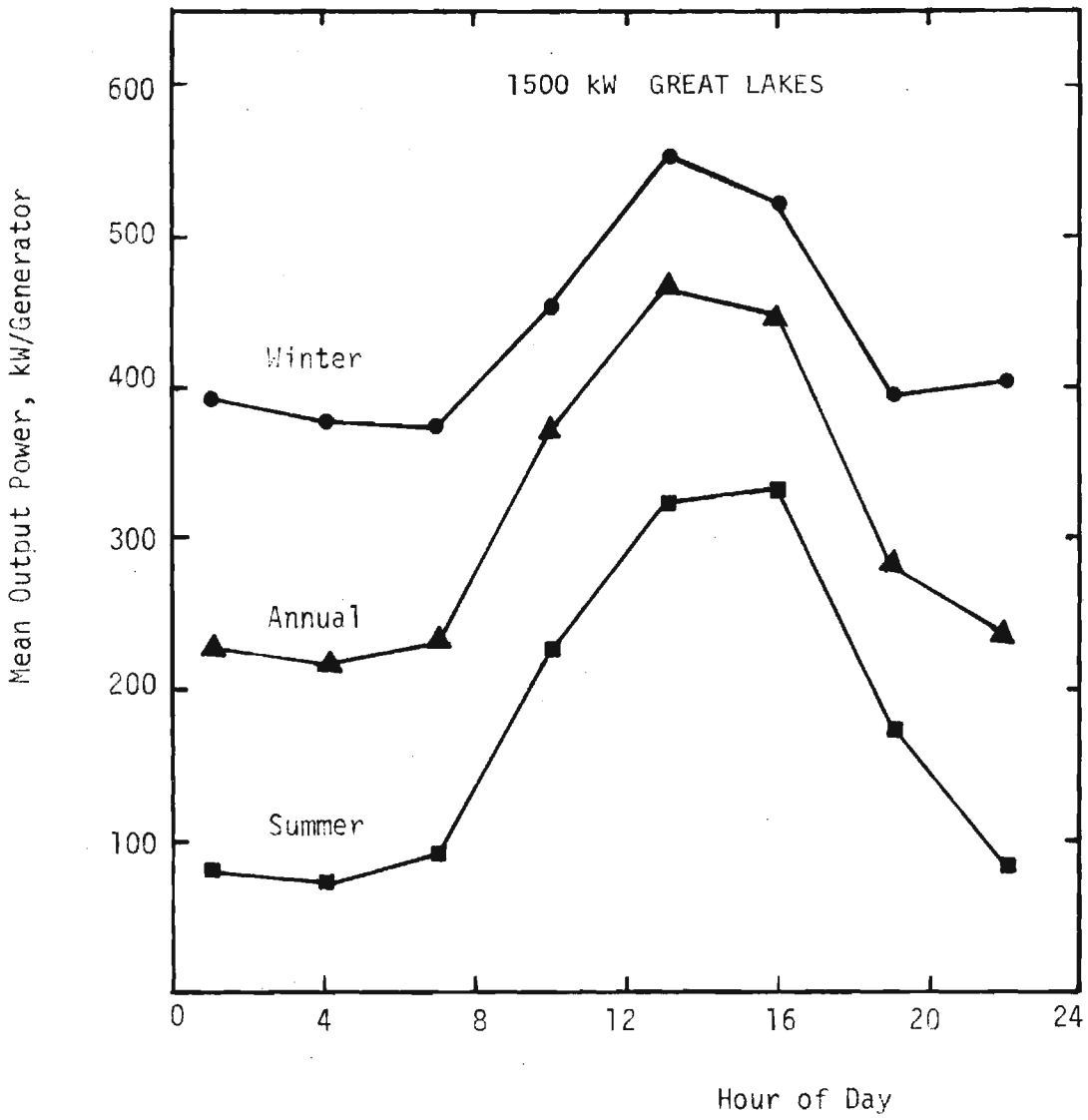

Figure C-2. As in Figure C-1 for 1500 kW WECS.

Table C-2

Seasonal and Diurnal Variations in Mean Output Power from Great Lakes Array of 1500 kW Wind Turbines (kW per Generator)

Season \ Hour	1	4	7	10	13	16	19	22	Avg
Winter	391	378	374	453	551	522	396	402	433
Spring	256	248	284	480	563	557	362	260	376
Summer	79	73	94	226	322	331	171	80	172
Fall	183	174	179	327	421	387	193	201	258
Annual	227	218	232	371	464	449	280	236	310

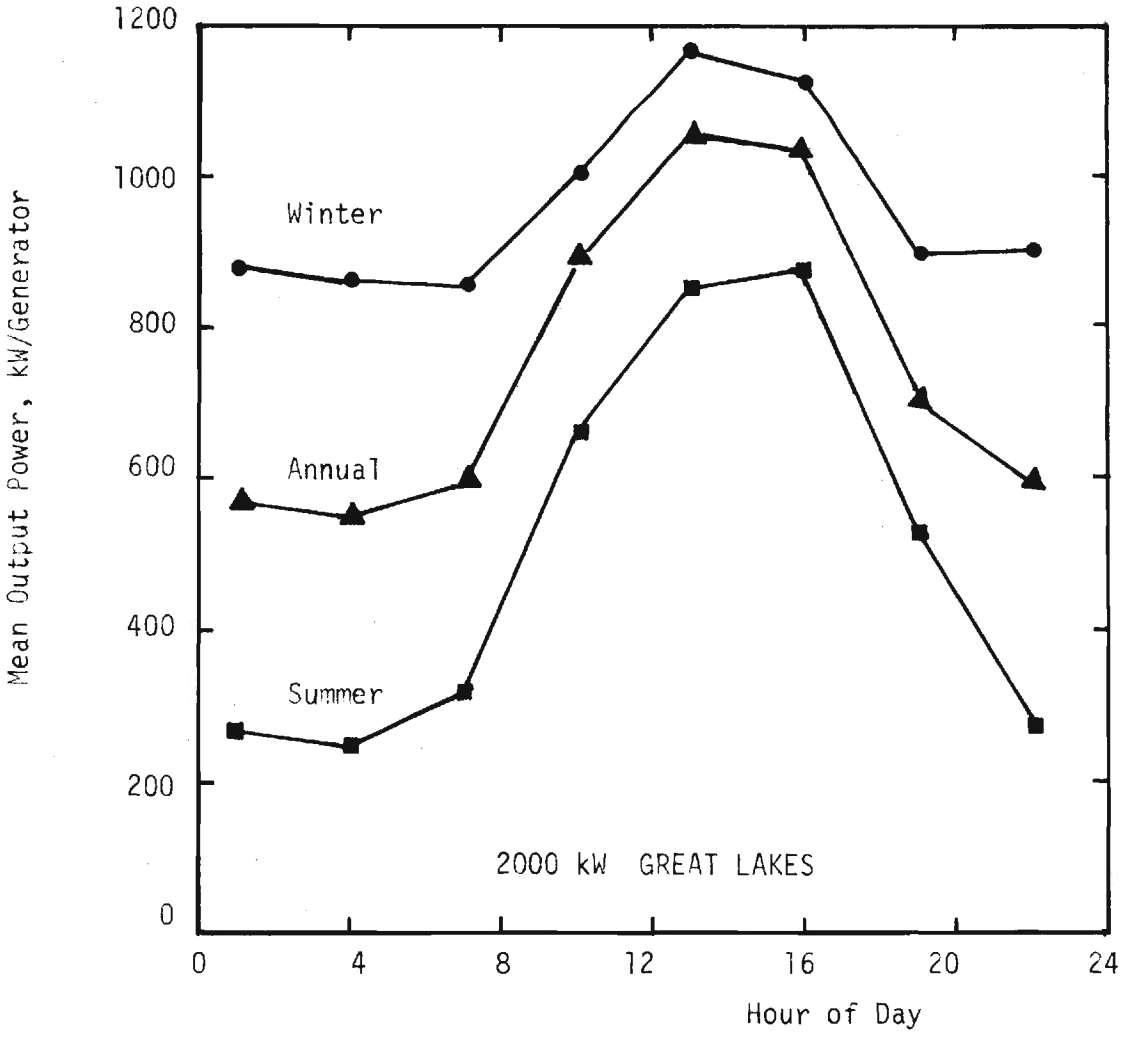

FigureC-3. As in FigureC-1 for 2000 kW WECS.

Table C-3

Seasonal and Diurnal Variations of Mean Output Power from Great Lakes Array of 2000 kW Wind Turbines (kW per Generator).

Season \ Hour	1	4	7	10	13	16	19	22	Avg
Winter	882	862	856	1006	1169	1130	896	906	963
Spring	631	619	699	1063	1189	1190	869	644	863
Summer	269	249	318	656	853	875	529	274	503
Fall	503	479	491	830	997	943	526	535	663
Annual	571	552	591	889	1052	1034	705	590	748

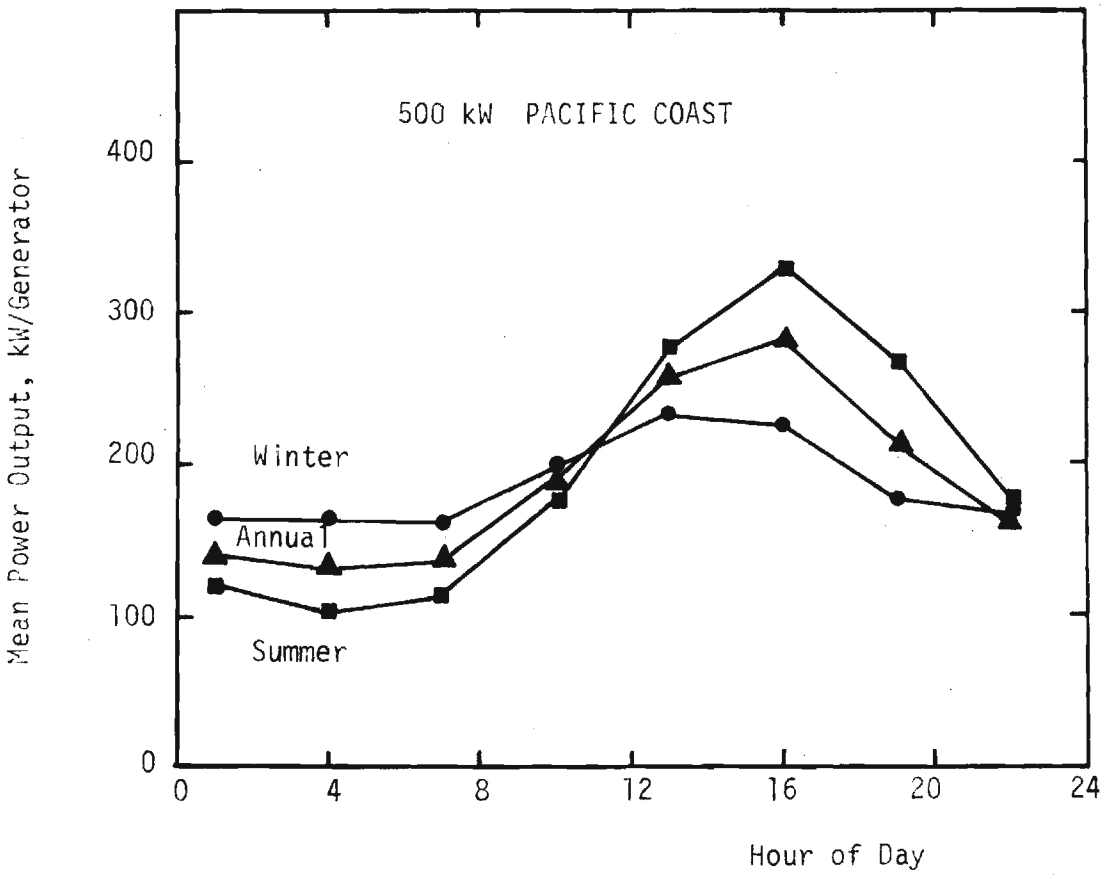

Figure C-4. Seasonal and Diurnal Variations in Mean Output Power for Pacific Coast Region 500 kW WECS Array.

Table C-4

Seasonal and Diurnal Variations of Mean Output Power from Pacific Coast Array of 500 kW Wind Turbines (kW per Generator).

Season \ Hour	1	4	7	10	13	16	19	22	Avg
Winter	164	163	162	197	232	226	176	168	186
Spring	153	144	154	222	290	319	243	177	213
Summer	121	100	114	178	274	330	267	172	195
Fall	120	116	117	166	230	251	167	135	163
Annual	140	131	137	191	257	282	213	163	189

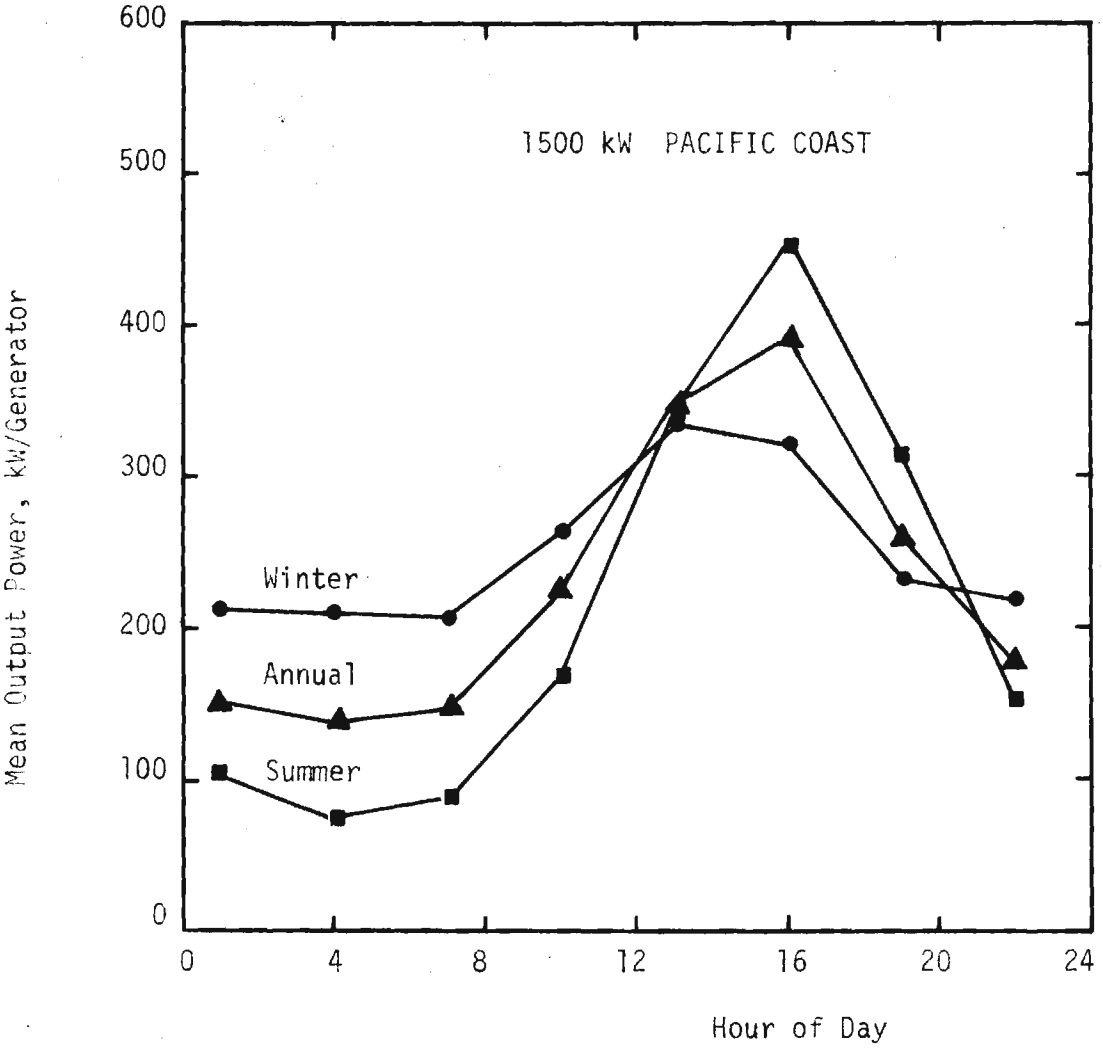

Figure C-5. As in Figure C-4 1500 kW WECS.

Table C-5

Seasonal and Diurnal Variations in Mean Output Power from Pacific Coast Array of 1500 kW Wind Turbines (kW per Generator).

Season \ Hour	1	4	7	10	13	16	19	22	Avg
Winter	213	210	208	262	333	320	233	217	250
Spring	173	156	176	282	419	478	305	196	273
Summer	101	76	89	169	342	453	313	156	212
Fall	117	117	114	178	285	315	181	133	180
Annual	151	140	147	223	345	392	258	176	229

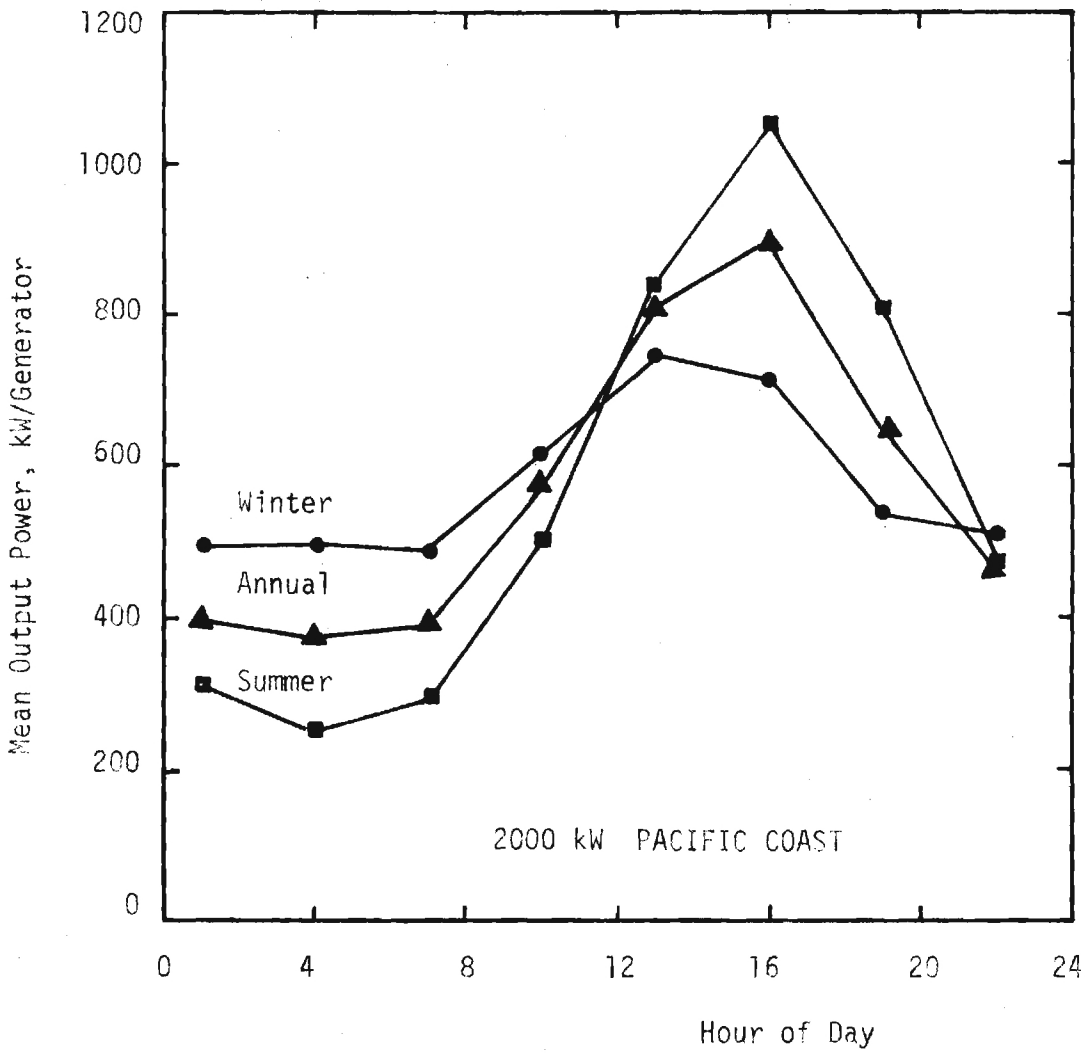

Figure C-6. As in Figure C-4 for 2000 kW WECS.

Table C-6

Seasonal and Diurnal Variations of Mean Output Power from Pacific Coast Array of 2000 kW Wind Turbine (kW per Generator).

Season \ Hour	1	4	7	10	13	16	19	22	Avg
Winter	496	495	490	609	742	716	538	509	574
Spring	443	411	450	682	937	1046	745	513	653
Summer	317	255	296	497	840	1054	805	470	567
Fall	332	321	322	478	701	769	483	377	473
Annual	397	370	389	567	805	896	643	467	567

APPENDIX D

SEASONAL AND DIURNAL VARIATIONS IN POWER AVAILABILITY PERCENTAGES FOR ARRAYS AND INDIVIDUAL SITES

This appendix gives tables of availability in percent of various array output power levels (100, 200, and 500 kW per generator) for the 3 WECS designs studied and for the two regions studied. Related data on array power availability are given in Chapter 5.

Example of how to read the following tables: For the Great Lakes Regions, at hour 16 (4:00 pm) in Winter (December-February), the power level 100 kW per 500 kW generator would be available 83.3% of the time from a single unit installation (Table D-1) and 95.1% of the time from the array studied. Thus if one sampled randomly at 4:00 pm in Winter, the output of a single 500 kW WECS in the Great Lakes Region, its output would be 100 kW or above 83.3% of the time and below 100 kW 16.7% of the time. For the array, the power output in this case would be 100 kW or more per array unit for 95.1% of the time and less than 100 kW per generator 4.9% of the time. For array power of 100 kW per generator, the total power from the array would be 100 kW times the number of generators in the array.

The diversity of the arrays studied significantly enhances the availability levels of 100-500 kW per generator, especially in the early afternoon (hours 13 and 16). Since these hours usually correspond to peak electric demand (especially for air conditioning load in the summer season), the increased availability of array power at these hours can have a significant impact on cost effectiveness of wind power to utilities.

Table D-1

Availability (percent) of 100 kW per 500 kW generator in Great Lakes Array

(Individual Sites and Whole Array)

Hour	Winter		Spring		Summer		Fall		Annual	
	Ind.	Array	Ind.	Array	Ind.	Array	Ind.	Array	Ind.	Array
1	71.5	89.4	57.9	73.5	36.3	39.6	52.4	64.8	54.4	66.7
4	69.9	86.7	57.2	70.4	34.2	38.0	50.6	60.7	52.9	63.9
7	69.6	85.1	62.4	76.7	42.7	50.4	51.4	62.2	56.5	68.6
10	77.7	92.7	82.3	97.6	70.0	86.3	74.8	91.0	76.2	91.9
13	83.9	96.7	87.1	99.3	79.7	98.5	81.6	97.4	83.1	98.0
16	83.3	95.1	87.8	99.8	80.8	99.6	80.7	97.6	83.1	98.0
19	72.8	89.1	75.7	96.7	62.9	84.6	55.2	69.7	66.7	85.0
22	72.8	89.6	60.5	77.2	38.0	42.8	54.5	68.1	56.4	69.3
All	75.2	90.5	71.3	86.4	55.6	67.5	62.7	76.4	66.2	80.2

Table D-2

Availability (percent) of 100 kW per 1500 kW Generator in Great Lakes Array

(Individual Sites and Whole Array)

Hour	Winter		Spring		Summer		Fall		Annual	
	Ind.	Array	Ind.	Array	Ind.	Array	Ind.	Array	Ind.	Array
1	54.0	79.2	39.6	60.0	18.1	25.0	32.4	51.6	36.0	53.8
4	52.8	76.1	39.3	58.0	16.8	23.9	31.0	47.9	34.9	51.4
7	52.5	74.5	44.8	64.3	22.0	29.6	31.9	47.7	37.8	53.9
10	61.8	85.4	66.4	90.9	46.7	71.1	54.8	77.8	57.4	81.3
13	70.4	92.2	73.0	96.7	59.8	88.0	64.2	88.8	66.9	91.5
16	69.0	89.6	73.8	97.8	61.1	92.4	62.0	87.7	66.5	91.9
19	55.1	79.2	55.7	83.7	38.0	57.4	34.2	52.3	45.7	68.1
22	54.6	80.0	40.8	64.1	18.3	25.0	34.8	53.2	37.0	55.5
All	58.8	82.0	54.2	77.0	35.1	51.5	43.2	63.4	47.8	68.4

Table D-3

Availability (percent) of 200 kW per 2000 kW Generator in Great Lakes Array

(Individual Sites and Whole Array)

Hour	Winter		Spring		Summer		Fall		Annual	
	Ind.	Array	Ind.	Array	Ind.	Array	Ind.	Array	Ind.	Array
1	71.5	90.5	57.8	77.0	35.2	44.8	52.2	68.4	54.1	70.0
4	69.9	88.9	57.1	74.1	33.2	42.6	50.6	66.2	52.6	67.9
7	69.6	88.0	62.3	79.6	41.7	53.9	51.3	66.6	56.2	72.0
10	77.7	93.8	82.0	98.0	67.2	90.0	74.5	93.2	75.3	93.8
13	83.9	97.8	86.6	99.8	75.8	98.5	80.9	97.8	81.8	98.5
16	83.3	95.8	87.3	100.0	76.5	99.8	80.0	98.2	81.8	98.5
19	72.8	91.4	75.2	97.6	58.2	88.7	54.5	74.5	65.2	88.1
22	72.8	90.2	60.3	80.2	36.0	47.6	54.4	71.6	55.3	72.3
All	75.2	92.0	71.1	88.3	53.0	70.7	62.3	79.6	65.3	82.6

Table D-4

Availability (percent) of 500 kW per 2000 kW Generator in Great Lakes Array

(Individual Site and Whole Array)

Hour	Winter		Spring		Summer		Fall		Annual	
	Ind.	Array	Ind.	Array	Ind.	Array	Ind.	Array	Ind.	Array
1	54.7	70.5	39.7	50.0	18.1	18.0	32.4	40.7	36.2	44.7
4	53.6	68.1	39.5	48.9	16.8	14.8	31.0	37.4	35.2	42.2
7	53.4	66.1	44.9	53.3	22.0	20.7	31.9	37.1	38.0	44.2
10	62.6	77.8	66.5	83.3	46.7	57.8	54.8	68.6	57.7	71.9
13	70.9	85.4	73.0	92.2	59.8	79.3	64.3	80.4	67.0	84.3
16	69.3	84.3	73.8	95.7	61.1	81.3	62.0	79.1	66.6	85.1
19	55.6	69.0	55.7	91.1	38.0	45.9	34.2	41.8	45.9	56.9
22	55.4	71.4	40.9	52.0	18.3	16.3	34.8	44.0	37.3	45.8
All	59.5	74.1	54.2	68.3	35.1	41.8	43.2	53.6	48.0	59.4

Table D-5

Availability (percent) of 100 kW per 500 kW Generator in Pacific Coast Array (Individual Site and Whole Array)

Hour	Winter		Spring		Summer		Fall		Annual	
	Ind.	Array	Ind.	Array	Ind.	Array	Ind.	Array	Ind.	Array
1	45.5	73.8	45.9	73.3	39.5	61.1	38.2	54.7	42.3	65.7
4	44.9	73.6	44.4	70.0	34.5	44.6	36.1	51.9	40.0	60.0
7	44.9	75.6	46.2	73.5	38.6	53.7	36.6	53.8	41.6	64.1
10	54.0	85.8	61.8	95.4	54.6	90.0	49.5	76.0	55.0	86.9
13	60.5	92.5	75.3	99.8	76.7	100.0	64.6	94.1	69.2	96.6
16	60.7	92.2	81.3	99.8	84.5	100.0	69.0	97.1	73.8	97.3
19	49.4	80.7	67.4	97.2	75.2	100.0	50.8	83.5	60.6	90.4
22	47.4	77.4	53.5	87.4	54.9	91.5	42.9	66.2	49.7	80.7
All	50.9	81.5	59.5	87.0	57.3	80.1	48.5	72.2	54.1	80.2

Table D-6

Availability (percent) of 100 kW per 1500 kW Generator in Pacific Coast Array

(Individual Site and Whole Array)

Hour	Winter		Spring		Summer		Fall		Annual	
	Ind.	Array	Ind.	Array	Ind.	Array	Ind.	Array	Ind.	Array
1	29.8	68.3	28.2	66.7	21.5	40.4	21.1	43.7	25.2	54.8
4	30.3	66.1	26.0	59.6	16.9	28.3	20.6	52.9	23.5	49.1
7	30.1	69.4	28.6	64.8	20.0	32.6	20.7	42.2	24.9	42.2
10	37.7	79.4	44.0	84.1	34.4	71.1	31.9	63.3	37.0	74.5
13	46.0	86.7	59.7	98.9	57.0	99.8	45.9	86.4	52.1	93.0
16	44.3	87.1	66.5	99.3	70.0	100.0	50.8	90.3	57.8	94.2
19	32.4	74.7	48.4	93.3	54.9	98.5	31.2	70.8	41.8	84.4
22	30.9	69.6	33.0	73.0	33.3	69.1	24.3	50.1	30.4	65.5
All	35.3	75.2	41.8	80.0	38.5	67.5	30.8	61.2	36.6	71.0

Table D-7

Availability (percent) of 200 kW per 2000 kW Generator in Pacific Coast Array

(Individual Site and Whole Array)

Hour	Winter		Spring		Summer		Fall		Annual	
	Ind.	Array	Ind.	Array	Ind.	Array	Ind.	Array	Ind.	Array
1	44.2	82.9	44.1	83.9	37.3	74.1	36.7	65.7	40.6	76.7
4	43.8	81.6	42.3	80.9	31.8	58.9	34.7	61.3	38.2	70.6
7	43.7	84.2	43.9	82.2	36.0	65.7	34.9	63.3	39.7	73.8
10	52.7	91.8	59.8	96.5	52.5	94.3	47.7	82.0	53.2	91.2
13	59.2	96.0	73.7	100.0	73.9	100.0	62.6	96.9	67.3	98.2
16	59.0	96.7	79.6	99.8	82.3	100.0	67.1	98.5	71.9	98.7
19	47.6	87.6	64.9	97.8	71.1	100.0	48.9	89.7	58.1	93.8
22	46.2	84.5	51.3	91.1	52.3	95.2	41.1	74.5	47.7	86.4
All	49.6	88.2	57.4	91.5	54.7	86.0	46.7	79.0	52.1	86.2

Table D-8

Availability (percent) of 500 kW per 2000 kW Generator in Pacific Coast Array

Array (Individual Site and Whole Array)

Hour	Winter		Spring		Summer		Fall		Annual	
	Ind.	Array	Ind.	Array	Ind.	Array	Ind.	Array	Ind.	Array
1	30.0	46.1	28.3	35.7	21.7	23.5	21.4	21.5	25.4	29.1
4	30.3	45.0	26.1	31.3	17.2	6.7	20.7	20.9	23.7	25.9
7	30.2	42.8	28.6	37.6	20.3	13.5	20.9	19.8	25.1	28.4
10	37.7	59.6	44.1	69.8	34.7	43.9	32.1	42.9	37.2	54.1
13	46.1	72.7	59.8	93.9	57.7	95.9	46.1	72.1	52.4	83.7
16	44.5	71.0	66.5	96.7	70.8	99.3	51.0	80.0	58.1	86.9
19	33.0	50.6	48.5	80.7	55.2	92.2	31.4	44.2	42.0	67.0
22	31.0	44.1	33.1	46.5	33.5	40.0	24.5	26.8	30.6	39.4
All	35.4	54.0	41.9	61.5	38.9	50.6	31.0	41.0	36.8	51.8

REFERENCES

Corotis, R. B. (1976): "Stochastic Modeling of Site Wind Characteristics", ERDA/NSF-00357/76/1.

Corotis, R. B. (1977): "Stochastic Modeling of Site Wind Characteristics", RLO-2342-77/1.

Crawford, K. C. and H. R. Hudson (1970): "Behavior of Winds in the Lowest 1500 ft in Central Oklahoma: June 1966-May 1967", NOAA ERLTM-NSSL-48.

Justus, C. G. (1976): "Wind Energy Statistics for Large Arrays of Wind Turbines (New England and Central U.S. Regions)", ERDA/NSF-00547/76/1, (NSF/RA-76-0191).

Justus, C. G. and Amir Mikhail (1976): "Height Variation of Wind Speed and Wind Distribution Statistics", Geophys. Res. Letters, 3, 261-264.

Justus, C. G. et al (1976): "Reference Wind Speed Distributions and Height Profiles for Wind Turbine Design and Performance Evaluation Applications", ORO/5108-76/4.

Ramsdell, J. V. (1975): "Wind and Turbulence Information for Vertical and Short Take Off and Landing (V/STOL) Aircraft Operations in Built Up Urban Areas - Results of Meteorological Survey", FAA-RD-75-94 (AD-A019216/1).

Singer, A. I. (1960): "A Study of the Wind Profile in the Lowest 400 Feet of the Atmosphere", BNL596 (T-170) (Physics and Mathematics) Progress Report No. 5.

Singer A. I. et al (1957): "Analysis of Meteorological Tower Data, April 1950-March 1952, Brookhaven National Laboratory", BNL 461 (T-102) (Physics and Mathematics", Brookhaven National Laboratory.

Singer, A. I. et al (1961): "A Study of the Wind Profile in the Lowest 400 Feet of the Atmosphere", BNL 697 (T-239) (Meteorology - TID 4500, 16th Ed) Progress Report No. 9.

Sissenwine, N. et al (1973): "Extreme Wind Speeds, Gustiness, and Variations with Height for MIL-STD 210B', AFCRL-TR-73-0560.

Wendell, L. C. (1970): "A Preliminary Examination of Mesoscale Wind Fields and Transport Determined from a Network of Wind Towers", NOAA ERLTM-ARL-25.

Wilson, R. E. and P. B. S. Lissaman (1974): "Applied Aerodynamics of Wind Power Machines", National Science Foundation, PB-238-595.